APL Materials

Roadmap on nanogenerators and piezotronics

Cite as: APL Mater. **10**, 109201 (2022); https://doi.org/10.1063/5.0085850
Submitted: 19 January 2022 • Accepted: 17 June 2022 • Published Online: 31 October 2022

Philippe Basset, Stephen Paul Beeby, Chris Bowen, et al.

COLLECTIONS

This paper was selected as Featured

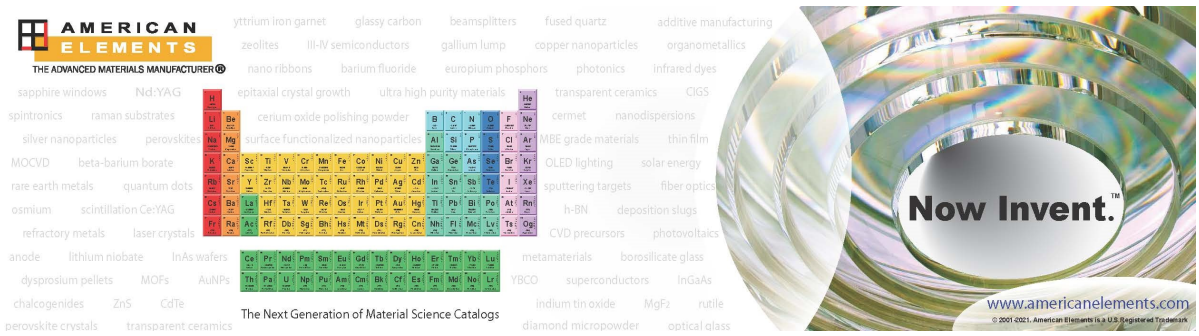

AIP Publishing

Roadmap on nanogenerators and piezotronics

Cite as: APL Mater. 10, 109201 (2022); doi: 10.1063/5.0085850
Submitted: 19 January 2022 • Accepted: 17 June 2022 •
Published Online: 31 October 2022

View Online Export Citation CrossMark

Philippe Basset,[1] Stephen Paul Beeby,[2] Chris Bowen[3] Zheng Jun Chew,[4] Ahmad Delbani,[1] R. D. Ishara G. Dharmasena,[5] Bhaskar Dudem,[6] Feng Ru Fan,[7] Dimitri Galayko,[8] Hengyu Guo,[9] Jianhua Hao,[10] Yuchen Hou,[11] Chenguo Hu,[9] Qingshen Jing[12,13,14,a)] Young Hoon Jung[15] Sumanta Kumar Karan[6,16] Sohini Kar-Narayan,[12,a)] Miso Kim,[16] Sang-Woo Kim[16,17] Yang Kuang,[4] Keon Jae Lee,[15] Jialu Li,[18] Zhaoling Li[18] Yin Long,[19] Shashank Priya,[11] Xianjie Pu,[9] Tingwen Ruan,[4] S. Ravi P. Silva,[6] Hee Seung Wang,[15] Kai Wang,[11] Xudong Wang,[19] Zhong Lin Wang,[20] Wenzhuo Wu[21,22,23] Wei Xu,[10] Hemin Zhang[1,24] Yan Zhang,[13] and Meiling Zhu[4]

For affiliations, please see the end of the Reference section

TABLE OF CONTENTS

I. PREFACE

Zhong Lin Wang (*zhong.wang@mse.gatech.edu)

Piezoelectric nanogenerator (PENG) was first introduced by using piezoelectric nanowires for converting tiny mechanical energy into electric power.[1] Research in nanogenerators has been vastly expanded in the last decade due to the invention of the triboelectric nanogenerator (TENG).[2,3] As of today, the definition of nanogenerator has far exceeded its traditional meaning, and it represents a field that uses the Maxwell's displacement current to convert mechanical energy into electric power/signal.[4–6] This field is attracting a wide range of interest due to the huge advances in the internet of things, big data, sensor network, robotics, and artificial intelligence.[7–13] TENGs are playing a key role in harvesting high entropy energy distributed in our living environment for effective driving of distributed electronics and systems.[14–20]

The piezotronic effect is about the use of piezoelectric polarization charges at an interface for effectively tuning/controlling charge carriers across a metal–semiconductor interface, which was first introduced in 2007.[21,22] The piezo-phototronic effect is about the use of piezoelectric polarization charges at a p–n junction for effectively tuning/controlling charge carriers recombination or separation at the interface, which was first introduced in 2010.[23,24]

From a recent SCI database search, there are 57 countries and regions, over 800 units and over 6000 scientists worldwide who are engaged in TENG research. The papers published in the public domain ever since the invention of nanogenerators in 2006 are given in Fig. 1, which unambiguously show that the research in nanogenerators is a focused field worldwide.

This special issue is about some of the current progress made in nanogenerators and piezotronics. Dudem *et al.* systematically reviewed the theoretical progress made for TENGs and how they can be utilized for optimizing the output power. Fundamental technical advances made for improving the performance of the TENG have been reported by Li *et al.*, Zhang and Bowen, and Basset, not only about the choice of materials but also about the power management system. Since the choice of materials for TENG is rather broad, Fan and Wu reported the use of 2D materials for nanogenerators and piezotronics, and Kim reported the use of metamaterials for energy harvesting. Wang, Hou, and Priya have reported the use of perovskites for TENG. Xu and Hao have elaborated on the use of smart polymer materials for TENG. The remaining articles are about the novel applications of TENGs for a variety of fields, such as acoustic sensors (Wand and Lee), biomedical research (Wand and Long), powering of wireless sensor systems (Chew, Kuang, Ruan, and Zhu), e-textiles (Beeby), human–machine interfacing (Pu, Guo, and Hu), and powering body-implantable medical devices (Karan and Kim). Although the collections of articles in this special issue is a small portion of the current progress in nanogenerators and piezotronics, a broad range of research is being carried out worldwide. Nanogenerators will find major applications in micro–nano power sources, self-powered sensors, blue energy, and high voltage sources. Piezotronics and piezophototronics will find applications

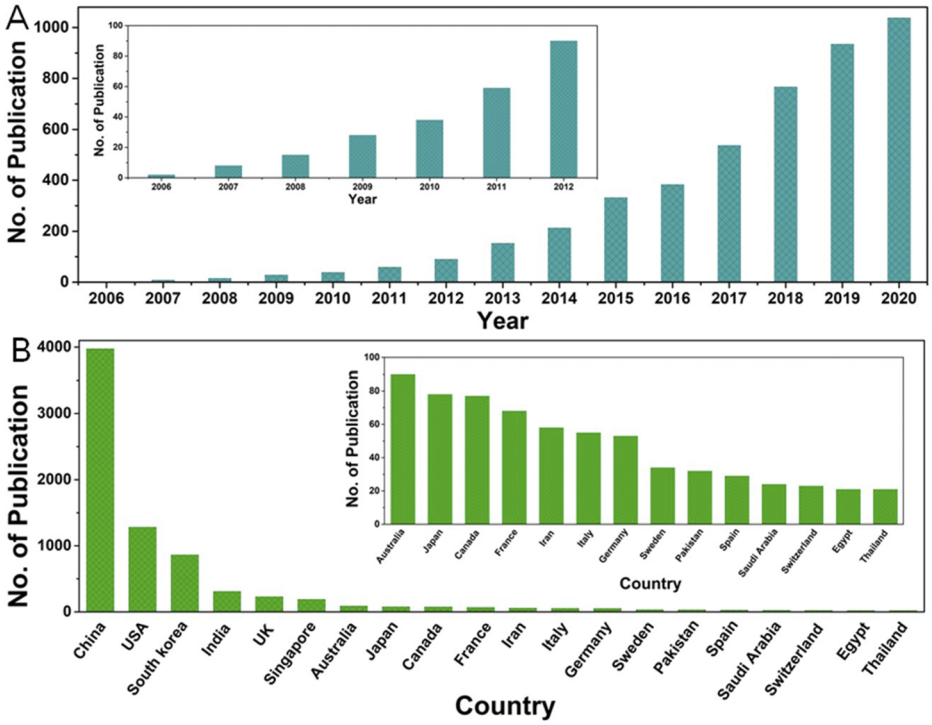

FIG. 1. Statistics of publications from Web of Science by 2020. The number of publications in each year (a) and country (b) when "Nanogenerator" was used as the keyword for search in Web of Science.

related to devices made for the third generation semiconductors. We anticipate that the field will be advanced very fast, which will soon impact industrial technology in specific areas.

II. THEORY

A. Theoretical progress and its implementation in the optimization of triboelectric nanogenerators

Bhaskar Dudem, R. D. Ishara G. Dharmasena, Sumanta Kumar Karan, S. Ravi P. Silva (*s.silva@surrey.ac.uk)

1. Abstract

Triboelectric nanogenerators (TENGs) are one of the most promising energy harvesting methods available for next-generation wearables, autonomous devices and sensors, and the Internet-of-things (IoT), which can efficiently convert ambient mechanical energy into useful electricity. It can be implemented in clothing, shoes, walkways, and moving parts in automobiles, harvest suitable energy to drive many types of portable/wearable/implantable electronics that at present, and are predominantly powered by batteries. In order to move the current state-of-the-art in practical devices to realistic technologies, much development is still needed. These requirements we envisage will be accelerated with the help of theoretical models and simulations, which can be verified and refined using an empirical route to best fit experimental data. This will give rise to self-validated models that allow for predictive design of TENG devices for specific applications using computer-aided design (CAD) and simulators.

2. Introduction

TENGs were first proposed by Yang *et al.* in 2012,[25] and it is well-known that they generate electricity based on the triboelectric effect, the frictional contact between two triboelectric materials resulting in static charge generation, and electrostatic induction resulting from the relative movement of such charged surfaces.[2,26–28] While contact-electrification (CE) is believed to be the fundamental phenomenon for charge generation during the friction of a TENG, the exact mechanism of this charge generation is not yet fully understood. In addition, the mechanism to enhance the output performance of TENGs by surface modification of the triboelectric materials is also not fully elucidated. Thus far, an extensive effort has been made to understand and optimize the output performance of TENGs by distinct types of theoretical models and simulations,[29–42] many of which are represented on a timeline as shown in Fig. 2.

3. Development of various theoretical models

a. Exploring the electrical response of TENGs based on mathematical modeling. TENGs typically contain triboelectric charges on their contact surfaces, and the relative movement of these charged surfaces causes the electric fields acting on their electrodes to vary, which results in an induced output current flow between the electrodes. The power output of the TENG is extracted by driving this current through an external load. This behavior is commonly expressed using Maxwell's displacement current[4]

$$J_D = \frac{\partial D}{\partial t} = \varepsilon \frac{\partial E}{\partial t} + \frac{\partial P_S}{\partial t}. \quad (1)$$

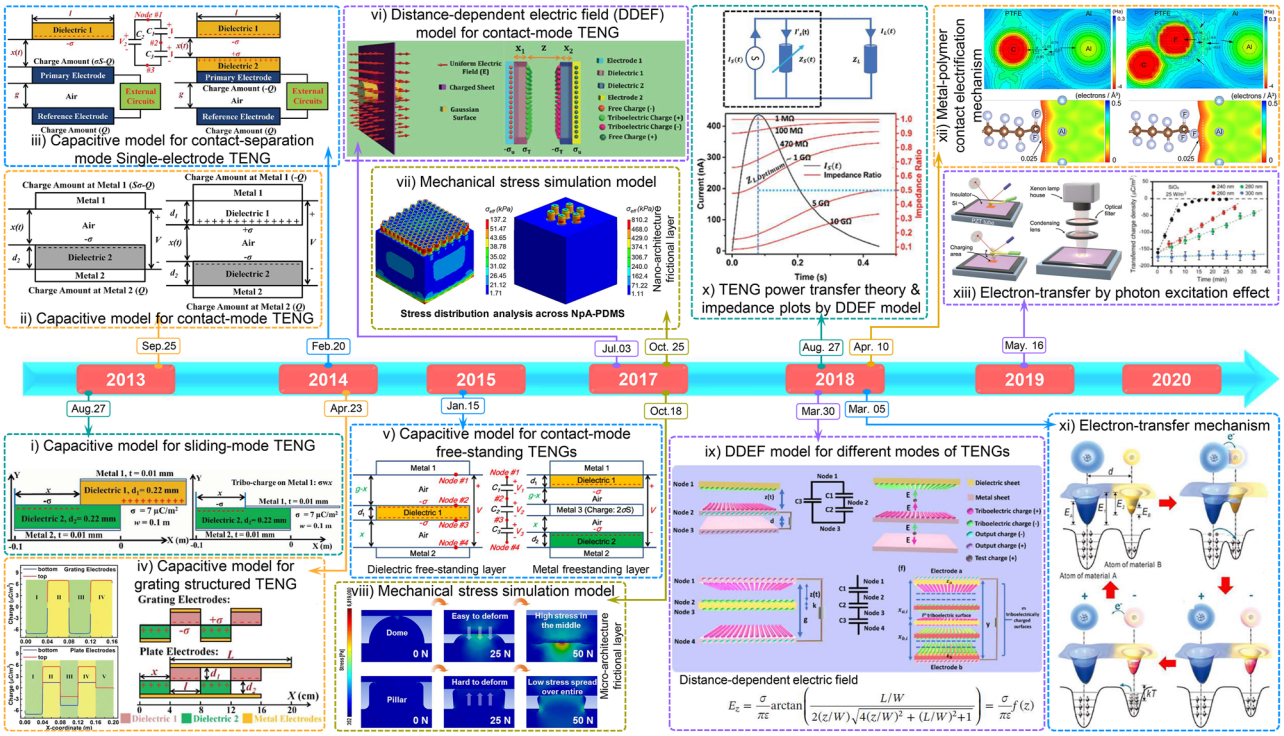

FIG. 2. Timeline displaying the progress in various types of theoretical approaches, thus far, to optimize the performance of TENGs. *2013 and 2014*: Capacitive model for (i) sliding-mode,[29] vertical contact–separation (ii) dual and (iii) single electrode mode,[30,31] and (iv) grating structured TENGs.[32] *2015*: (v) Theoretical prediction for contact-mode free-standing TENG.[33] *2017*: (vi) Distance-dependent electric field (DDEF) model of a vertical contact–separation mode TENG;[35] (vii) and (viii) stress simulation analysis across the nano-architecture triboelectric layers.[36,37] *2018*: (ix) the universal DDEF models to simulate and optimize different modes of TENGs[38] and (x) TENG impedance pots and TENG power transfer theory to understand its output power transfer;[39] (xi) electron-cloud-potential-well model for elucidating electron transfer mechanism in contact electrification;[40] (xii) the electrostatic potential distribution generated across the distinct atoms like F–C–Al and C–F–Al during the superposition of Al and the PTFE.[41] *2019*: (xiii) photon excitation effect to explain the charge transfer mechanism in triboelectrification.[42]

Herein, J_D = displacement current density, D = displacement field, t = time, E = electric field, and P_S = polarization of the medium. Two fundamental approaches have been presented so far to simulate the output behavior of TENGs: the parallel plate capacitor approach and the distance-dependent electric field approach.

The first generation of theoretical models representing TENGs was derived using the parallel-plate capacitor approach [Figs. 2(i) and 2(ii)]. In this approach, each TENG architecture was represented using a unique combination of parallel plate capacitors [Figs. 2(i)–2(v)] to approximate their output trends. Using these capacitor assemblies, a relationship between the voltage (V), charge (Q), and the separation distance of TENG layers (x) was developed (known as the V–Q–x relationship), which is given by

$$V = -\frac{1}{C}Q + V_{OC}. \tag{2}$$

Herein, V_{OC} is the open-circuit voltage, and C is the overall capacitance of the TENG. Initially derived for the vertical contact separation mode TENG (VCSTENG), this concept has been expanded to represent other contact modes as well as sliding mode TENG architectures [Figs. 2(i)–2(v)].[29–31,33] An universal edge approximation-based equivalent capacitance method has also been proposed as an extension of this concept, in which the capacitances of the edge effect are taken into consideration to estimate the V–Q–x relationship that applies to all modes of TENGs.[43] However, the parallel plate capacitor models contain drawbacks, such as the relatively low accuracy in predicting TENG outputs, the necessity of deriving bespoke capacitor models for each TENG architecture, difficulty in explaining the polarization of dielectrics, induction of output charges on electrodes, etc.[35,38,39,44,45]

More recently, the distance-dependent electric field (DDEF) concept has been presented based on Maxwell's equations as a universal platform to describe the output trends of TENGs [Fig. 2(vi)]. As opposed to the parallel plate capacitor model, the DDEF model studies the electric fields originating from triboelectrically charged surfaces by considering their finite dimensions. For instance, according to the DDEF model, the overall electric field originating from a triboelectrically charged surface (along its perpendicular axis) E_z, with charge density σ, dimensions L, W, permittivity ε, and at a perpendicular distance of x, is presented by

$$E_z = \frac{\sigma}{\pi\varepsilon}\arctan\left[\frac{\frac{L}{W}}{2\left(\frac{x}{W}\right)\sqrt{4\left(\frac{x}{W}\right)^2+\left(\frac{L}{W}\right)^2+1}}\right] = \frac{\sigma}{\pi\varepsilon}f(x). \tag{3}$$

The DDEF equation [Eq. (3)] can be applied to triboelectrically charged surfaces as well as the electrode surfaces to derive the outputs of TENG. Assuming a TENG with m number of triboelectric surfaces where the charge density (of an i-th surface) is given by $\sigma_{T,i}$ and output charge density is σ_u [Fig. 2(ix)], the potential (Φ) of the electrodes [a (Φ_a) and b (Φ_b)] are calculated as[39]

$$\Phi_a = \frac{-\sigma_u}{\pi\varepsilon_a}\int_0^y f(x)dx + \frac{1}{\pi}\sum_{i=1}^{m}\left(\frac{\sigma_{T,i}}{\varepsilon_a}\int_{x_{a,i}}^{\infty} f(x)dx\right), \quad (4)$$

$$\Phi_b = \frac{\sigma_u}{\pi\varepsilon_b}\int_0^y f(x)dx + \frac{1}{\pi}\sum_{i=1}^{m}\left(\frac{\sigma_{T,i}}{\varepsilon_b}\int_{x_{b,i}}^{\infty} f(x)dx\right). \quad (5)$$

Therefore, the current, charge, voltage, and power outputs can be derived using Eqs. (4) and (5). The DDEF approach results in several advantages over the parallel plate model, providing a detailed understanding of the electric field propagation, TENG polarization, and output induction, along with higher accuracy in describing the TENG outputs.

Furthermore, some of the recent studies have expanded on these developments based on Maxwell's displacement current theory to develop three-dimensional theoretical models to describe the output power generation of TENGs.[46]

b. Optimizing TENG electrical outputs using mathematical modeling. The DDEF model has been used to understand the power generation behavior of the TENG, resulting in the derivation of the TENG power transfer theory and TENG impedance plots [Fig. 2(x)].[38] TENG power transfer theory consists of a combination of the DDEF model and Norton's theorem, presenting the power output of a TENG by means of current output and an impedance element. This allows for its implementation more readily into circuit simulators by means of circuit blocks. TENG impedance plots are a similar strategy that helps in visualizing the maximum power generation conditions. Both these techniques, along with the DDEF model simulations, have been used to examine the outputs of a TENG and to optimize its power generation conditions. Accordingly, the primary factors affecting the power generation of a TENG have been defined, which are divided into the material, structural, and kinetic parameter sub-categories.

Considering material parameters, triboelectric charge density and dielectric constant of the TENG layers hold critical importance.[38] Higher charge densities help in increasing the power outputs, which can be achieved via appropriate material selection, surface structuring, and physical and chemical surface modifications.[47–49] Theoretically, having lower dielectric constants have been shown to enhance to electrostatic induction,[38] however, some experimental studies have shown that the use of high dielectric constant nanomaterials results in an overall increase in the power output. Structural parameters, such as the area of the TENG layers and their thickness, also affect the TENG outputs. Larger surface areas of triboelectric layers result in higher power outputs as well as the reduction of the internal impedance of the device, both of which are desirable for TENGs. On the other hand, smaller thicknesses of dielectric triboelectric surfaces are desirable to increase the electrostatic induction, hence the power output. However, it has been shown that a minimum level of thickness of the (dielectric) triboelectric layers (typically few micrometers) is required to ensure that the triboelectric charges can accumulate stably. With regard to the motion parameters, higher rates of movement of TENG layers (high velocity or high frequency) increase the power output while reducing the TENG impedance. The behavior of a TENG at increasing amplitudes (maximum separation) of movement shows a relatively similar trend up to a threshold value. Furthermore, conformal contact between TENG surfaces has been shown to provide higher power outputs and reduced impedances, in comparison to the non-contact mode TENG operations. Therefore, the design of a TENG for a given application needs to be conducted considering an appropriate balance of the above parameters, in which the theoretical models, TENG power transfer theory as well as TENG impedance plots will act as design tools.

In addition to these theoretical models, a standard method has been proposed to quantitatively evaluate the performance of TENGs, which consists of a structural figure-of-merit (FOM) related to the design of the TENG and a material figure-of-merit (FOM_m) as the square of the surface charge density.[50] Within the built-up V-Q, the TENG operation cycle with maximized energy output is initially proposed. Based on this maximum energy output per cycle and considering both the maximized energy conversion efficiency and the maximized average output power, the performance FOM was derived to evaluate each TENG design, composed by a FOM and a FOM_m. However, the breakdown condition is not considered in this process, which can seriously affect the maximum energy output. Therefore, a standardized method that considers the breakdown effect is further proposed for output capability assessment of nanogenerators, which is crucial for the standardized evaluation and application of nanogenerator technologies.[51] In addition, these structural FOM of TENGs are extended to quantitatively evaluating and comparing output performance under different load resistances as well as in charging systems (powering capacitors).[52,53] Therefore, these FOM standards will set the foundation for all further applications and industrialization of the TENGs, including operation in a hybrid energy storage system.

c. Optimizing the electrical response of TENGs based on the mechanical stress simulation models. The surface modification of the frictional materials by creating nano- or micro-architectures is one of the major routes to improve the performance of TENGs.[3,27,36,54–59] This is because such architectures can be expected to increase the surface roughness and result in an enhanced contact area as well as a high output performance of TENG.[36] However, the exact mechanisms by which they influence the performance are not yet fully clear. For example, even though some of the surface morphologies exhibit a high surface roughness, the resultant contact area can be rather reduced while they contact together. As a result, finite element method (FEM) simulations have been utilized to estimate the mechanical stress at the contacting interface between the nano-architecture polymer [such as polydimethylsiloxane (PDMS)] and metallic layers [Fig. 2(vii)].[36] In this study, the mechanical stress distributed across the surface of nano-pillars is considered as a crucial parameter, since the number of trapping electrons and electron transportation at the higher stress sites can be expected to maximize owing to the higher deformation of internal structures. Thus, by estimating the contact area and mechanical stress together (i.e., the product of contact area and stress is defined as contact force), an optimal structural dimension such as diameter and period of

nano-pillars is determined to attain a high electrical output response of TENGs. These studies are elucidating that an effective contact force distributed across the surface of nanostructures can largely contribute to the effective charge density as well as the electrical output performance of TENGs. Along with the dimensions, the geometric shape of the nanostructures may also expect to influence the durability and performance of TENGs. Thus, the effect of geometric shapes on the output characteristics of TENG is also investigated by considering again the contact force as a reference [Fig. 2(viii)].[37] The similar type of mechanical stress simulations used and realized within the nano-architectures that undergo greater deformation (like dome-shape) can result in a larger contact surface as well as the higher electric output owing to the larger contact force or mechanical stress distributions across their surface. Such nano-architectures are force sensitive, and less durable or not reliable against long-term contact/separation cyclic operations. In contrast, nanostructures with moderate deformability (like pillar-shape) can significantly improve the performance and are durable and longer-lasting under repetitive cyclic operations. Therefore, such mechanical simulation models can be used as a roadmap to decide on the optimistic shapes and dimensions of nano-architectures on polymer for designing the force sensitive, durable, and high-performance TENGs. Along with these surface features, the mechanical forces applied on TENG devices also play a key role to improve its surface charge density and output performance. Thus, a comprehensive theoretical model has been proposed to understand the energy conversion in various TENG modes, in which both the mechanical energy inputs indicated by the *F-x* (force–displacement) plot and electrical energy output as reflected by the *V-Q* (voltage–charge) plot are simulated and analyzed.[60] Such a model can also play an important role for optimizing the energy conversion efficiency in TENGs by considering both the mechanical and electrical energies, simultaneously.

d. Theoretical models to explain the charge transfer mechanism in contact–electrification. All the above mathematical and mechanical simulation models postulate that the electrical output of TENGs is mainly dictated by the triboelectric surface charge density and it is enhanced by altering the surface features of triboelectric materials. This is despite the fundamental mechanism of contact–electrification is still not fully understood.[61] Therefore, along with optimizing the parameters of TENGs, understanding the charge transfer mechanism in contact electrification is crucial for the TENG research community. Previous literature suggests that either the electron or ion transfer is involved in the contact electrification processes.[61–65] However, Xu *et al.* recently examined this age-old problem by the study of surface charge density evolution across the surface of triboelectric material with time at various high temperatures, with data consistent with the electron thermionic emission model.[40] From the results, they have reported that the contact electrification is dominated by the electron transfer in solid–solid materials, rather than the ion transfer.[40] They have also proposed an electron cloud/potential-well model [Fig. 2(xi)] based on fundamental electron cloud interactions to explain all types of contact–electrification phenomena for general materials in the contact–separation mode TENGs. As is well known, atoms in the materials consist of electrons within the inner atomic or molecular orbitals that are tightly bound, whereas electrons in the outermost orbits are mostly loosely bound. Therefore, here an atom was considered as a potential well in which the outermost loosely bound electrons form an electron cloud around the atom. As shown in Fig. 2(xi), the electron clouds of two atoms belonging to two different materials are separated by an interatomic distance before an external compression force is applied, while the electrons cannot transfer due to the local trapping effect in their potential wells. Once the force is applied, the electron clouds overlap owing to the physical contact between the corresponding materials, and their initial single potential wells become an asymmetric double-well potential. Consequently, the electrons can transfer from the atom of one material to the atom of another, resulting in contact–electrification. The key role of the external compression force is to bring the two materials into contact as well as to shorten the distance between the atoms that can cause a strong overlap of their electron clouds in the repulsive region. Likewise, the charges/electrons can be transferred if one material rubs against the other. After the separation of these materials, most of the transferred electrons can remain as static charges on the surface of materials owing to the energy barrier present in the corresponding material if the temperature is not too high. As a result, one of the materials gets charged positively and the other charged negatively. With the elevated temperature, the electrons transferred into negatively charged material atoms are more likely to hop out of the potential well, and they either return into the positively charged atoms or emit thermionically into the air. This study is one of the breakthroughs to understand the charge transfer mechanism in TENGs, which can be generally applied to explain all types of contact electrification processes in conventional materials, such as the combination of metal–semiconductor, metal–polymer, and polymer–polymer. Furthermore, a typical aluminum (Al)–polytetrafluoroethylene (PTFE) material pair of TENG has been tested by Wu *et al.* [Fig. 2(xii)] to analyze the mechanism of metal–polymer contact electrification, and the outcomes provide direct evidence for the above-stated cloud/potential-well model.[41] In 2020, a modified electron cloud-potential well model has been expanded for explaining the contact–electrification and charge transfer and release between two materials in the sliding-mode TENG.[66] Lin *et al.* further examined the effect of photon excitation on contact electrification [Fig. 2(xiii)].[42] By illuminating the surface of an insulator (such as SiO_2 or PVC) with UV light at a specific wavelength and intensities, the surface electrostatic charges can be released under photon excitation. To verify the photoelectron emission of electrons in contact electrification, the surface of an insulator (such as SiO_2 or PVC) illuminated with the light and effects of its wavelength and intensity on the irradiation-induced triboelectric charge decay were studied. These studies show that there exists a threshold photon energy above which surface electrostatic charges will be released. Therefore, both the electron thermionic emission and photon excitation studies indicate that the electron transfer plays a dominant role in contact electrification, particularly in solid–solid cases.

4. Concluding remarks

A number of theoretical approaches have been presented in the literature to explain the working principles and the output trends of different TENG architectures, which can be categorized under the parallel-plate capacitor approach and the DDEF approach. These models, along with the accompanying tools, such as the TENG

impedance plots and TENG power transfer theory, have revealed a number of new methods on the optimization of the TENG power outputs, targeting enhanced power generation, efficiency, and effectiveness as energy harvesters and self-powered sensors. Moreover, recently presented theoretical models have shed new light toward the origin of the triboelectric effect, as well as the surface modification related performance enhancement, which will potentially contribute toward designing better TENGs. Such theories and advancements can be further customized to suit a range of different applications, for example, textiles, large-scale energy harvesting, such as ocean waves, and IoT applications.[67–70] Therefore, the work related to TENG theoretical modeling continues to develop a comprehensive understanding on the origin of the triboelectric effect, static charge transfer between surfaces, novel material developments, and output induction of TENGs and their fine tuning on macro-, micro-. and nanoscales, leading toward the design and fabrication of practical and sustainable TENG applications.

With regard to TENGs, their typical large internal impedance has been a major issue (which normally is in Mega-Ohm to Giga-Ohm range at low operating frequencies) in using them for practical energy harvesting applications, with typical electronic devices or energy storage units containing relatively lower impedance (several Ohms).[38] This makes the transfer of power from the TENG to such practical loads extremely low efficiency due to the load mismatch. However, theoretical works on impedance characterization, impedance engineering, and device engineering have the potential to provide a viable solution to this issue as evident in recent studies,[38,71–73] which will significantly impact the overall energy conversion efficiency of TENGs. Furthermore, this can help to manage the high voltage and low current outputs, which are characteristic to TENG outputs, that need to co-exist with the high impedance issue. Moreover, designing efficient energy storage systems backed by the theoretical advances, which match to the TENG impedance characteristics, would also help to manage drawbacks caused by the high voltage generation within the TENGs.

5. Acknowledgments

The authors would like to acknowledge the support from the EPSRC Research Project (Grant No. EP/S02106X/1) for funding this work. This work was also supported by the Royal Academy of Engineering under the Research Fellowship Scheme.

III. METHODS

A. Sustainable textiles for utilization of high entropy energy by triboelectric nanogenerators

Jialu Li, Zhaoling Li (*zli@dhu.edu.cn), Zhong Lin Wang (*zhong.wang@mse.gatech.edu)

1. Status

Nowadays, the rapid development of human civilization requires the support of a large amount of energy supply. However, the world's energy structure is still dominated by low-entropy energy that is high-concentration and high-quality, such as coal, oil, and natural gas.[74] In comparison with low-entropy energy, energy, widely distributed in the environment, that is low-quality and irregular is called high-entropy energy, such as wind, water wave, mechanical vibration, and human activities.[10] After combustion, transportation, and application, low-entropy energy eventually becomes high entropy energy dissipated in nature. According to the first law of thermodynamics, the massive use of fossil energy will inevitably increase the disordered and low-quality high entropy energy distributed in the environment, aggravate the greenhouse effect, and cause global climate warming, which is contrary to the strategy of low carbon and sustainable development. Meanwhile, with the advent of the Internet of Things, the demand for social development is distributed, and our energy supply needs to be distributed. Currently, China has changed from "concentrated energy" to "distributed energy" in the global energy transformation. Therefore, how to collect high entropy energy with instability, low quality, low frequency, and wide distribution into effective output electric energy is a hot issue that urgently needs to be solved.[75] Triboelectric nanogenerator (TENG) is proposed for effective collection and utilization of high entropy energy. In 2012, we fabricated the first TENG that is an energy acquisition method based on the coupling effects of contact electrification and electrostatic induction.[2] This emerging technology is capable of converting extensively existed environmental mechanical energy into continuous electricity.[76]

At present, most TENGs are fabricated based on thin polymer films or elastic rubbers. The advantages of these triboelectric materials include lightweight, prominent mechanical properties, large power output, and high stability. Simultaneously, breathability is very crucial factor for the practical application of TENGs in the field of intelligent wearables. Meanwhile, hydrogels and aerogels are also common constructing materials. Unfavorably, most hydrogels are prepared with organic solvents, which are not environmentally friendly. Besides, hydrogels are prone to collapse when subjected to repeated mechanical stretching. Aerogels are porous materials with space network structure exhibiting low density and prominent gas permeability.

Alternatively, sustainable textiles could be an optimal option to construct breathable and high performance TENGs. To start with, textiles have favorable softness and flexibility to conformably comply with human's skin with ease. Moreover, they possess high specific surface area and diversified micropore structure, endowing textile-based TENGs with excellent portability, brilliant breathability, and high power output. Additionally, the low-cost and simple fabrication process is indispensable for sustainable textiles, which is more conducive to the realization of large-scale production and industrialization of textile-based TENGs. For instance, Huang *et al.*[77] developed a washable textile TEGN by adopting commercially available knitting method, and it delivered an open-circuit voltage of up to 800 V and a maximum power density of 203 mW/m^2. This washable and comfortable energy textile can drive warning indicator and smart watch or act as a motion sensor to monitor human movement signals. As portable and reliable power supply sources, textile-based TENGs have opened up promising possibilities for broad application prospects,[78] ranging from mechanical energy harvesting, wearable electronics driving, to self-powered environmental sensing and health monitoring (Figs. 3 and 4).[79]

2. Current and future challenges

Textile-based TENGs with compelling features have emerged as an effective energy conversion device and renovated the

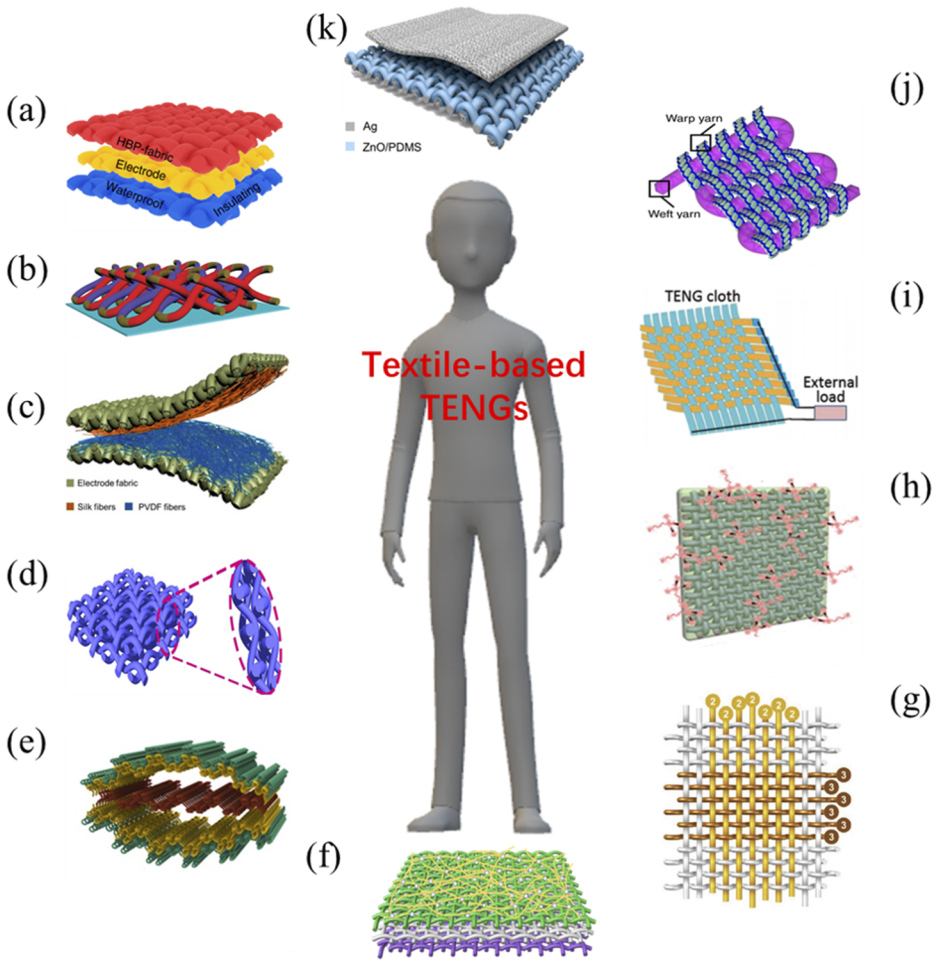

FIG. 3. Schematic illustrations and application demonstrations of wearable textile-based TENGs. (a) Reproduced with permission from Xiong *et al.*, Nat. Commun. **9**, 4280 (2018). Copyright 2018 The Authors, published by Springer Nature. (b) Reproduced with permission from Sun *et al.*, Nat. Commun. **11**, 572 (2020).[80] Copyright 2020 The Authors, published by Springer Nature. (c) Reproduced with permission from Guo *et al.*, Nano Energy **48**, 152 (2018).[81] Copyright 2018 Elsevier. (d) Reproduced with permission form Zhou *et al.*, Sci. Rep. **7**, 12949 (2017).[82] Copyright 2017 The Authors, published by Springer Nature. (e) Reproduced with permission from Kwak *et al.*, ACS Nano **11**, 10733 (2017).[83] Copyright 2017 American Chemical Society. (f) Reproduced with permission from Qiu *et al.*, Nano Energy **58**, 750 (2019). Copyright 2019 Elsevier. (g) Reproduced with permission from Zhao *et al.*, Adv. Mater. **28**, 10267 (2016).[84] Copyright 2016 Wiley-VCH. (h) Reproduced with permission from Guo *et al.*, ACS Appl. Mater. Interfaces **8**, 4676 (2016).[85] Copyright 2016 American Chemical Society. (i) Reproduced with permission from Pu *et al.*, Adv. Mater. **27**, 2472 (2015).[86] Copyright 2015 Wiley-VCH. (j) Reproduced with permission from Gong *et al.*, Nat. Commun. **10**, 868 (2019).[87] Copyright 2019 The Authors, published by Springer Nature. (k) Reproduced with permission from Seung *et al.*, ACS Nano **9**, 3501 (2015).[88] Copyright 2015 American Chemical Society.

mechanical energy harvesting technology. Qiu *et al.*[98] designed a single-electrode TENG textile by one-step surface coating method via simultaneously electrospinning and electrospray processes. This TENG textile possessed satisfactorily tailorable and washable properties, but the power density and durability were still far away from enough. Comparatively, Cheng *et al.*[99] designed a flame-retardant textile-based TENG with high electrical output and mechanical stability. However, it cannot be washable owing to the adoption of layer-by-layer self-assembly technique for self-extinguishing ability. Even though tremendous progress has been achieved in textile-based TENGs, there are still many problems to be well addressed.

First, the electrical output performance is supposed to be further enhanced for practical applications. Generally, the electrical output of TENG largely depends on the effective contact area of those two friction materials. Textiles have intrinsically porous structure to obtain excellent gas permeability. The more holes textiles possess, the less triboelectric charge density they can produce, causing an inefficient energy conversion. Besides, substantial pore spaces will induce capillary effect, especially for hydrophilic fabrics, which absorb massive moisture from the air and results in a low power generation.[100]

Second, multiple working models are needed to be integrated to efficiently harvest versatile and various human motions. TENG specifically includes contact–separation mode, sliding mode, single-electrode model, and freestanding layer mode. Since body motions concurrently cause mechanical friction and deformation in many forms, including contact, extrusion, and sliding, textile-based TENGs using single working model cannot take full advantage of these biomechanical motions to achieve an optimized energy harvesting efficiency.[101–105] The structural design with complex geometric configuration is required to maximize the power output.

Third, washability is one of the key prerequisites for sustainable textiles to construct wearable TENGs. After washing in water for many times, actually, most textile-based TENGs would be prone to creep deformation, either volume expansion or volume reduction, thereby having poor dimensional stability. Worse still, moisture and liquid contaminants are common in daily scenarios, which will speed up the electron dissipation and largely impair the power

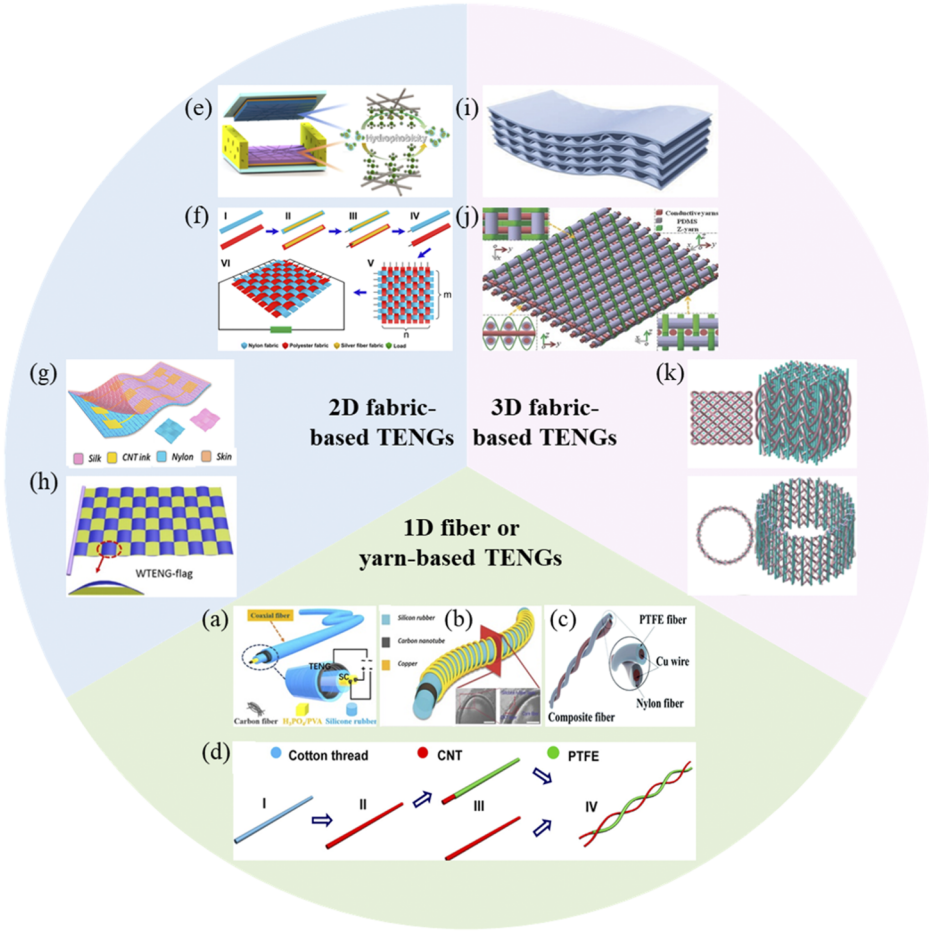

FIG. 4. Categories of textile-based TENGs according to the internal geometries and structural dimensions: 1D fiber or yarn-based TENGs, 2D fabrics-based TENGs, and 3D fabrics-based TENGs. (a) Reproduced with permission from Yang *et al.*, ACS Appl. Mater. Interfaces **10**, 42356 (2018).[89] Copyright 2018 American Chemical Society. (b) Reproduced with permission form He *et al.*, Adv. Funct. Mater. **27**, 1604378 (2017).[90] Copyright 2017 Wiley-VCH. (c) Reproduced with permission from Liu *et al.*, Nanoscale Adv. **2**, 4482 (2020).[91] Copyright 2020 Royal Society of Chemistry. (d) Reproduced with permission from Zhong *et al.*, ACS Nano **8**, 6273 (2014).[92] Copyright 2014 American Chemical Society. (e) Reproduced with permission from Li *et al.*, Nano Energy **36**, 341 (2017).[93] Copyright 2017 Elsevier. (f) Reproduced with permission from Zhou *et al.*, ACS Appl. Mater. Interfaces **6**, 14695 (2014).[94] Copyright 2014 American Chemical Society. (g) Reproduced with permission from Cao *et al.*, ACS Nano **12**, 5190 (2018). Copyright 2018 American Chemical Society. (h) Reproduced with permission from Zhao *et al.*, ACS Nano **10**, 1780 (2016).[95] Copyright 2016 American Chemical Society. (i) Reproduced with permission from Li *et al.*, Adv. Energy Mater. **7**, 1602832 (2017).[96] Copyright 2017 Wiley-VCH. (j) Reproduced with permission from Dong *et al.*, Adv. Mater. **29**, 1702648 (2017).[97] Copyright 2018 Wiley-VCH. (k) Reproduced with permission from Dong *et al.*, Nat. Commun. **11**, 2868 (2020). Copyright 2020 The Authors, published by Springer Nature.

output of textile-based TENGs.[106] It is very necessary to improve the dimensional stability of textile materials while maintaining excellent power output in the presence of the water scrubbing.

Finally, in practice, a single fiber may have perfect electrical conductivity and mechanical flexibility, but after spinning and weaving, the resistance of fiber assembly or fabric increases sharply and the flexibility decreases dramatically. Conductance-stable triboelectric materials and advanced textile processing techniques are of significance to ensure the uniformity and stability of mass produced textile-based TENGs, while not sacrificing the electrical performance and flexible texture in the course of real applications.[107]

3. Advances in science and technology to meet challenges

There are many approaches in science and technology available to address current and future challenges in textile-based TENGs. First, for the insufficient power output, one simple and straightforward way to further improve the power output is rational selection of triboelectric materials. Although all textiles exhibit triboelectricity, finding the right paired positive and negative materials can generate maximum output. Other effective way is surface functionalization on textiles. By using nanoparticles and possibly nanocomposites, nanomaterials demonstrating stronger capabilities to gain or lose

electrons can be successfully introduced. Besides, surface roughening and three-dimensional (3D) textile TENGs configuration can considerably increase the effective contact area and separation distance during operations, respectively,[108,109] and, in consequence, generate a distinctly high power output.

Second, for the sake of solving the restriction of single working model, at present, TENG has developed from the single working model to the multiple working models, which can be divided into the spherical 3D TENG, rotating-disk-based direct-current TENG, cylindrical spiral TENG, etc. Using multiple working models is more conducive to the effective collection of various mechanical energies in the ambient environment, which will perform a high charge density output even triggered by tiny deformations. In addition, to scavenge waste energy from all kinds of human motions, piezoelectric nanogenerators (PENGs) can be combined with TENGs and exhibit their own advantages and characteristics.[103] The hybrid energy harvesters are quite compatible and can complement each other.

Third, waterproofing modification treatment enables the textile-based TENGs with outstanding washable property. For instance, hydrophobic or oleophobic coating materials, such as hydrophobic nanoparticles, can be adopted to endow liquid repellence.[110] Also, it is applicable to directly use commercial waterproof fabric (i.e., Gore-Tex) as sacrificial substrate to accommodate the triboelectric materials.[106] Since the TENG is based on the surface charging effect, its performance is greatly affected by the environmental humidity. Packaging technology is required to protect the device from vapor contamination or liquid permeation, but without reducing too much of the flexibility. Preserving its hydrophobicity and flexibility is important for improving the washability and energy conversion efficiency.

Finally, efficient modern textile technology lays the foundation of realizing commercially mass production of textile-based TENGs with favorable flexibility. Improving and perfecting the spinning and weaving techniques are beneficial to fabricate the prominent textile-based TENGs, especially in producing very soft yarns and fabrics. For example, in terms of textile TENGs with coaxial yarn intersection, a roller-guided assembly line has demonstrated impressive efficiency in scalable manufacture. Besides, liquid metals are proved to be conductance-stable materials in comparison with conventional metals, and liquid metal can be widely used in fabricating high performance textile-based TENGs.

4. Concluding remarks

Mechanical energy exhibits the characteristics of abundant source, wide distribution, diverse forms, and easy conversion, which is a preferred choice for effective environmental energy collection. With continuous advancement and development in recent years, textile-based TENGs have attracted worldwide attention and achieved remarkable research results. Textile-based TENGs open up a new possibility for mechanical energy harvesting and is expected to relieve the shortage of world energy problem and promote the sustainable development. The TENG not only represents an emerging type of energy conversion technology but also demonstrates versatile functions in self-powered sensing. Even though vast progress has ever been made to realize the widespread application of textile-based TENGs, it is still essential to further optimize the structure design and material selection, enhance the power output, develop multiple working models, improve the washable property, boost the flexibility and stability, and expand the industrial production. In the future, textile-based TENGs have great potential in the extensive fields of high-efficiency energy harvesters, high sensitivity sensors, human–machine interaction, Internet of Things, environmental monitoring, and intelligent wearable.

5. Acknowledgments

This work was financially supported by the National Natural Science Foundation of China (Grant Nos. 52073051, 51873030, and 51703022), the National Key R&D Program of China (Grant No. 2018YFC2000900), the Natural Science Foundation of Shanghai (Grant No. 18ZR1402100), and Shanghai Committee of Science and Technology (Grant No. 19QA1400100).

B. Design and optimization of porous piezo-composites for energy harvesting application

Yan Zhang, Chris Bowen (*c.r.bowen@bath.ac.uk)

1. Abstract

Piezoelectric energy harvesting has attracted substantial interest from both academia and industry due to its potential to achieve long-lifespan sensing and self-powered autonomous operation of low-power electronics. Porous piezo-composites that combine a low dielectric constant with a high piezoelectric coefficient are promising materials with respect to an enhancement of energy harvesting capability. Here, we review recent achievements in the field of design and optimization of the material and provide insights and an outlook for the current and future challenges of the materials and their applications.

2. State-of-the-art

Energy harvesting, or energy scavenging, is a process that harvests small amounts of energy present in the ambient environment that would otherwise be wasted, such as heat, light, sound, vibration, or movement. This ambient energy can be converted into electricity for autonomous and self-powered low-power electronic devices and is a promising technology of interest to both academia and industrial applications to reduce or remove battery replacement and provide power in inaccessible or remote conditions. Among the range of harvesting approaches, piezoelectric energy harvesting converts oscillatory mechanical energy into electrical energy and is attracting due to its high energy conversion efficiency, ease of implementation, and potential for miniaturization.[111]

If we consider a piezoelectric material in an energy harvester with the surface area of A, thickness of h, that is subjected to a mechanical force of F, the energy E generated can be generally estimated by $E = \frac{1}{2}CV^2$, where C and V are the material capacitance and the voltage between the opposite electrode surfaces of the piezoelectric element, respectively. Based on this, the energy E from a mechanical load F can be calculated as $E = \frac{1}{2}\frac{d_{ij}^2}{\varepsilon_0 \varepsilon_{33}^T}\frac{F^2 h}{A}$, where ε_{33}^T is the relative permittivity (or dielectric constant), ε_0 is the permittivity of free space, and d_{ij} is the piezoelectric charge coefficient. *Figures-of-merit* that include the physical properties of the material

have been developed from this simple analysis to assess the performance of energy harvesting materials for practical applications. For the selection and design of materials for piezoelectric energy harvesting, the harvesting figure-of-merit FoM_{ij}, derived from the energy described above and has been widely used,[112–114] where $FoM_{ij} = \frac{d_{ij}^2}{\varepsilon_0 \varepsilon_{33}^T}$. The FoM_{ij} can be viewed as a direct indicator of the amount of piezoelectric energy harvested for a specific force, area, and thickness of material.

In order to achieve the desired optimized functional property with a high value of FoM_{ij}, significant effort has been made to improve the FoM_{ij}, such as chemical doping,[115] growth of single crystal materials,[116] and the combination of both;[117] all of the above-mentioned methods mainly focus on the enhancement of the piezoelectric charge coefficient d_{ij}, which is a measure of the charge generated from an applied load. In many cases, the increase in the piezoelectric charge coefficient also leads to an increase in the dielectric constant, therefore limiting the degree of improvement in the $FoM_{ij} = \frac{d_{ij}^2}{\varepsilon_0 \varepsilon_{33}^T}$. Moreover, chemical doping is highly sensitive to the subtle changes in the stoichiometry of the material and needs complex processing steps due to the requirement for the close control of the composition for each element in the composite. In addition, single crystal materials normally exhibit poor mechanical properties and are often high cost and have a low Curie temperature, which can limit their operating temperature. Another promising approach to increase the FoM_{ij} is the careful introduction of porosity into the piezoelectric, which can lead to a large decrease in the dielectric constant while being able to simultaneously maintain a relatively high piezoelectric charge coefficient.[113,118] Therefore, the formation of piezoelectric composites that consist of a piezo-active ceramic and a passive polymer, or air phase, can lead to high performance materials for energy harvesting applications.

There are five main preparation techniques to create energy harvesting materials based on porous piezoelectrics:[119] the burnt-out polymer spheres method (BURPS), the replica template method, gel casting, freeze casting, and additive manufacturing. The common approach to realize an effective device is to make it as a piezo-composite with a 0-3-0, 3-0, 3-1, 3-2, 3-3, and 2-2 connectivity by introducing a polymer into the pore space. The polymer can either act as a porous structure with a piezoelectric active phase that dispersed within the polymer using ferroelectric particles, with pores as an air phase to create a 0-3-0 structure,[120] or as a polymer that acts as a second phase as it infills the pore space of the porous piezoelectric ceramic to form a 3-0,[121] 3-1,[122] 3-2,[123] 3-3,[124] or 2-2[118] structure.

Based on the distribution of the pores in the composite, there are two types of pore structures, which can be regarded as *isotropic* and *anisotropic* architectures. In an isotropic porous piezoelectric composite, the pores are randomly distributed with a spherical-like or net-like morphology achieved via traditional processing techniques, such as gel casting,[125] BURPS[126,127] ("burned-out plastic spheres"), the replica method by coating the ceramic suspension on the wax/coral,[128] or using a polymeric sponge[129] that is burnt out during sintering, and additive manufacturing that allows for the fabrication of complex structures without the need for a mold.[130] Gel casting has attracted attention due to its simplicity and low cost, but many of the organic solvents used in this process are toxic and carcinogenic. The BURPS process has the advantage of being an easy and low-cost fabrication method, while its disadvantages include the relatively poor dispersion of the additive in the ceramic powders and the potential of gases to form cracks/defects during the volatilization process. Additive manufacturing is gaining increasing attention since it can produce a wide range of shapes with geometrical complexity; however, the pores generated can be relatively large in size and the integrity between printed layers can limit mechanical or dielectric properties.

By tailoring the amount of porosity and pore morphology, the piezoelectric performance and dielectric constant can be controlled to achieve a combination of high piezoelectric activity and low dielectric constant. A near three-fold increase of the FoM_{ij} compared with the dense material was observed in an isotropic porous $BaTiO_3$ composite with the porosity level of 60 vol. %.[127] In order to increase the piezoelectric coefficient in a porous composite with reduced dielectric constant, a sandwich structure with "dense layer–isotropic pores–dense layer" arrangement has also been proposed.[131,132] An optimum volume fraction of the porous layer was found to be 20 vol. %, with a relative thickness of the porous layer of 0.52 and the porosity within of ~60 vol. %, which were shown to exhibit the highest piezoelectric energy harvesting capability.[132] The typical morphologies of the isotropic pores and sandwich structure are shown in Figs. 5(a) and 5(b).

Due to the inherently low mechanical properties, such as compressive strength, of the isotropic porous composite, new materials with aligned pore channels and exhibiting an anisotropic structure have been considered for improving both the mechanical properties and piezoelectric coefficient. An efficient route to achieve a highly anisotropic morphology is *freeze casting*, where ice crystals in a ceramic suspension [see Fig. 5(c-i)] are grown unidirectionally along a temperature gradient [see Fig. 5(c-ii)]. These ice crystals act as a replica of the aligned pores [see Fig. 5(c-iii)] in the piezoelectric composite, thereby forming an aligned pore morphology after ice-sublimation and sintering, as shown in Fig. 5(c-iv). The benefit of this structure is the improved connectivity of the piezo-active ceramic and the reduced electric field concentration in the pore space under the application of an external electric field during the poling process.[113,121,132] As an example, an energy harvester fabricated from a highly aligned porous $BaTiO_3$ ceramic exhibited a 2.4-fold increase in capacitor charging during piezo-energy harvesting compared to the dense material under the same conditions.[113] A comparison of the harvesting Figure of Merit (FoM_{ij}) of porous ferroelectric materials is summarized in Table I.

In addition to the formation of porous ceramics, there has also been recent interest in forming porous polymers. A porous polymer with elongated unidirectionally pore channels can form a dipole-like structure by applying an external electric field that charges the pores to form a *ferroelectret* material. Such piezoelectrically active polymer composites are also promising for piezoelectric energy harvesting applications due to their combination of low permittivity and high piezoelectric coefficient.[147]

3. Current challenges and future prospects

Over recent decades, flexible device technologies have developed at an unprecedented rate, resulting in the improvement of wearable, stretchable, bendable, foldable, and lightweight electronics. Polymer based piezoelectric composites have been widely

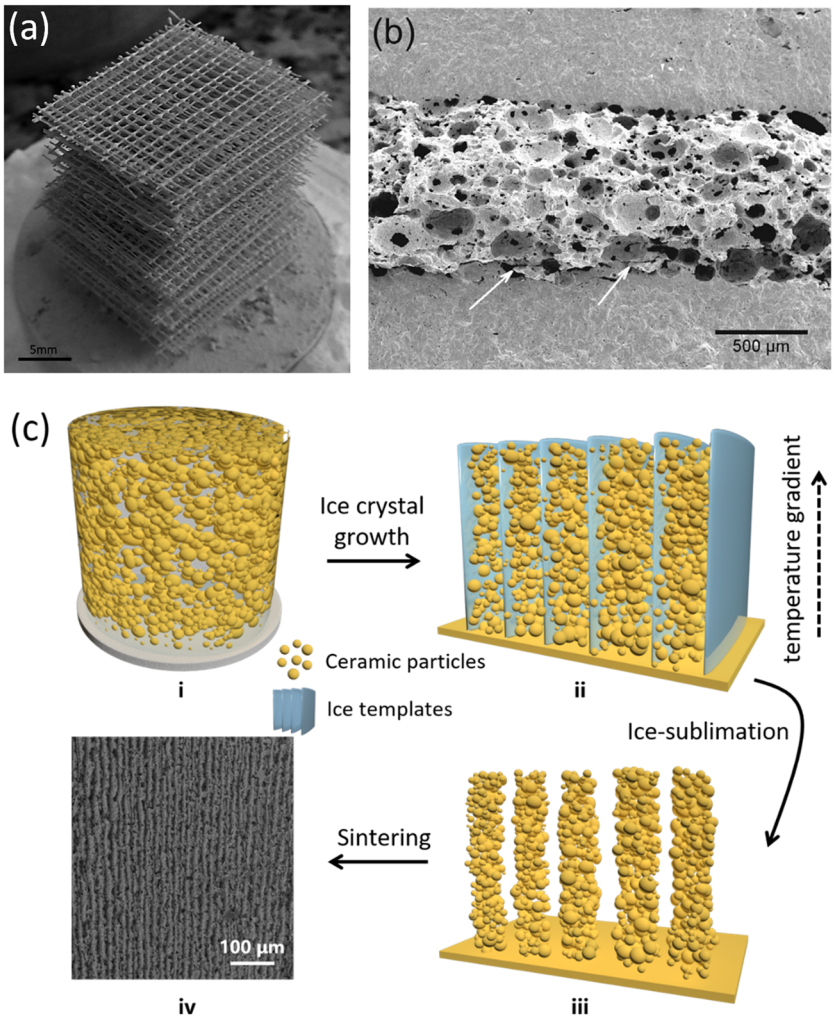

FIG. 5. (a) PZT-coated polymeric net by applying several layers of ceramic suspension.[129] (b) SEM of fracture surface of cross section of $BaTiO_3$ with porous sandwich layer (porosity ~60 vol. %).[132] (c) Schematic of freeze casting technique and the corresponding pore morphology with aligned pore structure: i. homogeneous ceramic suspension, ii. the frozen ice crystals grow unidirectionally along the temperature gradient, iii. aligned porous ceramic after ice sublimation, and iv. aligned pore morphology after sintering.

employed due to their low permittivity, low density, and high flexibility. However, the low piezoelectric coefficient of piezoelectric polymers (for example, PVDF and its copolymers have a d_{33} ~ 20 pC/N, compared with that of PZT ~ 500–700 pC/N), together with the low working/Curie temperature, T_c (PVDF and its copolymers have T_c ~ 100 °C, compared to PZT with a T_c > 300 °C) are the main factors that constrain the development of such materials in energy harvesting applications. For porous piezoelectric ceramics, while the introduction of porosity can provide some mechanical flexibility, effort is needed on the micro-structural design and polymer infiltration to improve the flexibility while retaining a high piezoelectric activity.[148] Impregnating the pore space of a porous ceramic with a polymer of high dielectric constant and lower stiffness would also be beneficial to piezoelectric properties since the electric field concentration on the passive polymer can be reduced,[121] and the applied mechanical load from the environment exerted on the active phase would not be shared by the passive polymer phase.

For practical applications on harvesting large-scale of energy sources, such as the vibrations of tall buildings, bridges, vehicle systems, railroads, ocean waves, and human motions, industrial scale up of processing methods is needed. Cracks/defects [such as those indicated in Fig. 5(b)], compositional homogeneity, and property stability are the main concern for the realization of the readily controlled materials and devices. Another challenge is that large-scale vibrations often vary with time and frequency, which makes efficient and reliable energy conversion difficult, in such a case, more efforts for the development of broader-band or off-resonance energy harvesting materials and systems are of interest.

There is also scope for the development of new materials, new architectures, and more efficient processing techniques for the creation of new ferroelectret candidates with moderate porosity, optimum ratio between the length and the width of pore channels, and enhanced piezoelectric capability.[149] Commercially available ferroelectrets are currently made of polypropylene (PP, Emfit, Finland) with a d_{33} of 25–200 pC/N, where the pore space is formed

TABLE I. Comparison of figure of merit (*FoM*) for energy harvesting using porous ferroelectric materials.

Method	Material/composite	Porosity vol. (%)	d_{33} (pC/N)	Relative permittivity, ε_r	*FoM* (pC/N)^2	References
BURPS	BCZT and air	10–25	285–424	1026–2158	8.9–9.4	133
	PZT-PCN and air	24–45.6	140–300	110–290	20.1–31.7	134
	PZT and air	35–54.5	161–312	241–1608	12.1–16.4	135
	PZT and air	5–45	208–350	300–1600	12.4–16.3	136
	BS-0.64PT	17.1	~485	400–1500	22.3	137
	PMN-PZT and air	33	510	~1580	18.6	138
	NKN and air	40	~100	...	...	139
Gel-casting	BCZT and air	20	381	~3350	4.9	131
	BT and air	30	~124	~1100	1.6	132
	PZT and air	27.8–72.4	260–560	400–3500	10.1–19.1	125
	PZT and air	31.3–58.6	424–635	446–3418	13.3–45.5	140
	PZT and air	28.1–68.7	608–690	1400–3500	15.4–29.8	141
Freeze-casting	PZT-PZN and air	~90	450	100–120	207.9	142
	PZT-PZN and air	50–82	380	284–853	29.9–57.4	143
	PZT and air	20–60	~350	~600	23.1	118
	NKNS	~60.5	~130	~1319	1.45	144
	PLZT	...	481	...	...	145
Direct ink writing	PZT and epoxy resin	...	~360	...	...	123
	KNN	...	280	...	...	146

by foaming process and stretching particulate filled polymers. Sandwich layer structures with a porous ferroelectret inner layer clamped between two dense polymer layers have also been realized by hot pressing, leading to an improved charge density. Hot pressing, therefore, provides an attractive route to create a variety of composite structures.[150,151]

The enhancement of the piezoelectric performance has been widely reported by forming single crystal with appropriate dopants; therefore, the formation of porous single crystal-like materials would truly combine a high piezoelectric activity with low dielectric constant for exceptional harvesting figures-of-merit. Li *et al.* presented Sm-doped $Pb(Mg_{1/3}Nb_{2/3})O_3$–$PbTiO_3$ (Sm-PMN-PT) single crystals that exhibit a d_{33} of 3400–4100 pC/N, compared with the traditional PMN-PT, PZN-PT single crystals that have a d_{33} of 1200–2500 pC/N.[117,152] It would be of interest to fabricate porous pseudo-single crystals to reduce the dielectric constant together with remaining this high piezo-response. This could be achieved by using freeze casting to align small single crystal templates [see Fig. 6(a)] and growing the templates during sintering to form complex porous architectures whose microstructure is single-crystal like,[153] as shown

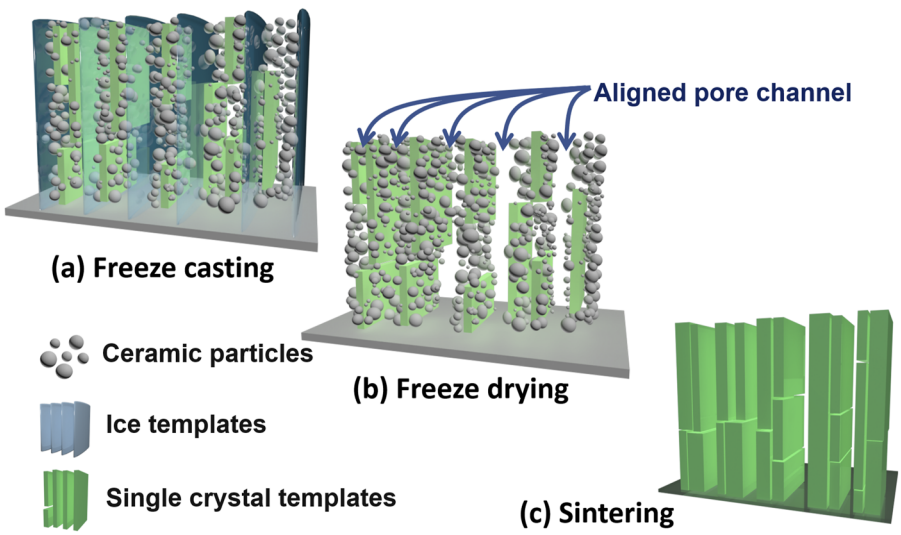

FIG. 6. Schematic of the fabrication of porous pseudo-single crystals via freeze casting. (a) Freeze casting small single crystal templates, (b) freeze drying the frozen green body, and (c) sintering for the realization of the porous pseudo-single crystals.

in Fig. 6. Such freeze casting could also be combined with 3D printing techniques to obtain complex and novel physical or geometrical configurations with customized design of shape, high d_{ij}, and low ε_{33}^{T} for variety of needs in piezoelectric energy harvesting and sensing sectors.

4. Concluding remarks

Piezoelectric composite materials that consist of the piezoactive and passive phases have been widely explored in energy harvesting applications due to their low dielectric constant and relatively high piezoelectric coefficient; such a combination of properties leads to a high harvesting figure-of-merit. The material selection and structural design have been utilized for the optimization of the energy harvesting capability. We expect significant progress in enhancing the poling efficiency of the porous composite by design of the pore space and impregnating a high dielectric constant but low stiffness polymer into the pore space. For harvesting large-scale vibrations, industrial scaling up of processing techniques and broader-band energy harvesting systems are of interest. The use of new materials, such as lead-free ferroelectrics and ferroelectrets, more efficient processing techniques, additive manufacture, and an ability to create porous pseudo-single crystals will be of increasing interest in the future development of this topic.

5. Acknowledgments

This work was supported by the Academy of Medical Sciences GCRF Fund (Grant No. GCRFNGR2-10059), ERC project (ERC-2017-PoC-ERC-Proof of Concept, Grant No. 789863), and The Leverhulme Trust (Grant No. RGP-2018-290). The authors acknowledge the Key Research and Development Project of Hunan Province (Grant No. 2020WK2004), Overseas Talent Introduction Project of China, and Hundred Youth Talents Program of Hunan.

C. Power management circuits for triboelectric nanogenerators

Philippe Basset (*philippe.basset@esiee.fr), Ahmad Delbani, Hemin Zhang, Dimitri Galayko

1. Abstract

Triboelectric energy harvesters, as for any electrostatic transducer, need to maximize their bias voltage and capacitance variation for maximizing the electrical energy conversion from the mechanical domain. Internal (almost) steady bias of several hundreds of volts can be easily obtained directly by triboelectrification with a good triboelectric material, and even higher bias, increasing with time, can be obtained with a poor material if using unstable charge pumps for rectification. However, whatever the chosen strategy, the high-voltage/low-current output of the TENGs need to be adapted to a lower voltage/higher current output to power typical electronics.

This section presents an overview of the architectures for power management systems proposed to date for triboelectric nanogenerators to improve the global energy conversion conditions efficiency in the future.

2. Introduction

Triboelectric energy harvesters (TENG) typically generate high AC open-circuit voltage of several hundred volts peak, with relatively low short-circuit current of few tens of μA peak maximum. However, most applications require DC voltages around a few volts, with DC currents of at least a few hundred of μA in order to generate a minimum average power of 100 μW. Therefore, a power management circuit (PMC) is needed to generate a low DC voltage for the load, while implementing a high voltage interface at the TENG's side to maximize the converted power. Hence, PMC for TENGs is an important topic that has recently attracted significant attention.

A complete PMC needs to fulfill two important tasks that are strongly interlinked: (1) the generation of a dynamic electrical bias on the TENG to optimize the mechanical-to-electrical energy transduction, while (2) performing the AC–DC conversion to a low DC voltage. For electrostatic transducers, such as TENGs, the converted power is proportional to the square of the bias voltage: hence, the first intention is to maximize the bias voltage level. A high bias is typically generated by the triboelectric effect, but may also be produced externally by some special conditioning circuits (CC), allowing high energy yield even with low cost TENG devices. In addition, the bias voltage generated by the CC on the TENG is necessarily variable and depends on the TENG motion: this represents the main challenge in the PMC implementation.

3. Passive charge pumps

Passive charge pumps are capacitive charge pumps where the switches are implemented with diodes (even if, for energy saving purpose, the diodes may be implemented with active switches[154–156]). These circuits can be classified into two categories: stable and unstable charge pumps. Stable charge pumps reach a constant saturation voltage after some time, for instance, full-wave and half wave rectifier, Cockroft–Walton multiplier, etc. On the contrary, unstable charge pumps, such as Bennet's electricity doubler, generate a DC voltage that is continuously increasing, until component limitations or electrostatic discharge occur: such charge pumps are able to generate high voltage biasing even with basic TENGs having low internal polarization.

4. Stable charge pumps: The diode rectifier based conditioning circuits

The full-wave (FW) diode rectifier is the most used CC for TENGs that can be found in the literature. It is a stable charge pump generating a saturation voltage proportional to the maximum transferred charge in the short-circuit mode.[157] The saturation voltage of the half-wave (HW) rectifier is higher by a factor $(\eta - 1)$, where η is the C_{max}/C_{min} capacitance ratio of the TENG.[158] Even higher saturation voltage can be obtained with a voltage multiplier, also known as the Cockroft–Walton doubler,[159,160] which is a generalization of the HW network.

During the early cycles, as the output voltage is close to zero, the output voltage of the FW rectifiers increases with twice the slope of the HW, although in that case both powers are far from the optimum of each circuit. However, if the output voltage of the rectifier can be set to half of its saturation voltage, HW outperforms the FW by a factor $(\eta + 1)/2$.[161] This can be seen from Fig. 7(c), where the extracted power is calculated as the time derivative of the energy of the load capacitor.

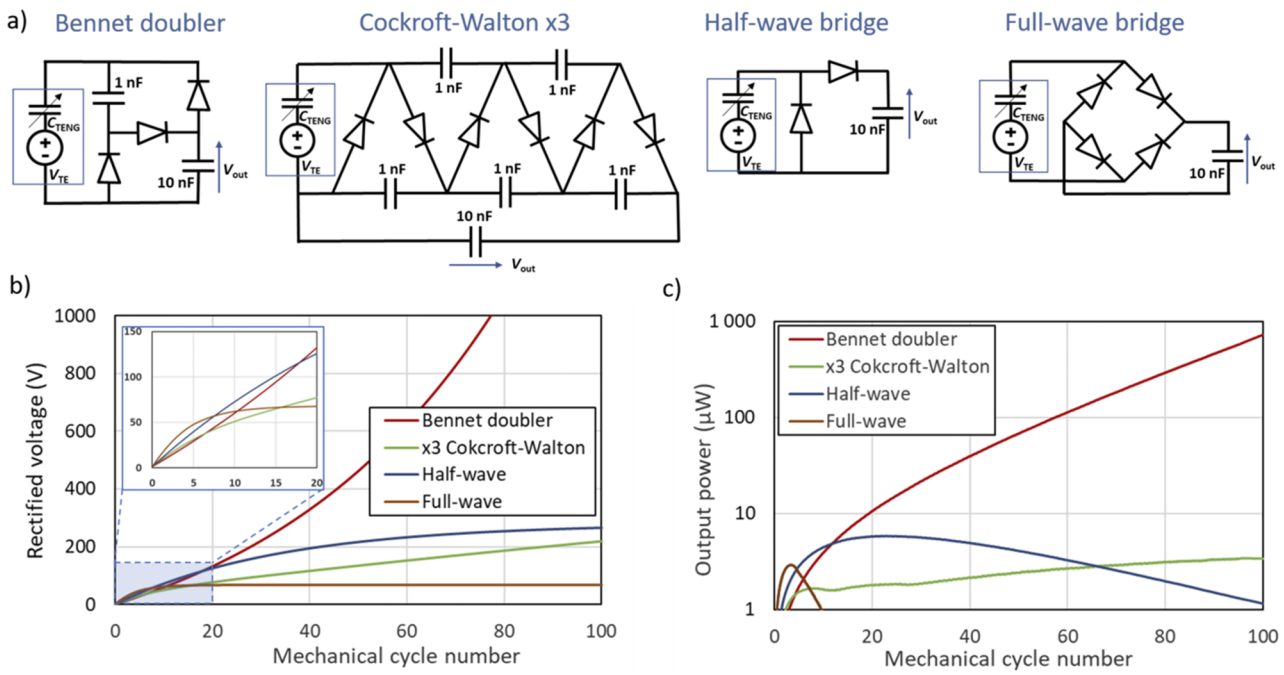

FIG. 7. Circuits (a), spice simulations (b), and output power (c) of a half- and full-wave diode bridges, a Bennet doubler, and a Cockroft-multiplier (×3) for a TENG having a charge density of 50 μC/cm^2 and a C_{max}/C_{min} ~ 1 nF/300 pF.

5. Unstable charge pumps: The Bennet's doubler family

A new class of CC, inspired from the electrical machines of the 18th century and also made of diodes and capacitors only, has recently emerged for TENGs conditioning: the Bennet doubler.[162] These circuits have the ability to exponentially increase the charge on the TENG's electrodes during operation and to increase its bias and conversion efficiency.[163] A minimum value of η is necessary, which is typically 2 for the simplest architecture, but it can vary depending on the circuit configuration.[164–166] While the output energy can be greatly improved by the unstable charge pumps, their main drawback is that it may take some time for reaching the conditions for a high energy conversion. This time is mostly depending on the value of η[163] and the ratio between C_{max} and the load capacitance. Figure 7 shows a simulation comparing the output rectified voltages and the output power for various CC.

6. Circuits based on active charge extraction

PMC based on synchronous techniques, such as SECE (Synchronous Electrical Charge Extraction) or SSHI (Synchronous Switching Harvesting on Inductor), consist in externally controlling the transducer's current by using an inductive DC–DC convertor activated synchronously with the motion of the mobile electrode. They can be seen as an improvement of the passive FW conditioning circuit: Their purpose is to actively enhance the correlation between the transducer's current and voltage to maximize the extracted power. The "charge extraction" term means that a negative (positive) current is generated at the phases of high positive (negative) voltage to maximize the average voltage–current product (the power). These circuits use a coil connected in series with a switch synchronously activated at the extremum voltages of the kinetic energy harvester, i.e., several times per mechanical cycle. We note that the term "synchronous" in their names is misleading: the passive conditioning circuits discussed earlier have also switches (diodes) activated synchronously with the mechanical motion, yet this synchronization is automatic, whereas in SECE and SSHI networks the synchronization needs to be external and requires sophisticated circuitry. Various implementations and variations of the basic SECE and SSHI techniques exist.[167–169] In the recent applications with TENG, the DC–DC convertor used for charge extraction has been controlled electronically,[170,171] by movement-induced electrostatic force[172] or movement-induced mechanical contacts.[155]

7. TENG generators for low voltage loads

A common limitation of the above-mentioned conditioning circuit is a high output voltage required for optimal energy conversion [cf. Figs. 7(b) and 7(c)], which is not compatible with the low voltage of the load supply. The FW and HW rectifiers work optimally when the output voltage is the half of the saturation voltage. The Bennet's doubler and the SSHI converter optimal output voltage is the maximum voltage supported by the technology and the used components. The SECE circuit is an exception: the output voltage may be as low as required for the load. Because of the generally requested high voltage at the output of the conditioning circuit, two-stage architectures are required: the second stage

is a DC–DC convertor achieving a voltage adaptation between the high output voltage of the primary conditioning circuit and the low voltage generated for the load.

The DC–DC converters used for the second stage are generally of two kinds. The first one, working in the continuous mode, performs an active impedance synthesis for the output of the conditioning circuit. This technique is mainly used for low coupling piezoelectric transducers used with full wave rectifiers to set the duty cycle or switching frequency of a Buck or Buck–Boost DC–DC converter at a frequency much higher than the mechanical oscillation.[173] The term "continuous mode" is due to the fact that the current in the inductor never goes to zero. However, a high-frequency control of the switch may be complex to implement and is power consuming.

Therefore, many works employ a DC–DC conversion in the discontinuous mode: first, the circuit accumulate the harvested charges in the output capacitor of the TENG CC, then this capacitor is fully or partially discharged to the load capacitance through the DC–DC converter by activating the Buck switch at a frequency much lower than the mechanical frequency,[174] and only when a significant energy is accumulated in the output capacitor of the TENG CC. This allows an event-based control of the DC–DC converter: the latter operates only when enough energy is harvested, and a significant reduction of the consumption needed for the power management is obtained. The event-driven control of the DC–DC convertor is achieved with a comparator provided with a hysteresis: either the hysteresis is narrow and then the CC output capacitor is discharged only partially or the hysteresis is wide and the output capacitor is fully discharged. The advantage of the narrow hysteresis is to keep the output voltage of the CC close to the optimal level. The wide hysteresis is easier to implement, it minimizes the activation frequency, but the CC operates suboptimally a non-negligible amount of time.

Moreover, a two-stage architecture allows the use a CC output capacitance of intermediate value (~10–100 times the TENG's capacitance) to minimize the set-up time required to reach the maximum harvested power. The output capacitor of the second stage (the load capacitor) is usually much larger (~10^3–10^6 times the TENG's capacitor), which provides a stabilization of the output voltage available for the load.

While actively driven MOS switches can be used to control the operation of the DC–DC stage of the power management circuit, recently self-powered/self-actuated switches have been proposed: a switch with wide hysteresis made of a SCR thyristor and a Zener diode,[175] and a high-voltage micro-plasma switch with a narrow hysteresis, to minimize the period while the TENG is biased at low voltage (Fig. 8).[176]

8. Comparison and choice criteria of power management architectures

The circuits described earlier have different features regarding the performances and the facility of implementation. Depending on the available triboelectric device and the design objective, one of them should be preferred. In the following, we list some typical situations that a TENG generator designer must face, and we provide guidance for selecting the most appropriate conditioning circuit.

Passive charge pumps: The great advantage of the passive charge pumps is their simplicity of implementation. However, they all need an additional stage in order to control the voltage at its output (with two-stage architectures or an LDO–low drop voltage–regulator).

The full bridge rectifier should be preferred when the output voltage [V_{out} in Fig. 7(a)] is much lower than V_{TE}, the build-in voltage of the TENG that is assumed to be high. Under this condition, this circuit provides the highest conversion power over all possible passive charge pumps. The half bridge rectifier should be preferred when V_{TE} is high and high V_{out} is possible. However, this usually involves additional DC–DC conversion to obtain a low voltage supply for the load.

When the built-in voltage of the TENG is low, unstable charge pumps should be preferred, as half-bridge and full-bridge circuits

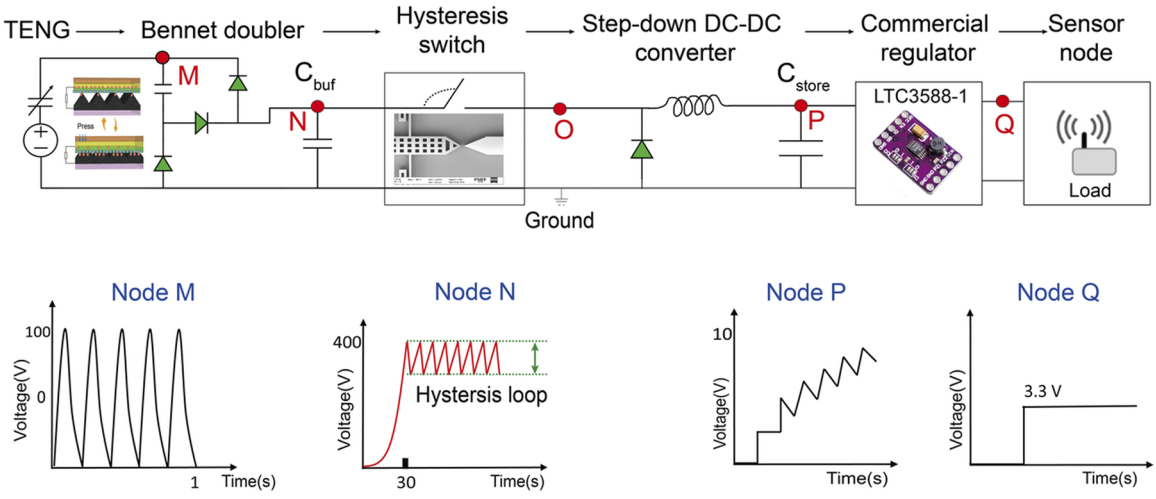

FIG. 8. A two-stage CC with an unstable charge-pump rectifier and high-voltage autonomous micro-plasma switch.[176]

would have poor performance. In this case, the unstable charge pump increases the output voltage V_{out} up to the optimal (high) value, independently on V_{TE}. As with the half-wave rectifier, these circuits must be supplemented with a DC–DC converter to generate a low voltage for the load.

Circuits based on the active charge extraction (typically, SECE) provides a very good compromise between efficiency and the complexity of the control. Its advantage is to generate a low voltage on the load without requiring an additional DC–DC stage. It should be preferred when the TENG voltage is high and when the technology used for the implementation of the circuit allows the use of a complex control involving an actively controlled switch, an internal inductive DC–DC convertor, etc. Usually, this involves using CMOS technology (on-chip integration) to minimize the parasitics and optimize overall circuit operation.

Two stage power management architectures are needed when the operational voltage of the TENG (the voltage on C_{buf} in Fig. 8) is much higher than the voltage on the load supply on C_{store}. Such architectures are necessary if we wish to maximize the energy extracted from the TENG by biasing it with a high voltage (on C_{buf}). The classical configuration shown in Fig. 8 corresponds to the combination of an unstable charge pump and of a DC–DC convertor regulating the voltages on C_{buf}. Note that a DC–DC convertor can only regulate one voltage, on C_{buf} or C_{store}. If both are to be regulated, the DC–DC convertor is designed to regulate the voltage on C_{buf}, and an additional stage (an LDO or another load management circuit) must be used for the regulation of the load voltage.

9. Conclusion

The conditioning electronics for TENGs remains a challenge that will continue to be addressed in the future. The main challenge is to match the high output voltage required for the biasing TENGs with the low voltage needed to power the load in most applications. Reconciling of these requirements requires the use of a two-stage power interface: the first stage is a conditioning (primary) circuit that generates power and the second stage is a DC–DC that matches the output voltage to the load. Variations in operating conditions may require the architectures to be adaptive. Adaptive behavior is typically implemented in the second stage (the DC–DC converter), which monitors the operation of the primary conditioning circuit and keeps it optimal. The high operating voltage of TENGs makes this task difficult to implement. In addition, another fundamental difficulty is the minimizing of the leakage in the system: at 100 V, 1 μA leak results in a power loss of 100 μW, which can be prohibitive.

In all cases, the two-stage power interface includes a switch to control the charge transfer between the two stages. Regardless of the switch technique chosen, the switch will induce significant losses with each actuation. Mechanical contact switches are easy to implement because they require no electrical control and can be operated precisely at the extreme variations in the TENG voltage. However, they are actuated at least once per mechanical cycle, which does not allow for charge accumulation over several cycles and therefore generates a lot of losses because of their high actuation frequency. Electronic switches need additional energy for their "cold" start-up, control, and actuation. They also drastically limit the allowable output voltage across the TENG, especially with IC technologies, which greatly affects the energy conversion. On the other hand, MPPT can easily be implemented to adapt the system to irregular mechanical inputs. Plasma switches can store energy up to very high voltages, they are self-actuated, and even a narrow hysteresis can be implemented by design. However, they also generate losses and their hysteresis cannot be matched to the external mechanical force, unless the gap between the switch electrodes can be adjusted by some MPPT electromechanical systems.

IV. MATERIALS

A. Atomically thin materials for nanogenerators and piezotronics

Feng Ru Fan (*frfan@xmu.edu.cn), Wenzhuo Wu (*wenzhuowu@purdue.edu)

1. Abstract

Nanogenerators and piezotronics have emerged as promising candidates to meet the needs in harvesting and interfacing the mechanical signals in numerous emerging technologies. The recent advances in atomically thin materials have promoted the development of 2D materials based nanogenerators and piezotronics with ultrathin form factors. In this roadmap, we intend to provide a brief discussion focusing on our perspectives on prospects and challenges associated with the fields of 2D materials for nanogenerators and piezotronics. The development of convergent, trans-disciplinary approaches is expected to remove the barriers in the design, synthesis, integration, characterization, and application of 2D materials for nanogenerators and piezotronics. Such collective efforts from the research community would also stimulate extensive investigations for piezoelectricity, electronic transport, triboelectricity, as well as many other scientific and technological aspects of atomically thin materials.

2. Background and state-of-the-art

The capabilities of devices to scavenge, detect, and interact with a rich spectrum of ubiquitous mechanical signals (e.g., force, strain, vibration, etc.) would allow the next-generation machines to sense, monitor, and communicate with the environment with greater intelligence in a multitude of emerging technologies, e.g., wearable devices, soft robotics, medical prosthetics, and human–machine interface.[177–181] Such capabilities are largely lacking in the state-of-the-art technologies for mechanical harvesters/sensors.[182,183] To this end, emerging technologies, such as nanogenerators and piezotronics, have attracted intensive interest. Wang and Song invented the piezoelectric nanogenerator (PENG) for harvesting the mechanical vibrations into electricity.[1] Wang and co-workers further demonstrated the concept of piezotronics, where the mechanically induced piezoelectric polarization function as the controlling signal.[21,23] Early studies in PENG and piezotronics were mainly exploring piezoelectric nanowires (e.g., ZnO and GaN).

The recent advances in scientific understandings and technological applications of 2D materials have promoted the development of nanogenerators and piezotronics, leveraging the unique characteristics of these materials.[184] 2D materials' atomically thin geometries and superior mechanical properties enable the introduction of enormous strain (e.g., >1%) without fracture, and broad tunability

inaccessible to bulk or thin-film materials.[185] 2D semiconductors and dielectrics (e.g., MoS_2, BN, etc.)[186–200] with noncentrosymmetric lattices have received significant attention owing to their unique electrical, optical, and other physical and chemical properties. Due to the strain-induced lattice distortion and the associated charge polarization, these 2D materials exhibit piezoelectricity. They are capable of direct mechanical-to-electrical transduction for static and dynamic signals and appealing for PENGs and piezotronics with ultrathin form factors. It should be noted that the piezoelectricity is closely related to the structure and thickness of 2D materials. For PENG, single-layer 2D materials with broken inversion symmetry has a strong intrinsic piezoelectric response, whereas centrosymmetric bilayers and bulk crystals are non-piezoelectric.[189] For TENG, the selection range of 2D materials is relatively wide, which can be either single-layer or bulk crystals. Figure 9 shows the chronological timelines for the milestones in the experimental efforts on 2D material based nanogenerators (PENGs and TENGs) and piezotronics.[189,197,201–204] We would like to point out that, due to the space limit, these only represent a small fraction of representative work in the related fields. Instead of comprehensively reviewing the progress in related fields, which can be found in recent publications, here we intend to provide a brief discussion focusing on our perspectives on prospects and challenges in related fields.

3. Challenges and opportunities

Despite the rapid progress achieved in related fields, roadblocks exist for the synthesis, integration, characterization, and application of 2D materials based nanogenerators and piezotronics. One of the biggest challenges in exploring the known 2D piezoelectric materials for practical applications is to induce consistent piezoelectric responses (e.g., aligned polarity) in all the 2D flakes using the external macroscopic mechanical strains (e.g., those induced by the substrates). Such a challenge is primarily due to the following facts: (1) most of these materials possess symmetries that lead to in-plane piezoelectricity; (2) the ionic nature of these compound materials results in orientation-dependent piezoelectric responses; and (3) these materials are often placed on the host substrate with poor or little control over the in-plane orientations due to the limitations in synthesis and/or assembly control. Many of the experimentally explored 2D piezoelectrics have small piezocoefficients, making applications elusive. Although a wide range of 2D materials has been theoretically predicted to exhibit intrinsic piezoelectricity,[186,187,198,199] most of these materials have yet to be investigated experimentally due to the challenges associated with the current approaches for preparing those materials, e.g., exfoliation and vapor depositions. These ongoing efforts have vague potential in scaling-up with desirable yield and material properties (e.g., shape, orientation, dimensions, carrier density, etc.), and suffer from the restrictions in growth substrates (e.g., for epitaxy) and process conditions (e.g., atmospheric control due to material instability). Also, the symmetry in most 2D piezoelectrics results in a thickness-dependence that imposes formidable challenges for the process control, where the piezoelectricity can disappear when the material thickness varies by only one atomic layer. The atomic thickness of the 2D materials also renders their sensitivity (and instability) to the environmental conditions. Moreover, the carrier concentration of 2D materials, which can significantly impact the piezoelectric property through charge screening, is prone to significant variations due to unintentional environmental doping. Such a challenge necessitates the development of stable 2D materials through the optimization of material properties, device structure, and the incorporation of the packaging process. An extensive understanding of the mechanism of electromechanical transduction and charge transfer at the atomic scale, which is still lacking, will facilitate the optimization of the output/sensing performance of related devices. The ultrathin nature and robust mechanical properties of 2D materials allow for potential integration into 3D architecture with diverse functionalities and boosted performance compared to planar counterparts. Still issues such as the electrical interconnection across layers and the robustness of the manufacturing process need to be addressed appropriately. The search, design, and production of 2D materials with robust out-of-plane piezoelectricity is favored for such 3D integration.[192,193,204]

These challenges also lead to abundant research opportunities. The reduction of dimensionality in 2D materials leads to strong, accessible piezoelectricity compared to its bulk counterpart. 2D piezoelectric materials are unique when compared to traditional piezoelectrics, which are brittle and insulating, and can host significant strain-induced electric field couplings through extremely strong Coulomb interactions in the 2D limit. Such characteristics offer unexplored possibilities for probing intriguing science in the atomically thin limit due to the strong coupling of piezoelectricity to various solid-state excitations involving charges, photons, and spins in 2D systems for engineering novel functionalities.[205–207] From a practical application point of view, 2D piezoelectrics have been explored as the active components for electromechanical sensors,[208] the optically active layers for strain-engineered optoelectronics,[194] and the interfaces for mechanically enhanced catalysis.[209] 2D materials, in general, can also be used to construct efficient triboelectric nanogenerators (TENGs)[2] due to their flexible structures and tunable surface/dielectric properties for engineered triboelectrification and electrostatic induction.[110,210–212] Such flexibility allows for the design and implementation of ultrathin triboelectric devices using 2D materials. The thin thickness of 2D materials also favors the occurrence/observation of flexoelectricity, a physical process that can induce electrical polarizations when a material is subjected to an inhomogeneous deformation.[213] The knowledge in the impact of flexoelectricity on the nanogenerator and piezotronics operations, as well as in 2D materials with centrosymmetry,[214] is expected to guide the design of future energy and sensor devices with enhanced performance.

The advances in material design and nanomanufacturing can enable new technology for scalably producing substrate-agnostic, high-performance 2D materials with designer properties. A comprehensive examination, through combined theoretical and experimental efforts, of the interfacial characteristics between 2D materials and electrodes will provide the fundamental understandings, e.g., the effects of metals and electrode configurations on the charge transfer/transport in metal-2D material contacts.[215] Such knowledge is critical for the rational design and optimization of future nanogenerators and piezotronics. The exploration of the fundamental doping mechanism and defect chemistry in 2D materials is essential for not only providing versatility in modulating the material properties by design[216] but may also enable novel device concepts and applications in nanogenerators and piezotronics.[217,218] The

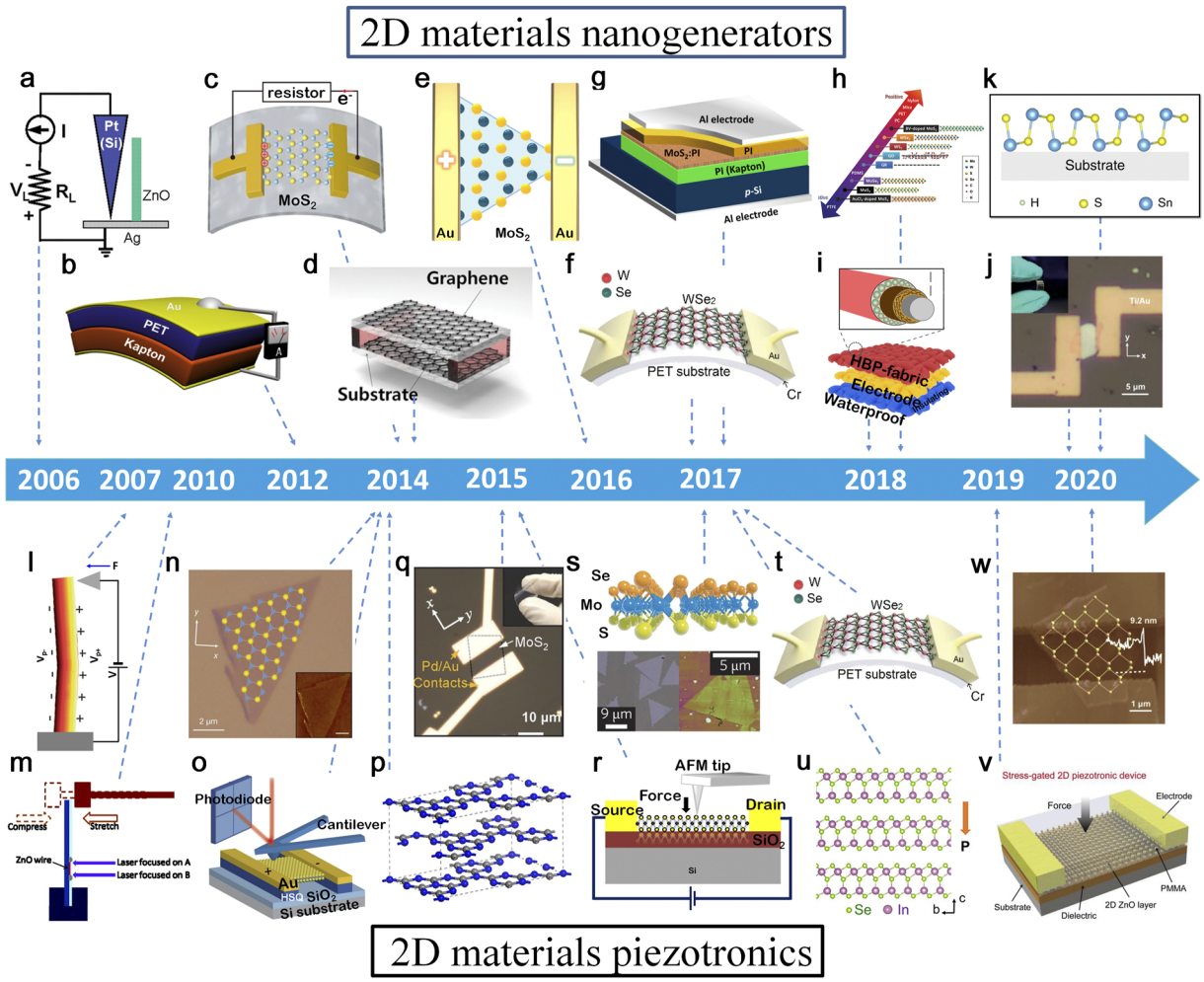

FIG. 9. The chronicle timeline showing the experimental milestones in 2D materials nanogenerators (above the timeline) and 2D materials piezotronics (below the timeline). (a) The first PENG based on the piezoelectric ZnO nanowires. Adapted with permission from Z. L. Wang and J. Song, Science **312**, 242 (2006). Copyright 2006 AAAS, USA. (b) The first TENG. Adapted with permission from Fan *et al.*, Nano Energy **1**, 328 (2012). Copyright 2012 Elsevier Ltd. (c) The first 2D materials-based PENG based on monolayer MoS_2. Adapted with permission from Wu *et al.*, Nature **514**, 470 (2014). Copyright 2014 Springer Nature. (d) Transparent TENG used monolayer graphene as electrode. Adapted with permission from Kim *et al.*, Adv. Mater. **26**, 3918 (2014). Copyright 2014 Wiley-VCH. (e) MoS_2-based PENG. Adapted with permission from Kim *et al.*, Nano Energy **22**, 483 (2016). Copyright 2016 Elsevier Ltd. (f) PENG based on chemical-vapor-deposition grown monolayer WSe_2. Adapted with permission from Lee *et al.*, Adv. Mater. **29**, 1606667 (2017). Copyright 2017 Wiley-VCH. (g) TENG based on monolayer MoS_2 nanocomposites. Adapted with permission from Wu *et al.*, ACS Nano **11**, 8356 (2017). Copyright 2017 American Chemical Society. (h) Triboelectric series of 2D materials. Adapted with permission from Seol *et al.*, Adv. Mater. **30**, 1801210 (2018). Copyright 2018 Wiley-VCH. (i) Textile-TENG based on BP composites fabrics. Adapted with permission from Xiong *et al.*, Nat. Commun. **9**, 4280 (2018). Copyright 2018 Springer Nature. (j) Flexible PENG based on multilayer BP. Adapted with permission from Ma *et al.*, Adv. Mater. **32**, 1905795 (2020). Copyright 2020 Wiley-VCH. (k) Flexible PENG based on SnS. Adapted with permission from Khan *et al.*, Nat. Commun. **11**, 3449 (2020). Copyright 2020 Springer Nature. (l) The first piezotronic device based on ZnO nanowires. Adapted with permission from Z. L. Wang, Adv. Mater. **19**, 889 (2007). Copyright 2007 Wiley-VCH. (m) The first piezo-phototronic device based on ZnO nanowires. Adapted with permission from Hu *et al.*, ACS Nano **4**, 1234 (2010). Copyright 2010 American Chemical Society. (n) The first 2D materials-based piezotronics prepared with the monolayer MoS_2. Adapted with permission from Wu *et al.*, Nature **514**, 470 (2014). Copyright 2014 Springer Nature. (o) The direct measurement of piezoelectric coefficient in monolayer MoS_2. Adapted with permission from Zhu *et al.*, Nat. Nanotechnol. **10**, 151 (2015). Copyright 2015 Springer Nature. (p) The piezoelectricity in 2D graphene nitride. Adapted with permission from Zelisko *et al.*, Nat. Commun. **5**, 4284 (2014). Copyright 2014 Springer Nature. (q) The first piezo-phototronic device based on monolayer MoS_2. Adapted with permission from Wu *et al.*, Adv. Mater. **28**, 8463 (2016). Copyright 2016 Wiley-VCH. (r) Piezoelectricity in CVD-grown monolayer MoS_2. Adapted with permission from Qi *et al.*, Nat. Commun. **6**, 7430 (2015). Copyright 2015 Springer Nature. (s) Piezoelectricity in Janus monolayers of transition metal dichalcogenides. Adapted with permission from Lu *et al.*, Nat. Nanotechnol. **12**, 744 (2017). Copyright 2017 Springer Nature. (t) Piezoelectricity in bilayer WSe_2. Adapted with permission from Lee *et al.*, Adv. Mater. **29**, 1606667 (2017). Copyright 2017 Wiley-VCH. (u) Piezoelectricity in a-In_2Se_3 nanoflakes. Adapted with permission from Zhou *et al.*, Nano Lett. **17**, 5508 (2017). Copyright 2017 American Chemical Society. (v) 2D piezotronics in ZnO nanosheets. Adapted with permission from Wang *et al.*, Nano Energy **60**, 724 (2019). Copyright 2019 Elsevier Ltd. (w) Piezoelectricity in multilayer black phosphorus. Adapted with permission from Ma *et al.*, Adv. Mater. **32**, 1905795 (2020). Copyright 2020 Wiley-VCH.

development of quantitative *in situ* or even *in operando* characterizations of 2D materials (e.g., for piezoelectricity, ferroelectricity, triboelectrification, and charge transfer) under controlled complex straining conditions, e.g., biaxial strain and patterned strain field,[219] will add to the critically required fundamental insights and instrumental toolbox toward physics-based design and development of 2D nanogenerators and piezotronics. Last but not least, the design and fabrication of 2D heterostructured artificial crystals can introduce more device physics and diversified functionalities.[218] The introduction of additional encapsulation layers (e.g., transferred boron nitride[220] or grown dielectrics[221]) can improve the stability of nanogenerator piezotronics devices based on 2D materials.

4. Conclusions

The development of convergent, trans-disciplinary approaches that bridge disciplines such as advanced manufacturing, data science, material science, device physics, and chemistry is expected to spur data-driven, physics-based theoretical and experimental advances in 2D materials based nanogenerators and piezotronics. Such a confluence of collective efforts from the research community would stimulate extensive investigations for piezoelectricity, electronic transport, ferroelectricity, triboelectricity, and many other scientific and technological aspects of atomically thin materials.

5. Acknowledgments

W.W. acknowledges the College of Engineering and School of Industrial Engineering at Purdue University for the startup support and the Ravi and Eleanor Talwar Rising Star Assistant Professorship. F.R.F. acknowledges Nanqiang Young Top-notch Talent Fellowship from Xiamen University.

B. Phononic crystals and metamaterials for energy harvesting

Miso Kim (*smilekim@skku.edu)

1. Abstract

Metamaterials are artificially engineered structures capable of yielding effective material properties not found in nature, which leads to desirable wave control functionalities not only in optics but also in acoustics and vibration regimes. Metamaterial-based energy harvesting has recently emerged as an enabling technology for drastic enhancement of harvesting performance by manipulating and amplifying input mechanical sources, such as vibration, sound, and elastic waves. Here, we review major achievements in the field of metamaterials-based energy harvesting using various kinds of phononic crystals and metamaterials, including phononic crystals with defects, gradient-index phononic crystals, locally resonant metamaterials, metasurfaces, and mechanical metamaterials. As in the early stage of development, metamaterial-based energy harvesting research entails challenges, which again form the basis for further development. Emergent directions, such as innovative metamaterial designs for broadband operation within a compact size, artificial intelligence-based design algorithms, and interface technology for efficient energy transfer between the metamaterial and energy harvesting devices, are addressed together with relevant challenges.

2. State-of-the-art

Energy harvesting (EH) technology has experienced a robust and remarkable development, thanks to high performance mechanical-to-electrical conversion materials, devices, and efficient power management circuits. Along with disruptive materials and systems for energy conversion and management,[222,223] researchers recently began to turn their eyes toward the idea of actively manipulating and amplifying input mechanical wave energies via metamaterials in order to drastically improve energy harvesting performance. As directly implied from the prefix *meta* that means "beyond" in original Greek, metamaterials are artificially designed structures that can exhibit material properties beyond the conventional scheme, such as negative mass density, negative bulk modulus, negative refractive index, and bandgap. Metamaterials derive their wave manipulation capability from these unconventional properties, providing a wide range of potential applications including super- and hyper-focusing lenses, cloaking, wave filtering, and absorbers in both optics and acoustics.[224–227] Here, we focus on metamaterials that are related to mechanical waves, such as vibration, sound, and elastic waves. Note that the term "metamaterial" can include phononic crystals, acoustic/elastic, and mechanical metamaterials in a broader sense while "metamaterial" or "acoustic metamaterial" sometimes denotes only the artificially engineered composite materials with functionalities due to local resonances. Metamaterials have provided a new paradigm for energy harvesting technology in that it is about active control of input wave energies rather than the conventional energy harvesting research focus: conversion and power management. When mechanical waves are amplified either through wave localization or focusing using metamaterials, subsequent mechanical-to-electrical energy conversion and management through high performance piezoelectric materials, devices, and harvesting power management circuits can make a synergetic effect to yield substantially enhanced harvesting performance.[228,229] Here, we review the present state-of-the art in metamaterial-based energy harvesting using various phononic crystal and metamaterial concepts ranging from phononic crystals, acoustic metamaterials, and metasurfaces to mechanical metamaterials.

Phononic crystals (PnCs) or sonic crystals are artificial structures consisting of a periodic repetition of unit cells. Similar to any periodic structure, interaction of acoustic waves with PnC structures results in a dispersive band structure with a bandgap due to Bragg' scattering, which is governed by the Bloch and Floquet theorem.[230] The characteristic length, i.e., unit cell size, of the PnC is of the same order of magnitude as the wavelength: a few millimeters to centimeters for acoustic and elastic waves. Within the bandgap frequency range, the energy trapped can be localized at a defect that is introduced inside a PnC structure, which can subsequently be converted into electrical energy by attaching a piezoelectric energy harvesting device at the defect. Locating a piezoelectric PVDF film in the cavity of PnCs consisting of periodic cylinders has proved useful for substantial enhancement in both vibration and acoustic energy harvesting when compared with the case without PnCs.[231–233] Similarly, elastic wave energy can be localized at the imperfection of a two-dimensional lattice constituted by stubs,[234] circular,[235] or

octagonal holes[236] in a metal thin plate (e.g., aluminum), leading to substantial amplification of harvesting performance. As highly dense energy localization occurs at the defect resonance frequency inside a phononic bandgap range, a systematic unit cell design for bandgap maximization is crucial for enhanced PnC-based energy harvesting. In this regard, octagonal hole-type unit cells with its optimized dimensions in an aluminum plate were numerically and experimentally demonstrated to yield more than 20 times of power enhancement when coupled with a PZT ceramic disk in comparison with a bare plate [Figs. 10(a) and 10(b)].[236] Parametric studies on the physical relation of PnC design parameters, such as material properties, supercell size (i.e., number of unit cells), and defect location, with PnC-based EH system characteristics, including bandgap size and frequency level, as well as mechanical and electrical output performance of elastic wave energy harvesting.[234,237,238] PnC-based energy localization and harvesting study has not been limited to a single defect. Creating double or more defects inside a PnC structure has unveiled different physical mechanisms not found in a single defect case, such as defect band splits and corresponding defect resonance modes, which can provide more versatile ways of exploring PnCs for broadband and tunable energy harvesting.[239] Instead of using only sonic crystals, researchers proposed a coupled resonance structure of sonic crystals and Helmholz resonators (HRs), the latter of which is one of the most conventional ways to amplify the sound pressure.[240–242] Hierarchical sonic crystals consisting of two different levels of periodic orders of PnCs are also an intriguing design proposed for broadband gaps and acoustic energy confinement, exhibiting potentials for broadband sound energy harvesting.[243–245] Phononic crystal cantilever beams coupled with a PEH device[246,247] or periodic arrangement consisting of piezoelectric cantilevers[248] have also been used to take advantage of both cantilever resonance and bandgap due to periodicity simultaneously.

Controlling directional nature of acoustic and elastic wave propagation toward the targeted location has also been a subject of significance for focusing and harvesting. Gradient-index (GRIN) phononic crystals, a periodic arrangement of unit cells with a spatial variation of the refractive index, have proved to be effective to manipulate the wave propagation direction for focusing both in acoustic[249,250] and elastic regimes.[251–254] Gradually changing indices in a GRIN PnC can be achieved by tailoring the geometric dimensions of the unit cell (e.g., the size of circular or cross-shaped holes and cylindrical stubs) that satisfy the desired target refractive index profile. When a piezoelectric device is integrated into the GRIN PnC structure particularly at the point of focusing [Figs. 10(c) and 10(d)], the focused energy can then be converted into substantially amplified electrical energy, exhibiting the wave manipulation capability in terms of direction as well as amplitude. Embedded acoustic black holes are another design framework that allows producing high energy density by tailoring the wave propagation characteristics. Tuning the local stiffness and thus wave velocity is possible by embedding structural tapering into the host structure. As vibration

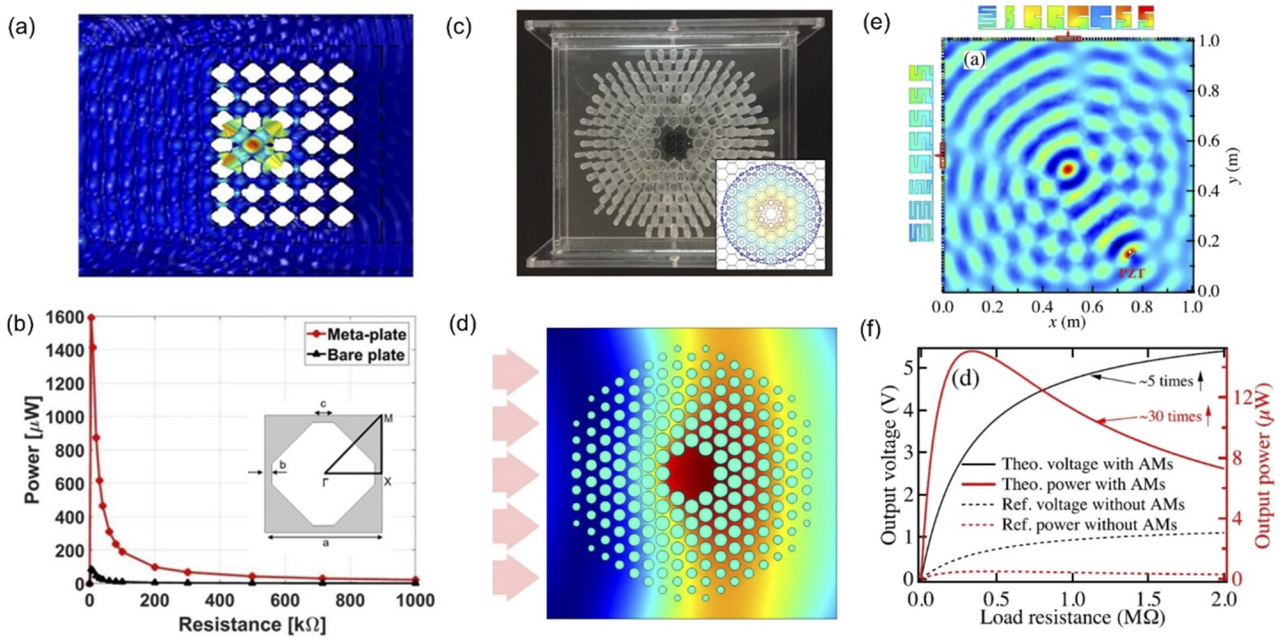

FIG. 10. Various concepts of metamaterials for mechanical wave energy focusing and energy harvesting: (a) harmonic simulation results showing energy localization at the defect of octagonal-hole type phononic crystals and (b) the resulting amplified output power, (c) an image of fabricated omnidirectional gradient-index (GRIN) phononic crystals (PnCs), and (d) its harmonic analysis results to show sound energy amplification at the center of the GRIN-PnCs, (e) numerical sound pressure field and (f) the output power of the two-sided multilateral metasurface. Figures taken with permission from Park *et al.*, Nano Energy **57**, 327 (2019). Copyright 2019 Elsevier Ltd. All rights reserved. Figures from Hyun *et al.*, Appl. Phys. Lett. **116**, 234101 (2020). Copyright 2020 with permission of AIP Publishing and S. Qi and B. Assouar, Appl. Phys. Lett. **111**, 243506 (2017). Copyright 2017 with permission of AIP Publishing.

energy can be trapped in the tapered acoustic black hole area, much enhanced harvesting is attainable.[255–258]

Locally resonant metamaterials are another innovative engineered structures that can possess extraordinary physical properties such as negative elastic modulus, negative mass density and negative refractive index.[226,259–263] Such unconventional features are associated with the phenomenon such as bandgap or negative refraction, which enables input acoustic wave localization and focusing for enhanced harvesting. Since PnCs require the unit cell size that is comparable to the wavelength, low frequency acoustic energy localization and harvesting can only be achieved with considerable lattice constants, inevitably causing volume issues for practical applications. In contrast, sub-wavelength structural designs of acoustic metamaterials (AMMs) based on local resonance allow us to achieve the desired functionalities with the benefit of much reduced operating volume. Considering the importance of spatial efficiency and easy fabrication, a planar defected AMM design was reported with the theoretical analysis on its acoustic bandgap, wave localization, and harvesting performance.[264] Ma *et al.* reported the dual functionality of a deep sub-wavelength membrane-type AMMs where hybridized resonances served the total sound absorption with no reflection with an additional harvesting functionality.[265] Similar membrane-type AMM designs with the dual functionality of noise insulation and harvesting follow as in Refs. 266 and 267. A coiling-up space structure offers a feasible way to tune and elongate the propagating path within a limited volume. A subwavelength-scale acoustic metastructure, consisting of an array of doubly coiled-up AMM cavities, was proposed for the strong confinement and harvesting of the sound energy.[268] Recent advances include a helix structure-based AMM,[269,270] a compact dual-layer of AMM[271] for low frequency acoustic energy harvesting, and mechanical locally resonant metastructures coupled with piezoelectric energy harvesters for enhanced vibration harvesting.[272]

The long wavelength of acoustic waves that can range up to the meter scales poses a fundamental limit on the miniaturization of relevant acoustic and elastic applications, including energy harvesting. Recently, the concept of a metasurface, a patterned planar structure with a deep subwavelength dimension, has emerged from the desire to manipulate and control acoustic waves on a subwavelength scale.[262,273,274] Phase control of the reflected or transmitted waves by tailoring material or structural designs is the key to the wave manipulation of metasurfaces. Metasurfaces opened doors for tremendous opportunities to realize novel wave functionalities including anomalous refraction,[275] total reflection,[276] full transmission,[277] and total absorption,[278,279] which enable perfect absorbers, broadband focusing lenses, acoustic cloaking, diodes, and vortexes. Various metasurface designs, not many yet though, have recently been demonstrated to implement acoustic or elastic wave focusing, energy confinement, and harvesting as well, including multilateral metasurfaces consisting of labyrinthine units[280] [Figs. 10(e) and 10(f)] and graded resonant metasurfaces based on rainbow trapping.[281]

One more important development we cover here is mechanical metamaterials. Mechanical metamaterials are architected materials that can exhibit unconventional properties or functionalities previously inaccessible, including but not limited to negative Poisson's ratio,[282,283] tunable stiffness,[284] and/or mass density, and even pattern and shape reconfigurability.[285,286] Auxetic metamaterials,[287] pentamode metamaterials,[288,289] and origami-based and kirigami-based metamaterials[290,291] are the representative mechanical metamaterials potentially useful for extensive structural and functional applications, which is well reviewed in Ref. 292. Pertaining to utilizing mechanical metamaterials for energy harvesting, only a few case studies can be found thus far yet. Unique properties and multifunctionalities of mechanical metamaterials are promisingly expected to contribute to flourishing the energy harvesting research field beyond enhancing output performance. Achieving controlled trapping of elastic strain energy via programmed structures that has been reported as energy absorbing materials[293] can be possibly utilized for energy harvesting. Triboelectric nanogenerators embedded in mechanical metamaterials demonstrated not only the tunable mechanical properties inherited by the mechanical metamaterials but also energy harvesting and self-powered deformation sensing capabilities.[294]

3. Challenges and future prospects

Manmade structures, such as phononic crystals and metamaterials, have experienced a remarkable development of uncovering unconventional effective material properties and wave functionalities that can break the traditional limits in acoustic and vibration engineering over the last two decades. A multitude of innovative concepts and designs have been proposed along with theoretical basis behind the novel characteristics of metamaterials, followed by experimental validations sometimes in the later years. Now the field is moving to enter the next level where real-world applications of the recently developed phenomena come into the picture. Viewed in this context, energy harvesting is one of the great candidate applications that can benefit from the wave manipulation capability of metamaterials. Research advances of drastic power-enhanced energy harvesting using various types of metamaterials reviewed in this article are the evidence. As still in the early stage of research, there remain substantial challenges to overcome, from which we can identify tremendous research opportunities.

First, we need more innovative metamaterial design schemes that can further increase the degree of input wave energy amplification either by focusing or localization toward the target location for harvesting. In addition, such energy focusing or localization should take place in a wide range of frequencies for broadband operation. Phononic crystals derive their bandgap features from the multiple scattering, thus not based on resonances. Maximizing the bandgap of phononic crystals via geometry or material property tailoring can be a solution to broaden the operating bandwidth. In contrast, local resonance-based acoustic metamaterials or metasurfaces have an inevitably intrinsic issue of narrow working bandwidth while offering advantages of subwavelength or even ultrathin subwavelength scales. Ideas for possible solutions can be drawn upon the coherent perfect absorption approach[295] and the integration of multiple metamaterials or metasurfaces over different frequencies,[296] both of which were utilized to realize broadband perfect absorbers. In order to develop metamaterials-based energy harvesting adaptable to the environmental changes including frequencies, active metamaterials that have capability to tune the bandgaps as well as the resonance properties by changing effective properties like stiffness in real-time can also be considered as well.

Size reduction also matters. The wavelength of acoustic and elastic waves range from millimeters to centimeters. In this regard,

subwavelength structures such as locally resonant metamaterials and metasurfaces have received considerable attention and deserve further study to realize focusing and harvesting functionalities. Mechanical metamaterials also offer compactness within a finite volume, making it possible to realize portable sensing and energy harvesting applications. Considering that the first experimental demonstration of pentamode mechanical metamaterials appeared only in 2012,[288] it is no wonder that only very few article can be found on mechanical metamaterial for energy harvesting applications. Hence, there are vast opportunities in exploring intriguing mechanical metamaterial concepts that already exist and will be reported in the near future for energy harvesting purposes.

Developing machine learning-based design algorithms is necessary to identify metamaterials suitable for specific target applications and such artificial intelligence-based design methodology is not just applicable to energy harvesting but to all metamaterial-related applications.[297–299] The present fabrication technology is limited to individual custom-made metamaterial specimens using laser-cutting or 3D printing. Together with the advances in 3D printing technology for mass production, automated fabrication processes for both metamaterials and energy harvesting devices are required in order to make this technology include viable commercialization.

Once input wave energy is amplified through metamaterials, efficient energy transfer from metamaterials to energy harvesting devices becomes important.[300] In that regard, acoustic or mechanical impedance mismatch between metamaterials and piezoelectric energy harvesting devices can pose a challenge. Therefore, it is required to identify energy harvesting device designs and operating conditions that allow impedance matching, which can vary depending on the input source: sound in air or underwater, elastic waves in a plate, mechanical vibrations. Frequency alignment between energy harvesting devices and metamaterials is also an important factor to consider. When the resonance and the bandwidth of the energy harvesting devices coincide with those of metamaterials, the output harvesting performance can be maximized. Both impedance matching and resonance tuning can be realized by tailoring constituent material and geometric properties of metamaterials and energy harvesting simultaneously.

4. Concluding remarks

Metamaterials, starting from optics and having been extended to acoustics and mechanics, have fascinated scientific community in various fields due to their novel properties and functionalities that break the conventional barriers. The wave control capability of metamaterials has recently infiltrated into energy harvesting research and proved their potential for drastic enhancement in harvesting performance using vibration, sound, and elastic waves. Metamaterials-based energy harvesting undoubtedly offers a promising way to realizing sufficient power generation suitable for practical applications but still poses challenges, such as broadband operation, size reduction, impedance matching, and frequency tuning. Innovative metamaterial designs and deep physical understanding of the mechanisms at the interface between the metamaterial and the energy harvesting device will underpin the next generation of metamaterial-based energy harvesting.

5. Acknowledgments

This research was supported by the National Research Council of Science and Technology (NST) grant by the Korean Government (MSIP) (Grant No. CAP-17-04-KRISS) and the Creative Materials Discovery Program through the National Research Foundation of Korea (NRF) funded by the Ministry of Science and ICT (Grant No. 2018M3D1A1058794).

C. New emerging materials for multi-modal piezoelectric generators: Organo halide perovskites

Kai Wang, Yuchen Hou, Shashank Priya (*sup103@psu.edu)

1. Abstract

Halide perovskites (HPs) have emerged as a promising solution-processible material in the field of photovoltaics and optoelectronics. Recently, broader applications of these modified perovskite materials in mechanical energy harvesting have been proposed due to their high dielectric and piezoelectric properties that are analogous to those of conventional inorganic piezoelectric materials. At this juncture, fundamental origin of ferroelectric and piezoelectric properties of organohalide perovskites remains under investigation. Results reported in literature, such as high piezoelectric coefficient of ~25 pm/V in $MAPbI_3$ perovskite[301] under illumination, ferroelectric domains,[302] and optically enhanced piezoelectric properties of halide perovskite films,[302,303] imply that these materials will have relevance in multimodal energy harvesting. In this perspective, we describe recent theoretical and experimental advances in understanding the dielectric and piezoelectric properties of halide perovskite materials followed by a brief outlook on the challenges and prospects for HP-based Multimodal Piezoelectric Generators (HP-MPG).

2. Motivation

Halide perovskites (HPs) have been well recognized in photovoltaics and hold the potential to be engineered into a piezoelectric material. This could induce the possibility to simultaneously harvest multiple type of energy sources using a single material. Prior reviews mostly focus on the single applied area of HPs. Besides the revisit to the frontier research on these materials, we also discuss the opportunities to simultaneously harvest different types of energies using an advanced device with HPs.

3. State-of-the-art in piezoelectric organohalides

Halide perovskites (HPs) are ABX_3 *"perovskite"* structured crystals with A-site occupied by monovalent cations caged in the $[BX_6]^{4-}$ corning-sharing octahedra network. Figure 11(a) shows the lattice structure of perovskites represented by formulation ABX_3. The wide range of options available for each crystallographic site enables thousands of combinations for developing new materials within the generic constraint of the Goldschmidt tolerance rule. Under the applied mechanical or electric field, dynamic tilting of the octahedra and orientations of the A-site polar cations drives the dielectric properties of perovskites. Figure 11(b) shows the molecular ordering based on the alignment of the A-site dipolar molecule.

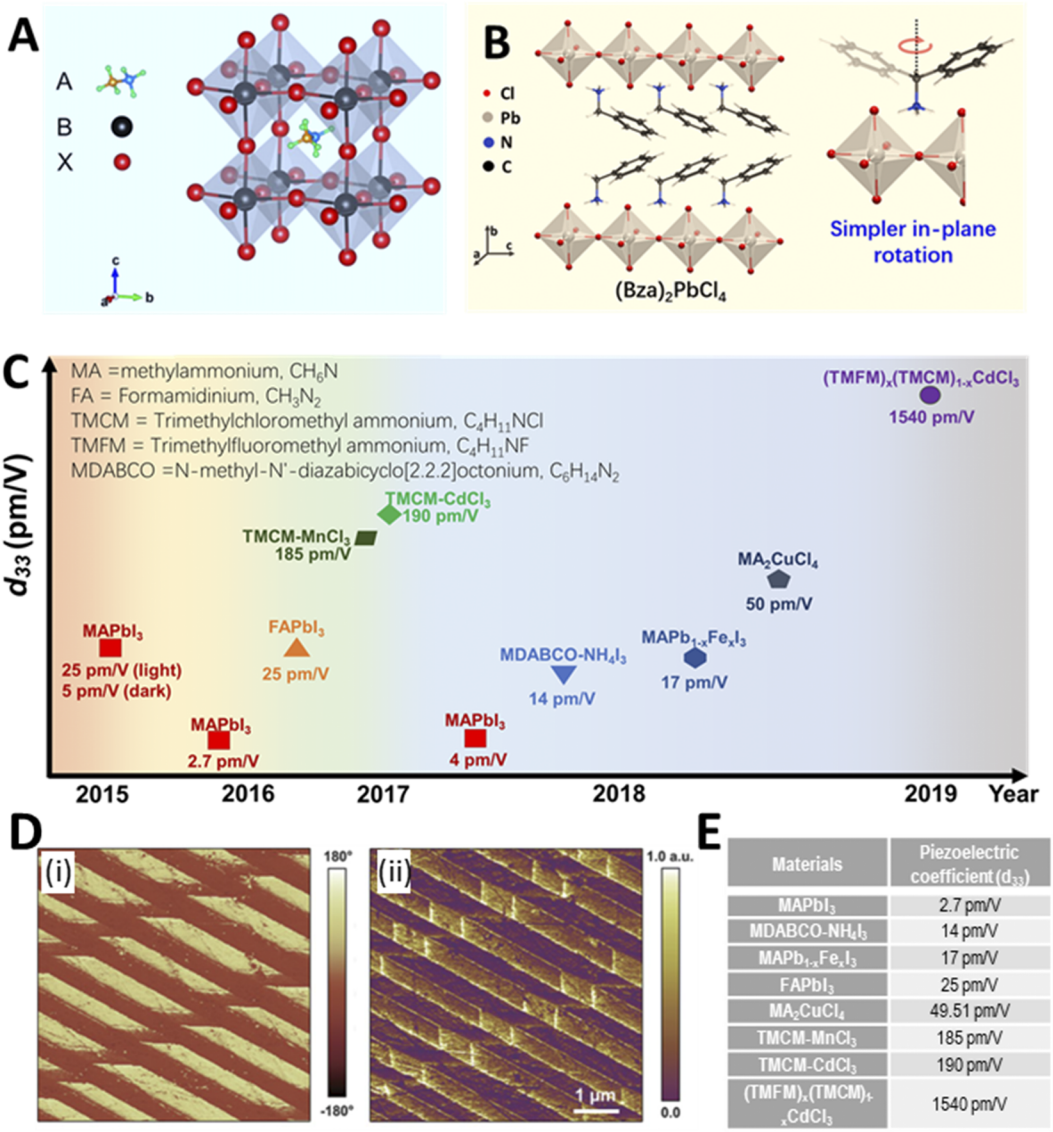

Materials	Piezoelectric coefficient (d_{33})
$MAPbI_3$	2.7 pm/V
$MDABCO\text{-}NH_4I_3$	14 pm/V
$MAPb_{1-x}Fe_xI_3$	17 pm/V
$FAPbI_3$	25 pm/V
MA_2CuCl_4	49.51 pm/V
$TMCM\text{-}MnCl_3$	185 pm/V
$TMCM\text{-}CdCl_3$	190 pm/V
$(TMFM)_x(TMCM)_{1-x}CdCl_3$	1540 pm/V

FIG. 11. (a) Schematic crystal structure of ABX_3 *"perovskite."* Adapted with permission from Wang *et al.*, Sol. Energy Mater. Sol. Cells **147**, 255 (2016).[312] Copyright 2015 Elsevier B.V. All rights reserved. (b) Molecular origin of polarization in a 2D perovskite: spinning of the A-site polar cation. Adapted with permission from Li *et al.*, Nat. Commun. **8**, 16086 (2017).[313] Copyright 2017 Springer Nature. (c) List of d_{33} values in multiple organohalide perovskites. Data are obtained from various resources. (d) Domain structures of $TMCM\text{-}MnCl_3$ seen in PFM images constructed by (i) phase and (ii) amplitude signal of the out-of-plane piezoresponse. Adapted with permission from You *et al.*, Science **357**, 306 (2017). Copyright 2017 AAAS. (e) Table summarizing the piezoelectric coefficient (d_{33}) of the reported organo halide perovskite materials. Data are obtained from various resources.

Recently, Govinda *et al.* reported the tetragonal–orthorhombic phase transition in both $MAPbI_3$ and $MAPbBr_3$ perovskite during a cooling process and suggested that the dipole from MA^+ units prominently contributes to dielectric value of the whole material.[304] In addition, illumination induced charge excitation also modulates the dielectric constant from ~10^3 (dark) to ~10^6 under AM 1.5 illumination.[301] Extrinsically doped/substituted HP materials, such as $(Me_2NH_2)PbI_3$, $(benzylammonium)_2PbCl_4$, $(3\text{-}pyrrolinium)CdCl_3$, $Me_3NCH_2ClMnCl_3$, $TMCM\text{-}CdCl_3$, show high dielectric properties and exhibit a characteristic Curie-temperature (T_c).[305–307] Coll *et al.*[301] first observed a giant increase of piezoelectric coefficient (~25 pm/V) upon illumination of HP, compared to 5–6 pm/V in dark, corresponding to the formation of large photoinduced dipole moments through the molecular orientation of MA^+ unit in the lattice. Dong *et al.*[308] directly measured the effective piezoelectric coefficient (d_{33}) of 2.7 pm/V in $MAPbI_3$ single crystal. Song *et al.*[309]

found that casting of the HP film on epitaxial PZT could further enlarge its d_{33} to ~4 pm/V. By engineering the composition derived from the prototype $MAPbI_3$, higher figure-of-merits such as effective piezoelectric coefficient (d_{33}) of ~25 pm/V in $FAPbBr_3$ nanoparticles, ~17.0 ± 6.0 pm/V in $MAPb_{1-x}Fe_xI_3$ films,[310] 49.51 pm/V in MA_2CuCl_4,[311] and 185 pm/V in TMCM-$MnCl_3$ (with a T_c of 406 K, higher than that of BTO[306]) have been achieved [Fig. 11(c)]. Figures 11(d-i) and 11(d-i) show the typical piezoelectric force microscopy (PFM) phase and amplitude images of the TMCM-$MnCl_3$[306] as an example, where the characteristic piezoelectric domains with lamellar-shape structure are clearly observed. The piezoelectric performance (d_{33}) of the above-mentioned HP materials is also listed in the table in Fig. 11(e) for better comparison. It should be noted that compositional engineering and thus design of the new HP material could provide effective d_{33} over 10^3 pm/V. Such a compositional design strategy provides foundation for developing the roadmap for HP-based piezoelectrics. In addition to piezoelectric properties, HP materials are also attractive due to their simplified processing such as low-temperature, solution-spinning and cost-effective single-step synthesis route. The large potential design capacity of this material in combination with optical and mechanical response could provide tremendous potential for developing new generation of multi-modal energy harvesting technologies. These materials will be responsive to mechanical and optical stimulations simultaneously due to their piezoelectric and photovoltaic behavior. Furthermore, these materials can be tailored to respond to thermal excitation by tuning their thermal conductivity and Seebeck coefficient.

HP based piezoelectric generators can scavenge mechanical energy from ambient environment and convert it into useful electrical energy. In comparison to traditional inorganic oxide perovskites, which require complicated synthesis processes such as high-temperature calcination and sintering, HP materials could be easily integrated onto target substrates using solution-processing based techniques. Furthermore, they can provide ability to respond to low acceleration levels (<0.1g). In 2015, Kim *et al.*[314] measured the output performance of piezoelectric generator based on the $MAPbI_3$ perovskite thin film casted by a spin-coating process. Figure 12(a) shows the device structure which consists of a $MAPbI_3$ thin film inserted between two electrode layers of PET/indium–tin oxide (ITO) and Au/Ti/PET. After poling, the device exhibits a peak voltage of 2.7 V with a current density of 140 nA/cm^2 under 0.5 MPa stress normal to the surface on an active area of 1 × 1 cm^2. Liu *et al.*[303] theoretically calculated the effect of the atomic substitution on the piezoelectric behavior. They found that the displacement of the lattice B-site cation contributes to most of the piezoelectric response of the material and the competition between A-X hydrogen bond and B-X metal-halide bond in HP material dominates its piezoelectric properties. Ippili *et al.*[310] developed the Fe-doped HP with formulation of $MAPb_{1-x}Fe_xI_3$ (x = 0.07) exhibiting polarization of ~1.6 μC/cm^2 and a corresponding piezoelectric device with output performance of ~7.29 V as well as a current density of ~0.88 μA/cm^2 after poling at 30 kV/cm. This magnitude is much higher than that from the $MAPbI_3$ device and could power a commercial red LED [Fig. 12(b)].

In addition to the mechanical energy harvesting, the HP-based devices can be used for sensing light due to their excellent optical properties. Eom *et al.*[315] reported self-powered pressure and light-sensitive bifunctional sensor using a CVD-$MAPbI_3$ HP films. They

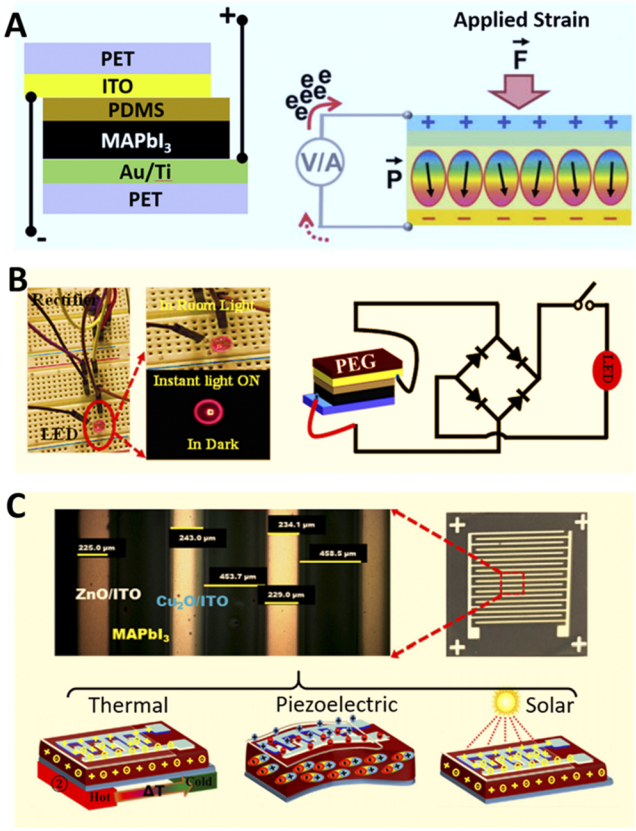

FIG. 12. (a) A piezoelectric device using $MAPbI_3$ and corresponding working mechanism. Adapted with permission from Kim *et al.*, J. Mater. Chem. A **4**, 756 (2016). Copyright 2016 The Royal Society of Chemistry. (b) Photograph of the instant LED light during applied mechanical pressure and its schematic rectifying circuit diagram for powering the LED. Adapted with permission from Ippili *et al.*, Nano Energy **49**, 247 (2018). Copyright 2018 Elsevier Ltd. All rights reserved. (c) Device configuration and working mechanism for harvesting thermal, mechanical, and solar energies. Adapted with permission from Jella *et al.*, Nano Energy **52**, 11 (2018). Copyright 2018 Elsevier Ltd. All rights reserved.

found that CVD-$MAPbI_3$ exhibits better stability than solution-prepared samples as solvents such as DMF and DMSO could induce the intermediate solvent–perovskite complexes that can interact with humidity. The device generates output voltage due to intrinsic piezoelectric coefficient of $MAPbI_3$ films and exhibits sensitivities of 8.34 mV kPa^{-1} and 0.02 nA kPa^{-1}. In terms of the light-stress bimode operation, the response time for applied pressure and light is 0.066 and 0.320 s, respectively, under a pressure of 30 kPa. Such a design could be the pathway for self-powered portable electronics and wireless sensors.

The multi-energy sensitivity of HP materials as well as their wide range of properties, such as excellent electronic band structure, ambipolar feature, ferroelectric nature, and ultra-high Seebeck coefficients, is opening new opportunities for multimodal energy conversion by harvesting multiple ambient energies, such as thermal, mechanical, and solar. Multimodal devices incorporating HP

materials to simultaneously harvest thermoelectric, piezoelectric, and solar (TPS) energies are being proposed recently. Jella *et al.*[316] developed the TPS-multimodal energy harvesting device consisting of interdigitated electrodes (IDEs) and multifunctional $MAPbI_3$ to harvest thermal, mechanical, and solar energies. Figure 12(c) shows the architecture and operating mechanism of the TPS-device. The device exhibits a thermoelectric performance of 0.012 nW at ΔT of 15 °C, a piezoelectric performance of 1.16 V and 0.61 μA under 0.2 MPa, and a solar cell performance with a V_{OC} of 0.8 V and J_{SC} of 0.014 mA/cm^2. This multimodal device design introduces an innovative framework for self-powered, portable, and mobile electronic systems. However, questions about the interaction between each type of energy harvesting mechanism remains unknown. For example, is there any coupling between harvesting energy from light, heat, and mechanical stress? How do they mutually affect each other and how to quantify these coupling effects? From molecular level, piezoelectric relies on the mechanical strain to change the lattice and induce the electric dipole alignment that eventually generates electricity. For semi-conductive materials, such as HP, not only the intrinsic leakage (semiconducting nature) but also the strain induced electronic band structure change will interfere the dipole dynamics during the piezoelectric process. Moreover, secondary or higher-level dynamics within the lattice (photon and thermal effect) will also be involved in these HP materials (due to their "soft lattice" nature) and eventually affect the piezoelectric process. These more complex questions and underlying physics will need expertise from cross-disciplinary teams and more investigations from different perspectives in a collaborative framework.

Another concept being investigated is the composite consisting of HP and polymeric matrix. Ding *et al.*[317] reported a composite film, comprising $FAPbBr_3$ HP nanocrystals uniformly distributed in a PDMS polymer matrix, and inserted between ITO/PET substrate and an aluminum foil to assemble a piezoelectric generator device. The poled device (50 kV/cm) exhibits an output voltage of 8.5 V and a current density of 3.8 μA/cm^2, when tested under 0.5 MPa of vertical compression at a frequency of 6 Hz. The generated output was stored in a capacitor to drive a commercial red LED. Dhar *et al.*[318] reported another polymer composite nanogenerator using $MAPbI_3$ and PDMS and observed a significant lattice-defect-induced piezoelectric responses. The increase in the lattice B-site defects will enlarge the ionic polarization, which in turn enhances the permittivity and thereby piezoelectricity. The device fabricated with 5 wt. % PDMS composite generated voltage of over 100 V with a maximum power density of 0.3 mW/cm^3, which could illuminate 30 commercial blue LEDs. PVDF has also been used as the matrix, which could provide better dispersion of the perovskite nanocrystals. Ding *et al.*[319] demonstrated a $FAPbBr_3$-PVDF composite for piezoelectric nanogenerators displaying highest outputs with a voltage of 30 V and current density of 6.2 μA/cm^2. A uniform-distribution is key to transfer the stress and induce a more efficient piezoelectric behavior at device level. Sultana *et al.*[320] synthesized $MAPbBr_3$ nanoparticles and embedded them into the PVDF matrix in the form of nanofiber processed by electrospinning. These composite fibers exhibit acoustic vibration with a high degree of acoustic sensitivity of ~13.8 V Pa^{-1} and efficiency of 58.5%. Due to the wide scope of variety of HP composition, other HP materials, such as $MAPbI_3$[321] and MA_2CuCl_4,[311] have also been incorporated as filler in the HP-PVDF composite for piezoelectric generators.

4. Current and future challenges

Self-sustainable, self-power technologies are becoming important not only because of the growing adoption of portable and mobile electronic implementations and edge/node sensors but also due to the fast integration of cloud computing, remote-communication, and Internet of thing (IoT) technologies. Harvesting ambient energy, such as acoustic and mechanical vibration, through piezoelectric effect can be one of the promising solutions. In the earlier discussions, we have highlighted intriguing facets of HP materials in terms of piezoelectric generators. Compared to their inorganic counterparts, these HP materials are advantageous in terms of facile low-temperature processing and hybrid material nature that combines both organic and inorganic solids at a molecular level. From manufacturing level, HPs are good candidates for the roll-to-roll fabrication and excellent compatibility to target systems with specific flexibility requirement. So far, there has been limited research on the HP-based piezoelectric generators, but the interest is growing rapidly. To achieve sustainable progress, several essential aspects that need to be investigated are summarized below:

(i) *Stability.* The intrinsic structural instability, such as phase instability and their extrinsic thermal/optical/ambient instability, need to be considered and addressed. Although multiple encapsulation techniques could boost their extrinsic stability against various environmental stimulus, improving their intrinsic instability still requires significant research efforts. Strategies, such as lattice strain engineering, and atomic-scale entropic modification might be potential directions.

(ii) *Novel material exploration.* The wide tunability of the perovskite ranging from crystallographic substitutions at atomic scale to crystal phase modulation and structural dimensionality, and to nanocomposites (0D, 1D, 2D, 3D, hierarchical nanoparticles, etc.) provides opportunity to design material architectures with suitable electromechanical parameters. Designing new compositions and microstructures and studying their piezoelectric and other relevant fundamental properties will provide pathway to improve the energy harvesting capabilities.

(iii) *Clarification between multiple energetic stimulus.* The HP materials are responsive to multiple energetic stimulus such as optical, thermal, mechanical, electrical, and even magnetic signals. Each of them may incorporate a coupling effect that could be mutually affected by each other from the material to device level. Decoupling them to gain more fundamental understanding, particularly at the nanoscale level, and/or manipulating their synergistic effects for energy harvesting might be excellent research direction.

(iv) *Device-level research.* Research and development at the device-level could provide practical direction to compare performance with current generation piezoelectric sensors and generators. This could improve the performance of HP-based piezoelectric device for mechanical energy harvesting, design of the photoferroelectric and photopiezoelectric devices, developing hybrid energy harvesters for multi-source energy harvesting, and developing eco-friendly, flexible, and high-performance devices.

5. Concluding remarks

In summary, HP materials are emerging as a new class of piezoelectric materials with advantages of simpler-processing and large compositional/structural tunability. The research on the HP-based piezoelectric materials is in early stages with much work required to improve the material properties and device implementation. With the growing research on inventing novel HP materials exhibiting variety of multifunctional properties, including piezoelectric, thermoelectric, and photovoltaic, there is significant opportunity to realize new generation of multimodal harvesters. We envision that future investigations in the field of HP materials will be more cross-disciplinary as it requires knowledge from multiple domains to resolve the intrinsically coupled effects.

6. Acknowledgments

K.W. acknowledges the financial support through SBIR Program through Nanosonic. K.W. also acknowledges IEE Stewardship Seed Grant Program (Penn State). S.P. would like to acknowledge the financial support from Office of Naval Research through Award No. N000141912461. Y.H. acknowledges the support through the National Science Foundation (Award No. 1936432).

D. Smart polymer materials for triboelectric and piezoelectric nanogenerators

Wei Xu, Jianhua Hao (*jh.hao@polyu.edu.hk)

1. Abstract

As important mechanical energy transfer devices, triboelectric nanogenerators (TENGs) and piezoelectric nanogenerators (PENGs) have achieved fast development and shown various applications. Polymers are playing critical roles in TENGs and PENGs, and especially, smart polymer materials (SPMs) possessing ability of responding to the external stimuli are attracting increasing attention for their combinations with TENGs and PENGs. Considering the outstanding advantages of these nanogenerators combining SPMs and the lack of relevant overview, here we briefly summarize the progress about the integration of SPMs with TENGs and PENGs. Meanwhile, some challenges and opportunities based on the status of this research field are presented and discussed.

2. State-of-the-art

Triboelectric nanogenerators (TENGs) and piezoelectric nanogenerators (PENGs) can generate electric output by converting ambient mechanical motions with broad frequency and scale range. This ability enables them to be the potential complement of traditional power sources and become an ideal candidate for forming self-sufficient system and powering emerging electronics.[20,28,322] Among them, TENGs, working based on triboelectric and electrostatic effects, possess various unique advantages and their fabrication requires using amount of polymers as contact materials, substrates, or spacers. The properties of the employed polymers will obviously affect the performance of TENGs.[323–327]

Compared to traditional polymers, smart polymer materials (SPMs), a special type of polymers that possess the inherent ability of making response to the external stimuli,[328] have been attracting considerable attention in the field of nanogenerators. The external stimuli to trigger SPMs could be temperature, light, and solvent. Under these stimuli, SPMs will generate the corresponding responses and show certain changes in one or more aspects, such as shape, color, and conductivity.[328,329] The common stimuli and corresponding responses for SPMs are shown in Fig. 13.

Given the unique stimuli-response ability, the integration of SPMs into TENGs is considered as a feasible approach to conceive devices with attractive functions. Based on the current achievements, the purpose of combining SPMs with TENGs can be broadly classified into two aspects:

a. To improve the certain performance of devices. In this case, the most typical example is to enhance output signals of TENGs by using piezoelectric and ferroelectric polymers, such as polyvinylidene fluoride (PVDF) and poly(vinylidenefluoride-*co*-trifluoroethylene) [P(VDF-TrFE)], as the triboelectric materials of TENGs. By means of the electrically induced piezoelectric/ferroelectric polarization, the surface charge density of triboelectric materials is significantly increased, leading to an enhancement in electric output. This improvement can be attributed to the shift in Fermi level of poled polymers instead of the piezoelectric effect.[330,331]

Another representative example is the use of healable polymers in TENGs for improving their lifespan and durability.[332–334] Healable polymer is one type of SPMs that enables fractures healing under certain stimuli. Specifically, the healing can be realized by means of the existence of some special bonds, including dynamic covalent bonds, reversible covalent bonds, and non-covalent bonds, in the molecular structures of healable polymers. These bonds enable the molecular chain diffuses on fracture interface and the re-building of broken bonds to achieve the recovery in structure and characteristics.[335,336] The healing process usually requires some external stimuli (e.g., temperature), while part healable polymers can

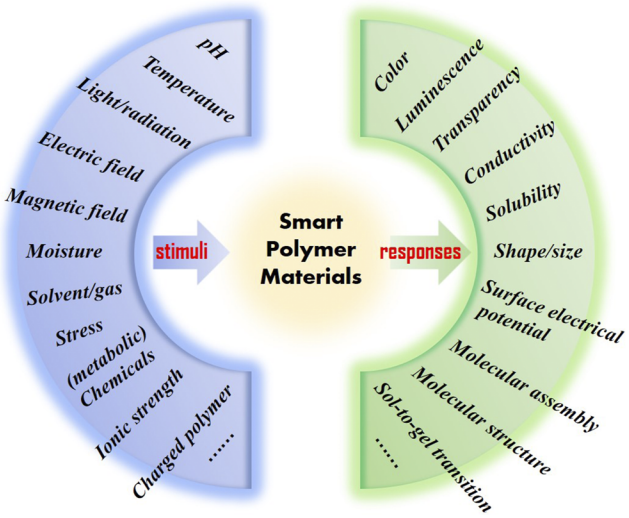

FIG. 13. The stimuli and response for smart polymer materials.

fulfill the healing process under ambient conditions, which is categorized as autonomously healable or self-healing polymers.[336,337] By employing healable polymers as constituent materials, the achieved healable TENGs are endowed with healability to recover the structure and performance when fracture has occurred, which could improve the durability, lifespan, and reliability of devices. On the other hand, the mechanical energy conversion of TENGs requires frequent mechanical impacts, which easily leads to the failure in both material and device. Therefore, the combination of healable polymers with TENGs is practically significant. In addition, attributed to healability, healable TENGs also present shape-tailorability and shape-adaptability for broadened application range.[338–340]

Numerous healable polymers have been prepared for forming healable TENGs, as summarized in Table II. Among them, self-healing TENGs using autonomously healable polymers can conduct the recovery without stimuli but usually show weak inherent mechanical strength. The reason is that autonomously healable polymers usually require the low glass transition temperature (T_g) for effective molecular chains diffusion under ambient conditions. In contrast, the stimuli triggered healable polymers perform higher mechanical properties. For instance, a thermal triggered healable polyurethane with tensile strength of about 10.5 MPa has been recently reported by our group for TENGs.[341] It should be mentioned that the recovery in electric output of TENGs mainly depends on the healing of electrodes conductivity.[342] The traditional electrodes used in healable TENGs usually consist of conductive fillers, and their conductivity recovery depends on the simple recontact of broken electrodes that need to be fixed and remained by the healed polymer substrates. Some TENGs, therefore, include intrinsically healable electrodes, such as hydrogel or magnetic electrodes, to arrive the fast healing of performance, where healable polymer substrates will mainly be charge of the mechanical property recovery of devices.[338,343]

To enhance the output performance of TENGs, microstructures usually are fabricated on the surface of the triboelectric layers. These microstructures can increase the effective contact area, but they may suffer from collapse and damage under strenuous mechanical impacts, causing the failure in performance and stability of TENGs. This obstacle can be overcome by employing shape-memory polymers as constituent materials of microstructures. Shape-memory polymer is a class of SPMs capable of retaining a temporary shape and recovering to its original permanent shape via transforming from any temporary shape in the presence of an external stimulus.[356] That means the deformed shape-memory polymer-based microstructures can recover to the original morphology under stimuli, leading to the recovery of device normal state and the improvement in stability and durability of TENGs.[356] Similarly, the recovery and renewal of distorted microstructures can also be realized by using the light-transformable polymer as constituent materials.[340] Another role of shape-memory polymers in TENGs is to serve as the main material instead of microstructures materials to improve shape-adaptability of device.[357]

TABLE II. Comparison of healable polymers employed in TENGs.

Polymer	Dynamic bonds or structure	Stimuli	Healing efficiency (%)	Tensile strength
H-PDMS[344]	Imine bonds	Room temp (12 h)	94	120 kPa
HTS-PDMS[345]	Bipyridine groups-zinc ions metal–ligand	Room temp (30 min)	~100	~70 kPa
CNT-putty composite[346]	Boron–oxygen bonds and hydrogen bonds	Room temp (40 min)	92	~12 kPa
IU-PDMS[347]	Imine bonds and quadruple hydrogen bond	Room temp (24 h)	~100	1.09 MPa
Healable PPUH polymer[348]	Fe(III)–PDCA interactions and quadrupolar hydrogen bonding	Room temp (24 h)	98.2	~1.4 MPa
Healable poly(dimethylsiloxane) elastomer[349]	H bonds	Room temp (72 h)	98	1.27 MPa
MWCNTs-UPy/IU-PAM[347]	Imine bonds and quadruple hydrogen bonds	Room temp (36 h) Near-infrared (NIR)	97 88	2.13 MPa
PVA/agarose hydrogel[350]	Boron–oxygen bonds and crystallites	Water/NIR	93	83 kPa
PVA/PDAP/graphene hydrogel[351]	Hydrogen bonds	Room temp (60 s) NIR (30 s)	98 94	85 kPa
Laponite/poly(AMPS-co-AA-co-DMAPMA)/GO–LiCl hydrogel[352]	Hydrogen bonds	Heat	99	106 kPa
Epoxy based polysulfide[353]	Disulfide bonds	NIR	90	2.6 MPa
Healable PU-PDMS[338]	Disulfide bonds and hydrogen bonds	Room temp (1 h) Heat	56 97	0.87 MPa
Vitrimer elastomer[354]	Disulfide bonds	Heat	~100	1.3 MPa
Healable polyurethane acrylate[339]	Multivalent H-bonds	Heat	45.1	~7 MPa
Healable PU[341]	Disulfide bonds	Heat	96.7	10.5 MPa
Poly(hindered urea)[355]	Bulky urea linkages	Heat	>95	1.7 MPa

Another strategy proposed by our group to improve the device's durability and robustness is the fabrication of magnetic-assisted non-contact TENGs by coating a magnetic responsive polymer composite layer on the surface of device. The interaction between triboelectric materials, therefore, can be remotely controlled by the motion of external magnet via magnetic field mediation. This will avoid the direct mechanical impact to TENGs and, therefore, delay the device failure, leading to improvements in the device's durability.[358,359]

b. To develop new application of TENGs. It is known that the amplitude of electric outputs of TENGs depends on the coupling effects of a few factors, including the contact area between triboelectric materials, the friction surfaces properties, and the electrodes conductivity. For the TENGs combining SPMs as constituent parts, the SPMs employed in the energy device may generate certain responses to the external stimuli. Once these responses of SPMs can affect the above factors, the electric output of TENGs will be correspondingly changed. This enables TENGs to serve as sensors that are capable of detecting these external stimuli by observing output signal change. Therefore, a series of stimuli sensors based on TENGs have been developed,[360–363] such as the ammonia sensor based on ammonia-responsive resistance change of polyaniline electrode,[363] and the temperature sensor based on heat triggered morphology recover of shape-memory polymer-based friction surface.[360]

On the other hand, the electricity generated by TENGs can perform as a stimulus to trigger the electrically responsive polymers. The common electrically responsive polymers mainly include piezoelectric polymers, dielectric elastomers, electroluminescence, and electrochromic polymers, and they can produce the corresponding responses, including the deformation, luminescence, and color change, to the electric stimuli for further application. By combining TENGs with electrically responsive polymers, a series of TENG driven systems have been developed as actuator, artificial muscle, and memorization.[364–367] Since the widely distribution of mechanical energy is available, these TENG driven systems will show self-powered ability of harvesting energy from operation environment as the power supply themselves. This brings them potential advantages for application in portable and implanting electronics, and some remote occasions.

Similarly, for PENGs working based on the piezoelectric effects, they can also drive electrically responsive polymers to arrive the self-powered smart systems.[368] Meanwhile, SMPs also contributes to the performance improvement of PENGs. The most important and representative SPMs used for PENGs are supposed to be the piezoelectric polymers, such as PVDF and its copolymers. Just as its name implies, piezoelectric polymers can perform the piezoelectric behavior of generating electricity when the mechanical force is applied on it (direct piezoelectric effect) and vice versa (converse piezoelectric effect), which directly leads to the birth of polymer-based PENGs.[369,370] Compared with the piezoelectric ceramics possessing higher piezoelectric coefficient in regular PENGs, piezoelectric polymers usually show better flexibility, facile processing, and lower density. This endows the polymer-based PENGs with good flexibility and robustness for suitable application in some occasions demanding large deformation and strong mechanical impact.[369,370] For acquiring piezoelectricity required by PENGs, piezoelectric materials usually need accept the "poling" treatment for oriented alignment of dipoles by being applied strong electric field at phase transition temperature. However, for some piezoelectric polymer nanowires prepared by electrospinning and template-wetting technique, the orientation of dipoles can be formed during nanowire's growth without further treatment.[20,371] The corresponding nanowire-based generators present an improved energy conversion efficiency. Besides, the ferroelectric polymer with the spontaneous polarization is also a good candidate for achieving polymer-based PENGs without poling procedure.[372]

Similar to TENGs, PENGs' durability is also challenged by mechanical impacts. The combination of healability into PENGs, therefore, is significant from the practical application level. Recently, a lactate-based piezoelectric polymer elastomer was designed by introducing flexible chain segments into the molecular structure.[373] Attributed to the decreased crystallinity, lower glass transition temperature and long linear molecular chain nature, this piezoelectric polymer shows electrical and mechanical healing ability at body temperature, leading to the formation of a healable polymer-based PENG. Besides piezoelectric polymers, PENGs can also be prepared based on piezocomposite, which is a mixture of the polymer matric and the inorganic piezoelectric material. For piezocomposite, the use of SPMs as matric will endow it with additional functions for performance improvement of PENGs. For instance, Yang *et al.* fabricated a self-healing piezocomposite through mixing piezoelectric PZT particles with self-healing PDMS for achieving a fully self-healing PENG.[374] The current achievements about the integration of SPMs with TENGs and PENGs are summarized in Fig. 14.

3. Challenges and future prospects

Despite many SPMs have been successfully coupled with TENGs and PENGs, some challenges and opportunities still exist for extending these concepts into practical operation. One of motivations of using SPMs in nanogenerators aims at improving device's performance. However, for current prototypes, the improvement in certain performance of a device usually accompanies with the sacrifice of some other performances. For instance, healable polymers may improve the device's lifetime and durability by means of the recovery of structure integrity. However, since the usually weaker mechanical strength of healable polymers (especially self-healing polymers), healable devices themselves become easier to be damaged and require more frequent recovery than regular TENGs. For those healable polymers with high strength, their healing process requires external stimuli and severe healing condition. Considering that TENGs and PENGs usually operate under mechanical impacts, to develop and employ some mechanical-compression-triggered healable polymers may be an ideal solution to obtain the devices containing satisfactory mechanical robustness and healing ability in operation environment.[375] Besides, to introduce some fiber fillers into healable polymers also shows the potential for the improvement of the materials' tear resistance for more robust devices. Another performance that is often sacrificed in TENGs combining healable polymers and shape-memory polymers is the electric output, which is because the triboelectric property of most currently prepared SPMs is not situated at extreme positions in the triboelectric series. The surface modification of SPMs may be a possible method for realizing the electric output improvement of devices without

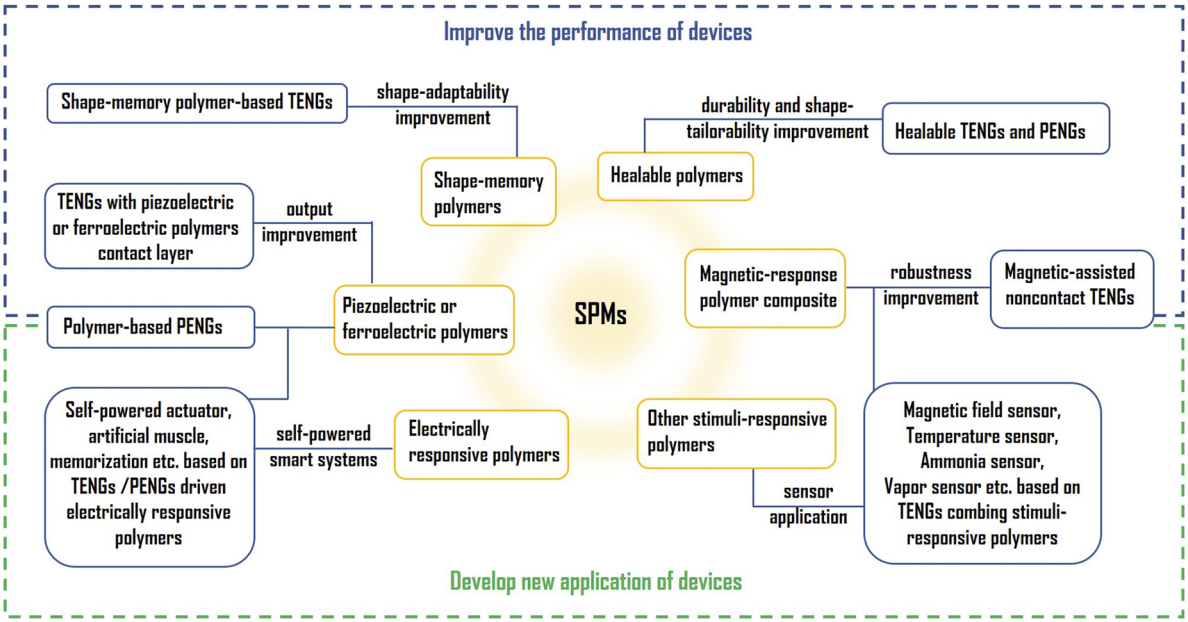

FIG. 14. Schematic diagram showing the motivation and achievement of integrating SPMs with TENGs and PENGs.

compromising the nature of the used SPMs. In our opinion, the key in the future development could be to design SPMs with better comprehensive properties. A compromise on constructing the mechanical energy devices is necessary when considering functionality, mechanical properties, and output performance of the device. Besides, for sensors based on TENGs with SPMs, they detect external stimuli by observing the change in electric output. However, the output of TENGs could be easily affected by various factors, which poses the challenge to the reliability, reproducibility, sensitivity, and selectivity of sensors. The optimized devices may be achieved by means of material and structural design. Because of the randomness of ambient mechanical sources in the nanogenerator driven self-powered smart systems, generating stable and expected electric stimuli by nanogenerators for system operation is still an arduous task. The development of hybrid system and circuit design could be considered as one of the future directions. On the other hand, the application of polymer-based PENGs is partly limited by their low piezoelectric coefficients and thermostability compared to piezoelectric ceramics-based PENGs. Further progress may depend on the development of polymeric candidates or polymer–ceramic composites that may have better piezoelectric properties combining with robustness, low-cost, and, in some cases, biodegradability. It is foreseen that the integration of SPMs with TENGs and PENGs would potentially lead to the formation of devices with more expected performance and application.

4. Concluding remarks

The integration of SPMs with TENGs and PENGs brings additional features and advantages. The purpose of using SPMs in TENGs and PENGs can be mainly classified into two aspects: (1) to improve certain performance of device and (2) to develop new applications. For PENGs, the piezoelectric polymers are the most main constituent materials for the fabrication of polymer-based PENGs. Besides, some challenges and further opportunities are also given.

5. Acknowledgments

This work was supported by the Research Grants Council of Hong Kong (Grant No. PolyU 153025/19P).

V. APPLICATIONS

A. Self-powered flexible piezoelectric acoustic sensors

Hee Seung Wang, Younghoon Jung, Keon Jae Lee (*keonlee@kaist.ac.kr)

1. Abstract

With the emergence of the artificial intelligence (AI) era, voice-based smart device controls have attracted significant attention due to intuitive bilateral communications for human–machine interaction (HMI) in a hyperconnected society. Resonant piezoelectric acoustic sensors are the core technology for highly sensitive and accurate voice recognition in internet of things (IoT) platforms. Future acoustic sensors can be extended to the fields of mobile electronics, smart home assistant, personalized biometrics, and autonomous vehicles. To advance the resonant acoustic sensors as potential candidates for AI-based practical applications, several essential factors should be addressed: frequency band control of flexible membrane, multi-channels for full-cover phonetic spectrum,

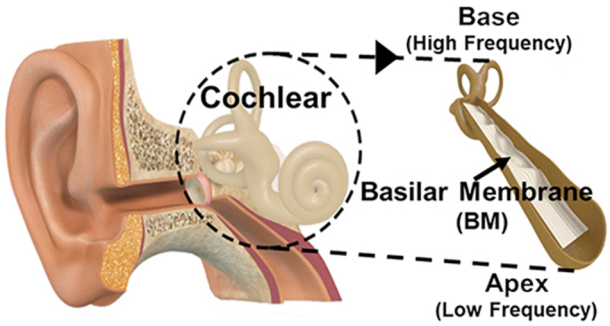

FIG. 15. Schematic illustration of basilar membrane in human cochlea. Asymmetric structure of basilar membrane enables resonant frequency separation over the audible spectrum. Elongated region with thin and elastic membrane (apex) resonates at low frequencies, while shortened region with thicker and stiff membrane (base) responds to high frequencies. Reproduced with permission from Han *et al.*, Nano Energy **53**, 198 (2018). Copyright 2018 Elsevier.

high sensitivity of piezoelectric thin films, and machine learning algorithms for resonant sensors.

2. State-of-the-art

Acoustic sensors convert mechanical oscillations of sound waves to electrical signals for voice recognition. Recently, resonant flexible piezoelectric acoustic sensors have been reported by mimicking the highly sensitive basilar membrane of human cochlea.[376–383] A trapezoidal basilar membrane with ~15 000 hair cell channels has an asymmetric structure to detect numerous resonance frequencies of voice signals.[384] Low frequencies can be resonated in the elongated region of the thin and elastic membrane, while high frequencies can be responded in the shortened region of the thicker and stiff membrane. The basilar membrane sensitively distinguishes the resonant frequencies by gradually changing the width, thickness, and stiffness, as shown in Fig. 15. Voice information converted into the frequency domain is transmitted to the brain in the form of electrical impulses by hair cell channels, which is similar to the piezoelectric mechanism. Inspired by the neuroscience of human nature, it is important to apply a broad coverage of multi-resonant frequencies to flexible piezoelectric acoustic sensors.

The most widely commercialized acoustic sensor is a condenser type microelectromechanical systems (MEMS) microphone measuring the capacitance between two vibrating membranes while applying continuous power.[385] The MEMS sensor presents a flat frequency response of low sensitivity by locating the resonant frequency above the audible sound spectrum. The non-resonant microphones also have drawbacks, including limited single channel, an unstable amplifier circuit, and high power consumption. A highly sensitive flexible piezoelectric acoustic sensor with a multi-frequency band was reported to overcome the disadvantages of a non-resonant MEMS microphone.[381–383] The characteristics of resonant and non-resonant acoustic sensors are compared in Fig. 16. The multi-channel interdigitated electrodes (IDEs) were integrated on the piezoelectric $Pb[Zr_{0.52}Ti_{0.48}]O_3$ (PZT) membrane to respond to sequential resonances induced by a tiny sound wave oscillation. The self-powered acoustic sensor has a curvilinear structure to linearly detect the resonant frequencies of 650, 1080, and 1440 Hz. The first, second, and third mode of resonance were measured in the region of the base, intermediate, and apex membrane, respectively. The combination of a low quality factor and multi-resonant channels enabled flexible acoustic sensor to cover the entire voice spectrum, as presented in Fig. 17(a). The thin membrane has a significant advantage in achieving a low quality factor, which is important for widening the frequency bandwidth. The quality factor is defined by dividing the resonant frequency into bandwidth below 3 dB of the peak value. The resonant acoustic sensor exhibited four to eight times higher sensitivity than the conventional condenser type microphone by resonating in a range from 100 Hz to 4 kHz.

Machine learning based speaker recognition was also demonstrated using the flexible piezoelectric acoustic sensor with multi-channel signals of abundant voice information.[382,383] Fast Fourier transform (FFT) and short-time Fourier transform (STFT) were utilized to convert the voltage waveforms of the time domain into frequency components, as exhibited in Fig. 18(a). Gaussian Mixture Model (GMM) was applied to training and test procedures of voice information for the speaker decision. Figure 18(b) shows the majority voting method for speaker recognition process, which calculates

	Non-Resonant Condenser Type	Resonant Piezoelectric Type
Measurement Type	Capacitance	Voltage
External Power	Required	Self-powered
Sensitivity (Open Circuit)	Low	High
Amplification	Required	Not Required
Data sets	Single Signal	Multi-Signals
Resonance Location	Above Audible Spectrum	In Voice Spectrum
Frequency Response	Flat	Tunable for Voice Band Coverage

FIG. 16. Characteristics comparison of non-resonant condenser type and resonant piezoelectric type acoustic sensor. Non-resonant sensor measuring capacitance has critical drawbacks, including high power consumption, low sensitivity, required amplification, and single channel. Resonant piezoelectric sensor overcomes these disadvantages by exploiting self-powered operation, high sensitivity, multi-channel signals, and tunable frequency response for covering voice spectrum.

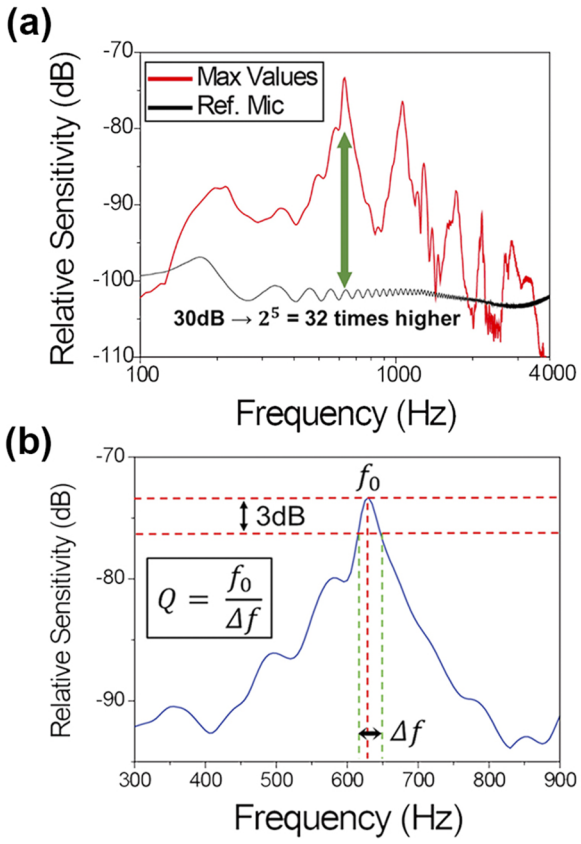

FIG. 17. Frequency response of flexible piezoelectric acoustic sensor. (a) Relative sensitivity of resonant acoustic sensor and conventional reference microphone over the voice frequency range from 100 to 4 kHz. Frequency response of the resonant sensor is achieved by selecting the most sensitive channel value at each frequency. (b) Enlarged relative sensitivity plot of a flexible piezoelectric acoustic sensor under sound frequencies from 300 to 900 Hz. Resonant frequency bandwidth below 3 dB of the highest peak is utilized for calculation of quality factor. Reproduced with permission from Han *et al.*, Nano Energy **53**, 198 (2018). Copyright 2018 Elsevier.

the likelihood of test voice according to each frame by comparing the training and testing results. Figure 18(c) presents the trained STFT features in t-SNE plot that embeds high dimensional data of similar data into a low dimensional space to visualize the probability distribution. The recorded TIDIGITS dataset of a flexible resonant acoustic sensor included 40 speakers consisting of 70 words data for training and 7 words data for testing. Signal averaging was applied to the multi-channel acoustic sensor by selecting the two most sensitive data at each frequency. An outstanding speaker recognition rate of 97.5% was exhibited using the resonant piezoelectric sensor, which reduced the error rate by 75% in reference to a commercial MEMS microphone. The machine learning algorithm was successfully combined with multi-channel data of abundant voice information, which resulted in a superior speaker recognition rate.

A brief overview of flexible piezoelectric acoustic sensors and speech processing was recently reported to suggest synergistic collaboration for AI-based voice user interface (VUI).[383] Biomimetic resonant acoustic sensors were demonstrated using various piezoelectric materials, such as polyvinylidene fluoride (PVDF), aluminum nitride (AlN), and inorganic perovskite PZT membrane.[376–381] In combination with a highly sensitive multi-channel sensor, machine learning methods for speech processing have been discussed, including the Hidden Markov Model (HMM), Deep Neural Network (DNN), and Convolutional Neural Network (CNN). The resonant based flexible piezoelectric acoustic sensors could be advanced by further developments, such as miniaturization, noise filtering, modularization, mass production, and efficient deep learning algorithms.

3. Current challenges and future prospects

Several important technical approaches are included in designing flexible piezoelectric acoustic sensors: resonance frequencies within the voice spectrum, multi-channels for covering the phonetic frequency range, sensitivity enhancement of piezoelectric membranes, and sound recognition based on a machine learning algorithm. The resonant frequencies of an acoustic sensor should be located in the voice spectrum range from 100 Hz to 4 kHz, where most vocal energy is distributed. The resonance frequency is proportional to the membrane thickness and elastic modulus while it is inversely proportional to width and density.[386] The device dimensions can be reduced for downsizing the resonant acoustic sensor by adjusting the geometrical and material parameters. The resonant frequency of the flexible membrane is positioned above the voice frequency range according to the miniaturization of sensors due to the inverse quadratic relationship with width. Advances in device structures using ultrathin and elastic membranes can be applied to miniaturized sensors to locate the resonance frequency in the phonetic spectrum through a methodology based on mimicking the basilar membrane of the human cochlea.

Sequential resonances under sound waves are generated in flexible membranes, which have constant correlation between the first, second, and third resonant frequencies. Multi-channels on a piezoelectric acoustic sensor can respond to mechanical oscillations of tiny voice pressure by mimicking the frequency separation mechanism of the human cochlea. The low frequencies of the first resonance can be resonated in wide channels while the high frequencies of the third resonance can be reacted in narrow channels. Broad bandwidth of a flexible acoustic sensor should be achieved by a low quality factor of the resonant frequency in the voice spectrum.[381] The frequency range coverage can be further extended by applying a flexible membrane with a gradual thickness change to a resonant acoustic sensor. The basilar membrane of the human cochlea utilizes asymmetric thickness with six-fold deviation to detect a wide resonant frequency range from 10 Hz to 20 kHz.

The sensitivity of resonant acoustic sensors should be enhanced for modularization, which requires robust characteristics under noise conditions. When integrated with commercial circuit electronics, a sensor module with high signal-to-noise ratio has advantages with respect to signal transmission and microchip interconnection. The piezoelectric constant of a flexible membrane is important to increase the sensitivity of the resonant acoustic sensor, which directly converts sound wave oscillation to output voltage. Flexible piezoelectric materials have been developed for higher device performance by improving the dielectric constant,

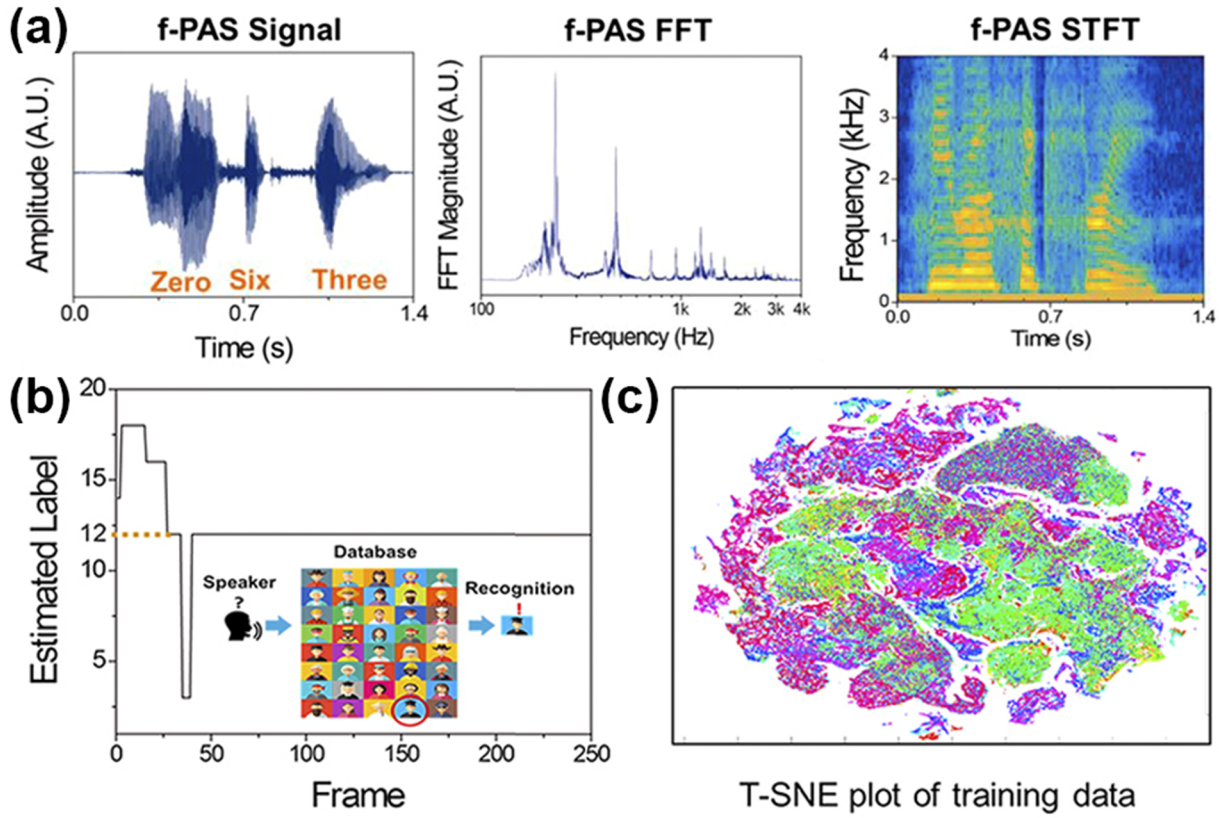

FIG. 18. Sound signals of a flexible piezoelectric acoustic sensor (f-PAS) (voice of 063). (a) Time domain voltage waveform, FFT analysis, and STFT spectrogram of f-PAS. The STFT is multiple frames of the sound FFT signal over a short shifting period to analyze the time-varying characteristics of frequency domain signals. (b) The majority voting method of GMM algorithm for speaker decision in recognition process over the frames in case of discovering 12th speaker. (c) t-SNE plot to visualize the trained STFT features of 2800 training data (40 people). The t-SNE plot shows probability distribution by embedding high dimensional data of similar objects into a low dimensional space. Reproduced with permission from Han *et al.*, Nano Energy **53**, 658 (2018). Copyright 2018 Elsevier.

polarization-electric field hysteresis loop and d_{33} value. Composites of piezoelectric nanoparticles and polymer matrix were reported using barium titanate [$BaTiO_3$ (BTO)], lead zirconate titanate (PZT), and alkaline niobate [(K, Na)NbO_3–$LiNbO_3$ (KNLN)].[387–392] The piezoelectric constant was improved by sol–gel based BTO and PZT thin film fabricated via inorganic laser lift-off (ILLO).[393–402] Highly sensitive perovskite piezoelectric membranes were developed including relaxor single crystalline PMN-PT, PMN-PZT, and PIM-NT, which achieved exceptional piezoelectric coefficients of d_{33} above 2000 pC/N.[403–405] Advances in piezoelectric thin films are demanded in order to achieve outstanding sensitivity of resonant acoustic sensors for modularization and miniaturization.

A combination of an acoustic sensor and optimized machine learning algorithms is essential for accurate voice recognition and speech processing.[383] The machine learning is a statistical model that analyzes the server database to perform specific computing tasks without explicit instructions. The machine learning datasets are utilized in training and testing procedures for voice processing. After the analysis function is defined in the training phase, the algorithm model can predict the detailed decision for the new input data. Subsequently, the performance of the machine learning algorithm is evaluated by comparing the pre-trained voice information with test data. Machine learning techniques can be applied to various applications of signal processing, such as speech recognition, speaker identification, voice localization, and language translation.[383] The multi-channel data of a resonant acoustic sensor can be analyzed by a machine learning algorithms, such as standard methods and deep learning approaches, which perform the signal processing of voice feature extraction utilizing mel-frequency cepstral coefficients (MFCC), STFT spectrogram, and auditory filter bank. Development of an appropriate algorithm and feature extraction method can lead to further progress of the flexible piezoelectric acoustic sensor for practical voice applications.

4. Concluding remarks

We have summarized the state-of-the-art and future prospects of resonant flexible piezoelectric acoustic sensors. Progress in voice user interaction opens avenues for practical voice applications by combining a highly sensitive acoustic sensor and an optimized machine learning algorithm. Frequency band control can be applied by adjusting the structural parameters of resonant sensors for

miniaturization. In addition, modularization is expected to be realized by enhancing the sensitivity of the piezoelectric membrane and decreasing the connection resistance with a commercialized microchip. To further extend the sound spectrum range, biomimetic resonant acoustic sensors are required by mimicking the basilar membrane of the human cochlea, which has a gradual thickness change with six-fold deviation in the thin and thicker regions. Machine learning algorithms can improve the capability of resonant acoustic sensors by optimizing the multi-channel signal processing for feature extraction and voice information analysis. Advances in these areas can suggest novel AI platforms for sensor node networks and touchless appliance control in the future hyperconnected IoT era.

5. Acknowledgments

This work was supported by the Wearable Platform Materials Technology Center (WMC) (Grant No. NRF-2016R1A5A1009926) and the Convergent Technology R&D Program for Human Augmentation (Grant No. NRF-2020M3C1B8081519) through the National Research Foundation of Korea (NRF) funded by the Ministry of Science and ICT. The authors would like to thank Fronics Co., Ltd., for their support.

B. Nanogenerators towards closed-loop electrostimulation in biomedical applications

Xudong Wang (*xudong.wang@wisc.edu), Yin Long

1. Abstract

Electrostimulation (ES) has long been utilized as a versatile therapeutic strategy for treating human diseases. The nanogenerator technology stands at a unique position for connecting biological ES to body motions by converting biomechanical energy to electric pulses. This process forms a closed-loop ES in both energy flow and function feedback. This article elaborates how the closed-loop ES operates as a close analog to how the body controls its own functions. The superb performance of the closed-loop ES is exemplified using an animal study of vagus nerve stimulation for effective diet and thus weight control. The NG-enabled ES is also discussed from the mechanism perspective to illustrate the similarity to biological systems, which led to successful results of facilitated skin recovery and hair growth. We recognize that the concept of closed-loop ES has been initially investigated in many other directions, such as bone growth, muscle stimulations, and deep brain stimulations. Supported by more focused study from materials and device engineering and biology science, the closed-loop ES will quickly grow into a very impactful application direction of nanogenerator technology for human wellbeing.

The nanogenerator (NG) technology emerged a decade ago as a new concept for nano- or micro-scale mechanical energy harvesting.[406] It relies on the electromechanical coupling principles, such as piezoelectric or triboelectric, to convert low-level mechanical energy from the ambient environment into electricity with impressive sensitivity and efficiency.[407,408] Currently, the NG technology has rapidly developed into a versatile power source for microelectronics owing to their broad materials selections and flexible design configurations.[409,410] Many research endeavors have been focused on materials innovations and design engineering to adapt this intriguing energy harvesting technique to a variety of mechanical energy sources, such as mechanical vibration,[411,412] wind blowing,[413,414] tire rolling,[415,416] water waving,[417,418] and body motions.[419–421] Among them, harvesting energy from human body possesses unique and perhaps the most irreplaceable merits, because human body is extremely restrictive to materials chemical and mechanical properties, and has a very limited access to other external energy sources, such as light. As a result, various body motions, such as muscle stretching,[422–424] hearting beating,[425] and breathing,[426] are considered attractive alternative energy sources for powering wearable and implantable bioelectronics.

The last five years witnessed a significant surge of NGs for biomedical devices. The applications can be divided into two directions, one for charging a power storage device (battery or capacitor)[426,427] and the other for directly providing biomedical functions [e.g., electrostimulation (ES) and sensing].[410,413] While early investigations have shown adequate biomechanical energy availability in human bodies (from milliwatt to watt level) for most microelectronics,[428] how to effectively collect this type of energy without introducing negative interference to the human body remains a key challenge.[429] Therefore, most implantable NGs only had a power output in the microwatt level, representing considerably low energy utilization efficiency.[427,430,431] With the rapid evolution of battery technology, many types of biomechanical energy are becoming more mismatched in terms of their energy volume density. It may take a significantly long period of time to charge a micro-battery using current NG technology.[154,171] On the contrary, directly applying the generated electricity to achieve certain biomedical functions becomes particularly intriguing. Without involving any energy storage component, such applications distinguish from other battery-driven devices by directly connecting the biomedical functions with biomechanical energy sources.

2. Closed-loop electrostimulations enabled by NGs

Considering the energy availability, effectiveness, and application irreplaceability all together, NG-driven ES might be a particularly practical and impactful direction for applying NGs on humans. Biologically, electrical signal is the essential element that human body uses to control all functions.[432] For example, brain, together with the complex neuron network, uses electrical signal to process information, communicate with all body parts, and interact with the external environment, to sustain a well-coordinated operation of the entire body system. Muscles rely on electricity to control their stretching and relaxing, performing all levels of body movement with great precession and responsivity. Cells, the fundamental building block of human body, perform their basic metabolic processes directed by local electric potential, e.g., opening and closing channels in cell membranes for ions and nutrition exchange. Besides, a few body parts themselves are piezoelectric, such as bone, cartilage, ligaments, and tendons.[433] They are able to generate electric potential in response to strain or force. It was believed that the endogenous piezoelectric potential was essential for bone growth and healing.[434]

Knowledge of the internal electricity in biological systems could be dated back to the 17th century when Luigi Galvani discovered animal electricity.[435] However, understanding of the electricity

effects in human body and applications of electricity for therapeutics are still evolving nowadays.[436,437] Many clinical approaches have implemented electricity to achieve a variety of therapeutic purposes, such as nerve stimulation,[438,439] pain relief,[440] diet control,[441,442] bone recovery,[443] wound healing,[444] and muscle restoring.[445] These clinical approaches typically used high frequency and short duration electrical pulses generated by a large electrical system. However, the optimal ES conditions are still mostly uncertain. Compared to these conventional ES treatments, NG might be able to yield more effective ES results to the targeted biological functions. As illustrated in Fig. 19(a), NG directly provides ES signals to human body, which are activated and solely powered by the biomechanical energy from relevant body motions. This forms a closed loop of both energy flow and function feedback. Therefore, we term this process as *closed-loop ES*. In a closed-loop ES, the stimulations are automatically responsive and synchronized to corresponding body motions and thus impose efficient therapeutic effects without any external manipulations. In the following content, we elaborate two unique perspectives of NG-enabled closed-loop ES, i.e., automatic correlation to stimulation targets and the bio-mimicking nature of ES generation.

3. Closed-loop ES for correlated nerve stimulation

The concept of closed-loop ES can be well illustrated by an example of vagus nerve stimulation for obesity control.[441] Research has shown that ES to the vagus nerve could induce multiple physiologic functions related to food intake, energy metabolism, and glycemic control, opening a new opportunity for therapeutic anti-obesity interventions.[446–448] A schematic of closed-loop ES for obesity control is shown in Fig. 19(b). The NG-based vagus nerve stimulator (VNS) is attached to the surface of the stomach and is able to generate biphasic electrical pulses when the stomach moves. Upon some food intake, the peristalsis of stomach activates and energizes the VNS to produce ES signals directly toward the anterior and posterior vagus nerves. The artificial signals travel through the cervical vagal trunk to the brain to help ceasing the eating action and thus reduce the overall food intake. In this scenario, the ES only actives when the to-be-controlled function (food intake) is taking effect, forming a closed activation-stimulation functional loop. This closed-loop ES could provide less number but more targeted stimulation so that the nerves might be more responsive to the stimulation and

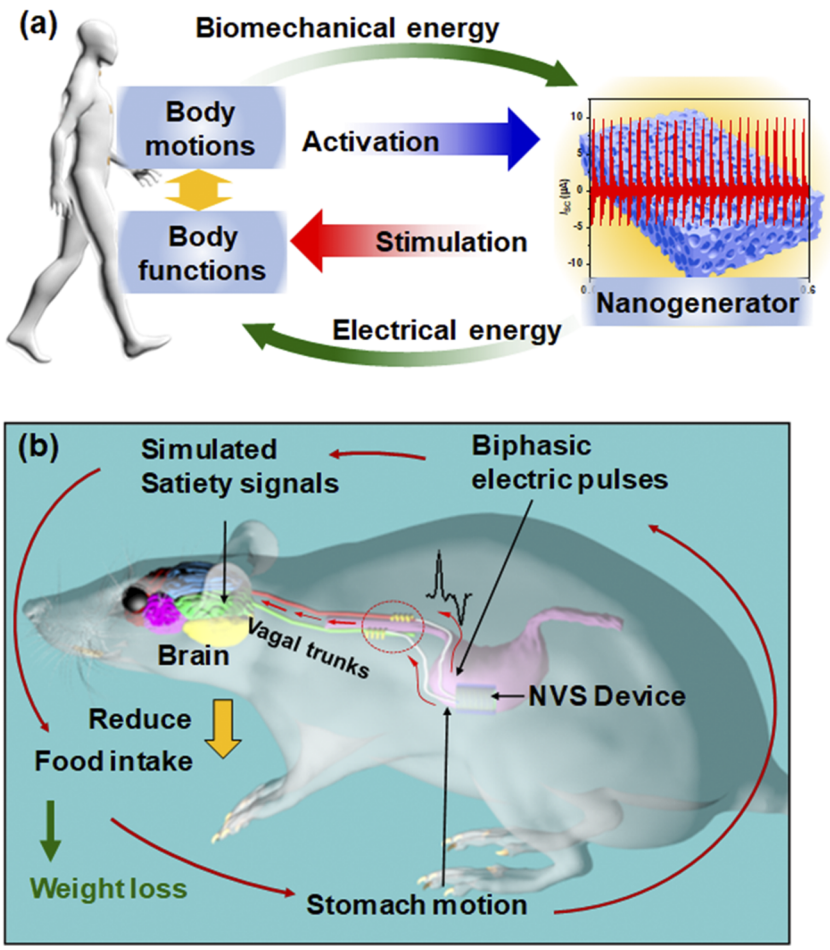

FIG. 19. Concept of closed-loop ES. (a) Schematic diagram showing the connection between human body motion and NG stimulation forming a closed loop of both energy flow and function feedback. (b) Schematic of a closed-loop ES example that used a NG-based vagus nerve stimulation (VNS) device to control diet and thus to achieve weight loss. Reprinted with permission from Yao *et al.*, Nat. Commun. **9**, 5349 (2018). Copyright 2018 Springer Nature.

thus more effective to control food intake. Animal studies on adult rats showed a rapid and stable 38% weight loss over a 75-day testing period, which was correlated with the reduced food intake of ~2/3 of the control groups. This result significantly outperformed other reported chronic microchip VNS systems based on similar rat models in terms of amount of weight loss and the time to reach the peak weight loss. This demonstration of closed-loop ES provides a promising alternative strategy of peripheral neuromodulation mechanism that might be more effective for obesity control compared to the miniaturized and implantable vagus nerve stimulators approved by the Food and Drug Administration (FDA).[449]

The application potential of nerve stimulations is far more than what shows above. Many neurologic and psychiatric disorders, such as Parkinson's disease,[450–452] essential tremor,[453,454] epilepsy,[457,458] and major depression,[457,458] have been broadly treated by ES. Introducing the closed-loop ES may bring new design concepts to nerve ES systems with largely improved wearability and efficacy. It is also relatively straightforward to build the closed-loop stimulations, particularly for tremors. The involuntary oscillatory muscle movements associated with tremor may perfectly serve as the mechanical stimuli that provide ES signals by a NG with naturally matching frequency and phase. Such a coordination can ideally eliminate the use of an electrical power source and a complex electronic system to tuning the stimulation intensity and frequency for ES treatments. Deep brain stimulation (DBS) is a neurosurgical procedure that uses electrical pulses to stimulate a specific brain area to treat neurologic and psychiatric disorders.[459] As DBS requires a relatively high current density in the range of 1.4–106.8 μA/cm^2,[460] it needs NGs with a rather high performance to reach the desired strength of stimulation. Hwang *et al.* used a single crystalline $Pb(In_{1/2}Nb_{1/2})O_3$–$Pb(Mg_{1/3}Nb_{2/3})O_3$–$PbTiO_3$ (PIMNT) with a remarkably high piezoelectric coefficient (d_{33} ~ 2700 pC/N) to develop a NG for DBS.[405] The PIMNT-based NG could generate an instantaneous current peak of ~45 μA at a load resistance of 200 kΩ through mechanical bending, which was proved to be able to introduce effective DBS in a mouse brain. However, unlike tremor treatments, it is not clear what mechanical energy source would be appropriate to close the loop for NG-driven DBS. If this hurdle can be overcome, it may revolutionize the implantable DBS technology.

4. Bio-mimicking nature of closed-loop ES for cell stimulation

Compared to conventional electrical signals used for ES, the electric pulses generated by NGs are closely analogous to those generated in biological systems. As a complex liquid-based ionic system, human body generates electric potential primarily by creating ionic displacements, such as redistribution of free ions, ionized groups, or molecular dipoles [Fig. 20(a)].[461] The electric potential is determined by the amount of charge carrying ions distributed at the interface. Considering the electric potential generation mechanism of NGs (both piezoelectric and triboelectric), piezoelectric potential is resulted from the surface charges induced by materials internal ionic displacement, while triboelectric potential is produced by surface charges exchanged during the contact of dissimilar materials with different electronegativities. Although the charge generation mechanisms are different, both effects share the same feature that the potential is determined by the limited amount of surface charges.[170] Therefore, when interfacing with human body, the surface charges would quickly attract ions toward the interfaces, naturally mimicking what the biological system does for internal potential generation [Fig. 20(b)]. Due to the limited amount of surface charge, the electric potential could be quickly screened, resulting in a sharp and transient voltage pulse for ES. The pulse width is typically less than 1 ms with a shape similar to degenerate waves.[462] The close similarity in pulsing mechanism and pulse features might be the reason that degenerate waves were found particularly effective for ES wound healing when compared to other electric pulse formats, including square, sinusoidal, and triangle.[463]

Our recent studies evidenced that the ES generated by a NG could significantly facilitate the biological processes in skin, including wound healing and hair regeneration. It is known that a natural skin wound healing process relies on the endogenous electric field to direct many cellular processes that lead to orderly healing.[464] By generating periodic biphasic electric pulses from breath motions using a NG, our group developed a self-activated electrical bandage that significantly accelerated skin wound recovery on rats.[465] The electrical potential was applied to the wounded area via a pair of parallel electrodes with a peak-to-peak voltage (V_{pp}) from 0.2 to ~2.2 V. On a 1 × 1 cm^2 full depth skin wound, the NG-dressing resulted a three-day full closure of the wound with minimal scare formation, while the control required 2 weeks for the recovery [Fig. 21(a)]. Mechanistic studies revealed that the on-skin ES was able to facilitate the proliferation and migration of the fibroblast cells and align them along the electric field. Three typical growth factors involved in wound healing, including transforming growth factor beta (TGF-β), epidermal growth factor (EGF), and vascular endothelial growth factor (VEGF) in wound tissues also showed elevated levels under ES. The bio-mimicking potential pulses from NGs were found advantageous compared to other conventional ES signals. Upon stimulation, the limited surface charge could be quickly screened by counter ion accumulation at the interface and thus minimize the interfacial charge transfer and suppress undesired redox reactions at the interface.[466] Therefore, a much lower reactive oxygen species (ROS) level was observed from the NG-stimulated system compared to other conventionally powered alternating ES.

Alopecia, a dermatological disorder due to a growth factor deficiency and/or hair cycle disorder,[467,468] is a common disease related to skin function and may share the similar effectiveness under NG-driven ES as that observed in skin wounds recovery. Early experiments have proved that ES could regulate secretion of multiple hair growth factors, promote hair follicle (HF) proliferation, prolong the anagen stage, and ultimately promote hair regeneration.[469–471] Our group introduced a NG that could convert random head motions into electric pulses for ES to promote hair regeneration.[472] The biphasic ES had a V_{pp} of ~320 mV, yielding a maximum dressing electric field of 3 V/cm. Significantly facilitated hair regeneration was obtained from Sprague–Dawley (SD) rats and genetically defective nude mice with higher HF densities and longer hair shaft length compared to controls treated with Minoxidil and vitamin D3 [Fig. 21(b)]. Mechanistic study revealed that ES largely enhanced secretion of VEGF and keratinocyte growth factor (KGF), and thereby overcame genetic defects (e.g.,, hair keratin disorder) and promoted hair regeneration. The HF proliferation percentage as a function of treatment time under NG-driven ES also largely outperformed other reported results by ES with different

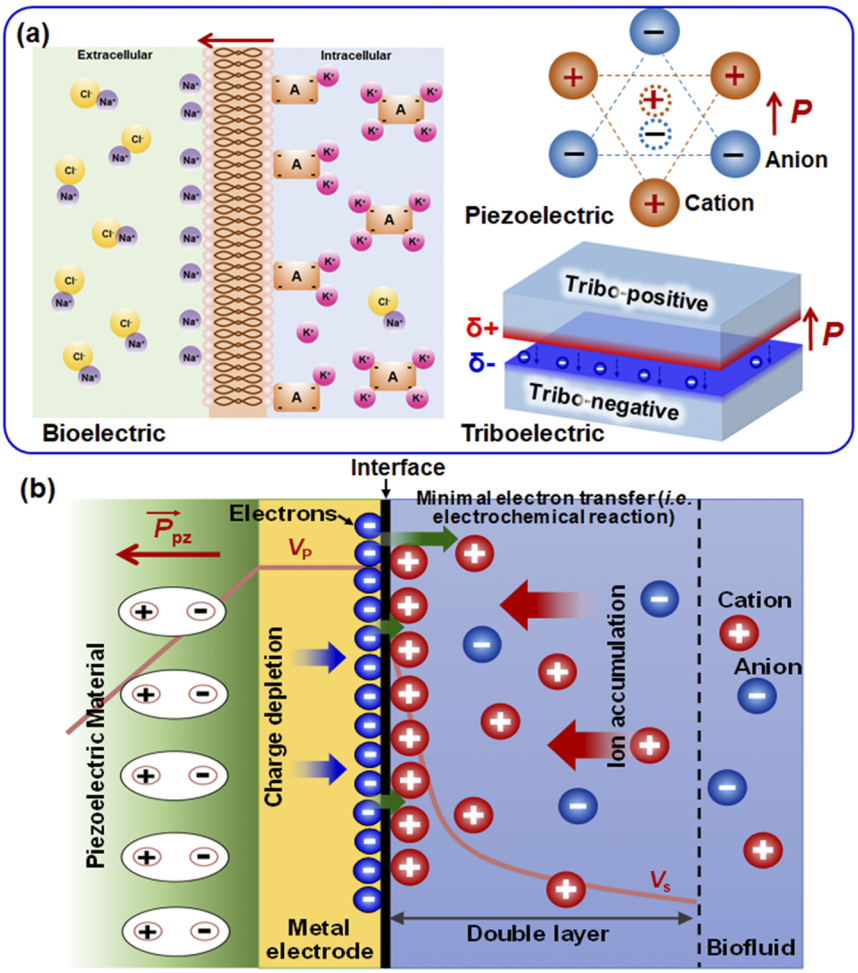

FIG. 20. NG-generated electric potential interfaced with a biological system. (a) Schematic illustration and comparison of electric potential generated in a biological system (left), a piezoelectric material (up-right), and a triboelectric pair (lower-right). (b) Schedule illustration of charge distribution and transport at the interface between a NG electrode and a biological system.

treatment parameters, further supporting the advantages of ES from NGs.

Above two examples of closed-loop ES enabled by NGs are not exclusive. We believe this strategy could be applied to most, if not all, ES therapeutic treatments with enhanced effectiveness and alleviated side effects. Bone healing is another well-known biological process that can be controlled by endogenous electric fields and externally applied ES.[473–477] In a preliminary *in vitro* study, Tian *et al.* showed that the ES generated by a NG would be able to stimulate bone cell proliferation, demonstrating the possibility that the NG-driven ES could promote osteoblasts attachment, proliferation and differentiation.[478] Nevertheless, the unique clinical advantages of using NG for bone healing still needs to be further demonstrated by more direct *ex vivo* and *in vivo* experiments and head-to-head comparison.

In addition to cell growth, ES also plays an important role in muscle stimulations. One typical example is artificial heart pacing, a common cardiac treatment for a variety of arrhythmias normally implemented by an implantable pacemaker. Current research on NGs for pacemakers are primarily focused on charging the pacemaker batteries by NGs using the energy from nearby body motions, such as hearting beating or breathing.[427,479] This strategy would enable a self-powered operation, i.e., the electrical power solely comes from the body motions. For closed-loop ES, more direct ES is expected that bypasses the energy storage component. For example, Hwang *et al.* used a piezoelectric NG to stimulate the heart of rat through two electrode leads directly from the NG without any electronic circuits [Fig. 21(c)].[403] This concept may revolutionize the pacemaker design with a much simpler and smaller configuration compared to current ones. Nevertheless, this demonstration was implemented only by using an external mechanical energy source. This strategy may raise risks to timely deliver ES to heart muscles with desired frequency and intensity. How to adapt a reliable biomechanical source with a sufficiently high energy to close the stimulation loop may not be an easy task to accomplish.

In conclusion, the NG technology stands at a unique position to connect biomedical ES with biomechanical motions. In this short roadmap article, we capitalize the concept of closed-loop ES that depicts a process where the electric pulses used for ES are generated by relevant body motions. It provides a close analog to how the

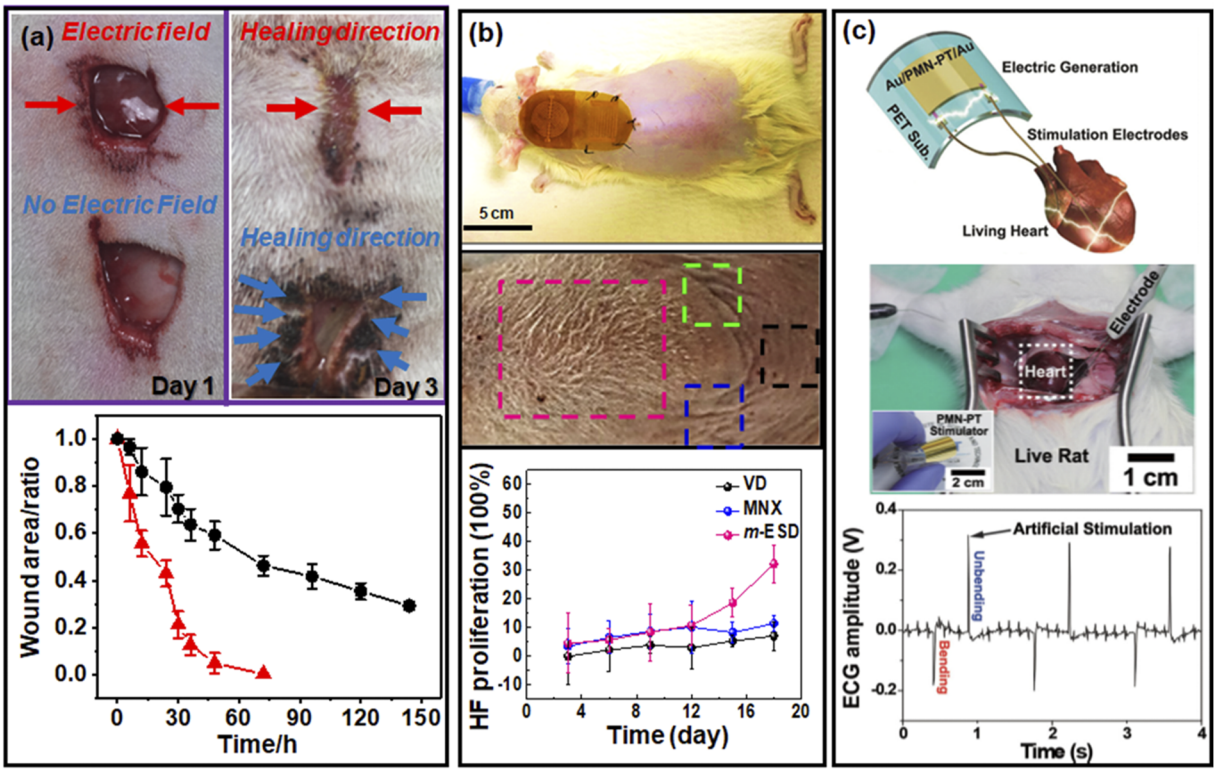

FIG. 21. Examples of closed-loop ES on cells. (a) ES accelerates skin wound recovery from 2 weeks to 3 days on rats. Reprinted with permission from Long *et al.*, ACS Nano **12**, 12533 (2018). Copyright 2018 the American Chemical Society. (b) ES accelerates hair follicle (HF) proliferation and hair growth on rats and nude mice. Reprinted with permission from Yao *et al.*, ACS Nano **13**, 12345 (2019). Copyright 2019 the American Chemical Society. (c) ES on heart muscle for direct heart pacing. Reprinted with permission from Hwang *et al.*, Adv. Mater. **26**, 4880 (2014). Copyright 2014 Wiley-VCH.

body controls its own functions. It may deliver the most direct and synchronized stimulations to the targets and thus impose efficient therapeutic effects without any external manipulations. Considering how our body uses electricity to communicate and to control, the concept of closed-loop ES would show very broad and promising application potential. Despite the few successful cases discussed in this article, research in this direction is still rather immature. From an engineering perspective, the first critical challenge is how to generate stable and sufficiently large electric pulses from small biomechanical motions *in vivo*. Different body parts have different motion patterns, most of which are non-linear with small strength and low displacement. In order to achieve high biomechanical energy-to-electricity conversion efficiency, flexible NGs and packaged devices need to be designed with specific motion and softness configurations to perfectly match the corresponding movement patterns without imposing a significant burden to the supporting organ or muscle. Biologically, many advantages of the NG-enabled closed-loop ES are hypothetical. Further in-depth cell-level understandings are particularly needed to quantify the relationship between ES from NGs and the targeting biological processes. Collaborations between material and biology scientists would be essential to reveal the unique correlation of NG-driven ES to specific bio-functions, from an interdisciplinary angle of biology, dielectrics, and electrochemistry. New engineering solutions and biology understandings will eventually lead the concept of closed-loop ES to a powerful toolset for both therapeutic and cosmetic treatments with unprecedented effectiveness.

5. Acknowledgments

This publication was supported by the National Institute of Biomedical Imaging and Bioengineering of the National Institutes of Health under Award Nos. R01EB021336 and 1R21EB027857. The content is solely the responsibility of the authors and does not necessarily represent the official views of the National Institutes of Health.

C. Energy harvesting powered wireless sensor system technologies

Zheng Jun Chew, Yang Kuang, Tingwen Ruan, Meiling Zhu (*m.zhu@exeter.ac.uk)

1. Status

The intended outcome from energy harvesting research is to power wireless sensor systems, as an alternative or supplement to batteries. This is because batteries, which have limited capacity and

charge cycles, need to be replaced once they are depleted to allow systems that rely on them as the power source to continue working. The rapidly growing number of wireless sensor systems for applications may soon incur a never-ending battery replacement and disposal maintenance routine that is too much to cope with. Therefore, harvesting ambient energy is a promising method to power wireless sensor systems for long term and sustainable deployment, with very little to no maintenance where the wireless sensor systems can be "fit-and-forget." Energy harvesting powered wireless sensor system technologies comprise energy harvesters that convert the ambient energy to electricity, power management circuits to convert the harvested electrical energy into a usable form, and energy stores to hold the harvested energy and supply energy for wireless sensors to perform sensing tasks. All these different subsystems of an energy harvesting powered wireless sensor system are inherently multidisciplinary that require research on materials,[228] applied physics,[480] mechanical designs,[481] electronics,[482] and communication technology.[483] While many promising innovations on the individual subsystems of energy harvesting technologies have been achieved,[484] it is still challenging for the subsystems from different domains to operate in synergy when they are integrated into one system. The challenge mainly lies in the mismatches among the different subsystems of energy harvesting technologies, which can be in terms of their coupling and the powers that are related to generation by the energy harvester and demand by the power management circuit and wireless sensors. These mismatches would not be easily identified or understood if these individual subsystems are being investigated in isolation. Therefore, successful real-world applications of energy harvesting powered wireless sensor systems are very limited so far even though energy harvesting has been extensively studied for almost two decades.[485,486] Many powerful techniques capable to analyze and improve the individual subsystems of energy harvesting technologies are available, which can be used to address the mismatches when they were applied in the perspective of a whole system by considering the interaction with adjacent subsystems. This "whole system approach" will be discussed by looking into the development of a piezoelectric energy harvesting powered wireless sensor system using a series of methodologies from the perspective of the energy harvester design, modeling, power management circuit, and the wireless sensor system.[487,488]

2. Advances

The development of an energy harvesting powered system always begins with the design of the energy harvester as the energy harvester is responsible for converting the ambient energy into electrical energy to power the rest of the system. Cantilever beams[489,490] and cymbal structures[491] are commonly used as piezoelectric energy harvesters. Piezoelectric transducers are one of the most dynamic energy harvesters as their frequency responses and electrical output vary with parameters of the transducers and succeeding circuits.[492] Modeling using finite element (FE) method is a powerful way to understand, predict, and optimize the transducers.[481] To understand the interaction of an energy harvester with its adjacent subsystem, which is the power management circuit, the model needs to include the circuit. However, the complete circuit is very difficult to be directly modeled and simulated in FE analysis. A way forward is to simplify the circuit as a load of its equivalent impedance.[492–494] Such a simplified system-level model that coupled the energy harvester with the load now forms the basis for FE analysis of an energy harvester as the load has been proven to affect the harvested power and the resonant frequency, which would not be revealed if only the uncoupled model is used in the modeling. From the FE analysis, the lumped parameters of an energy harvester in its equivalent circuit model can be determined. A system-level coupled electrical model that consists of the energy harvester and the circuit can then be built and analyzed using circuit analysis software to simulate the operation of the circuit that is connected to energy harvester.[493]

To obtain a close to accurate simulation results, a transducer model with very detailed features that resembles the actual device is essential, but it would lead to an unprecedentedly complex model that is extremely time-consuming to solve. For example, the macro-fiber composite (MFC) is a very popular piezoelectric transducer with an interleaving multi-material layered structure for energy harvesting, sensing and actuation applications.[495] Modeling an MFC with its detailed structure has been proven to be quite complex that encouraged many research efforts to devise homogenized models of MFC as a single piezoelectric material with equivalent properties.[494] A good solution is to use the representative volume subsystem of a MFC to determine the equivalent properties of a homogeneous MFC model in FE analysis.[496,497] However, the equivalent properties are subjected to variations according to the chosen electrical assumption and boundary conditions. Considering that output power is the key parameter of interest from an energy harvester, an equal power-output method FEM was proposed to evaluate the equivalent properties by applying electrical boundary conditions that ensure equal voltage, electrical charge, and, thus, equal power output between the heterogeneous and homogeneous MFC models when connected to a given load.[494] Apart from electrical output, FE analysis can also be used to study mechanical and material properties of a designed transducer,[492] which is vital to understand its reliability that ensure a long-lasting operation in the real-world.[492] Thus, an initiative has been taken to study and develop a transducer with high reliability, high output power, and broadband operational frequency using a novel deformable force amplification structure with a strongly coupled piezoelectric transducer that is pre-stressed by a mechanical transformer.[492]

A power management circuit in its simplest form generally comprises a rectifier to convert the AC electrical energy from an energy harvester into DC energy and a DC–DC converter to convert the rectified DC voltage into an appropriate level for charging up the energy storage as well as powering the wireless sensor. The optimum value of the impedance that is connected to an energy harvester for maximum power transfer changes with the vibration frequency applied onto the energy harvester. Therefore, maximum power point tracking (MPPT) is an indispensable feature in a power management circuit. Many design methods of MPPT control circuits are to track the electrical output from an energy harvester and varies the duty cycle of a DC–DC converter as the effective impedance of a DC–DC converter changes with its duty cycle.[498] Most methods are based on that maximum power transfer occurs when the impedances of both the power management circuit and the energy harvester match. Popular MPPT techniques in energy harvesting applications include hill-climbing[499] and fractional open-circuit voltage (FOCV).[500] The hill-climbing method periodically samples the output power obtained from the energy harvester using

different control parameters and gradually tunes the parameters until maximum power is obtained.[501] Thus, the power consumption of this method increases with the duty cycle of the MPPT control circuit. A simple way of keeping the average power low is to carefully reduce the duty cycle of the MPPT control circuit so that its operating frequency is still higher than the excitation frequency on the energy harvester to maintain a relatively high MPPT accuracy.[499] An algorithm that linearizes the system with control parameters independent of nonlinear functions was also proposed to simplify the control as well as save power.[501]

The FOCV is an increasingly popular method based on the findings that the voltage across a load is half of the open-circuit voltage when it matches the intrinsic impedance of the source for maximum power transfer.[502] General implementation of this method also requires periodical sampling of the open-circuit voltage of the energy harvester as the reference to determine the half open-circuit voltage by temporarily disconnecting the energy harvester from the DC–DC converter. Similar to the hill climbing method, the sampling frequency for the open-circuit voltage is directly related to the power consumption of the MPPT control circuit and accuracy of the MPPT. One method to reduce the power losses is to use a small sensing capacitor for sampling the open-circuit voltage. It allows a short sampling time, which reduces the time that the energy harvester is disconnected from the DC–DC converter for power transfer.[503] Another innovative method is derived from the equivalent circuit model of the energy harvester that forms an RC circuit with the rectifier. The voltage waveform of the RC circuit formed by the energy harvester and the rectifier is used to determine the half open-circuit voltage of the energy harvester by using analog filter circuit and differentiator without the use of a microcontroller.[500] This method occurs in real-time, has a low power consumption of around 3–7 μW, and does not disconnect the energy harvester from the DC–DC converter.[482]

Given that the instantaneous power from energy harvesters is usually lower than the power requirement of wireless sensor systems to operate, the harvested energy needs to be accumulated in energy storage devices. In energy harvesting applications, supercapacitors are preferred over rechargeable batteries as the energy storage device because they are more rugged against factors such as temperature variations, unregulated voltage, and current charging and have much higher charge–discharge cycles than rechargeable batteries. However, the voltage across a capacitor is dependent on the energy stored in the supercapacitor. This is unlike a battery, which provides a relatively steady voltage, regardless of its state of charge. On the other hand, wireless sensor systems can only start working properly above a specific threshold voltage. Therefore, a supercapacitor has to be charged up first to accumulate sufficient energy and also to reach the voltage level that is required by the wireless sensor system. Early designs failed to start-up or properly operated the wireless sensor system, which is directly connected to the supercapacitor.[504,505] The wireless sensor system, which draws energy, can be simply modeled as a resistor, which dissipates power. In that sense, the wireless sensor system will simply discharges the supercapacitor once they are connected. This prevents energy accumulation and voltage increment across the supercapacitor to the minimum required level for a proper operation of the wireless sensor node. Therefore, an interface that is aware of the energy level in the supercapacitor is required to control the energy flow. Early design of such an energy-aware interface (EAI) mainly consists of a voltage detector and a switch.[504,505] Once the voltage across the supercapacitor exceeds the threshold voltage of the voltage detector, the switch will be turned on to connect the wireless sensor system to the supercapacitor. However, with only one threshold voltage used, the capacitor voltage may drop quickly below the threshold voltage once the wireless sensor system starts operating. The wireless sensor system will then be turned off again or operating with an unpredictable behavior.[505]

A more practical design of the EAI consists of two different thresholds for connecting and cutting off the capacitor to the wireless sensor system.[506,507] There are important considerations to determine the appropriate threshold values.[508] The turn-on threshold voltage has to be higher than the turn-off threshold voltage where their absolute limits are equal to the operating voltage range of the wireless sensor system, which provides a sufficiently large operating window. The hardware energy-aware approach is essential to reduce the sleep power consumption of wireless sensor systems and power the systems without the start-up issue in the condition of mismatch between the energy generated by harvesters and demanded by the systems. For the turn-off threshold voltage, there could still be energy wastage with just the hardware implementation. It may be possible that the wireless sensor system is turned off by the EAI when the capacitor voltage reaches the turn-off threshold even though the wireless sensor system has not finished its tasks. The wireless sensor system may also finish its tasks early and keep draining the energy without doing any meaningful tasks until the EAI turns it off. To better use the harvested energy, an energy-aware algorithm was developed to provide a flexible turn-off threshold voltage.[507] The algorithm was programmed in the microcontroller of the wireless sensor system to determine the usable energy in the capacitor. The wireless sensor system varies its tasks or active time according to the energy availability. The wireless sensor system will be able to switch off earlier when it finishes its tasks or end its task in an orderly and prepared manner so that it is not turned off abruptly by the EAI, before the capacitor voltage reaches the turn-off voltage of the EAI.

3. Challenges

The very narrow power bandwidth of many piezoelectric energy harvesters, such as cantilever beam structures, is one of the biggest challenges for their applications in the real world as most of the vibration sources exhibit broadband spectrum. Many research efforts have been put into the design of broadband piezoelectric energy harvesting. There were some success with very specific designs that utilize frequency up conversion[509] and resonance frequency tuning techniques,[510] but they are limited to very niche applications or operating conditions. Usable output power, at least a few millwatts power for applications,[487] is also a main challenge. There is generally a size constraint on the energy harvesting powered wireless sensor systems due to limited space in the area for deployment. The output power scales according to the size of the energy harvester, which means a reduction in the size lowers the power.[511] There are some ongoing research efforts in using novel deformable force amplification structures with strongly coupled transducers as discussed earlier but that has not been sufficiently studied yet.[492] Studies on power management for piezoelectric energy harvesters using analytical model have resulted in many variants of

techniques, such as SSHI[512,513] and SECE,[514,515] to extract power from the inherent capacitance of piezoelectric energy harvesters that tends to hold some of the energy. However, practical implementation of many of the techniques as a standalone system is still limited. Some of the issues include the requirement for stringent control using digital signal processing from a computer,[514,515] the need for a large transformer,[516,517] and overdamping of the energy harvester,[514] which reduces the vibration displacement and harvested energy.

There is no general energy harvester design method that suits different applications due to factors such as narrow bandwidth of the transducer and different environmental conditions. Application-oriented bespoke designs are necessary on a case-by-case basis to achieve a high performance system by choosing optimal design parameters such as capacitor size and duty cycle based on the energy availability.[518] Therefore, the lack of real-world environmental data will make it almost impossible to design a working system for a given application. Apart from the data, the system design requires different software, tools, and expertise, which is a complicated process. For instance, important design parameters, such as material properties and geometry of energy harvesters, for a reliable long-term operation can be optimized using FE analysis and simple analyses of electrical power from the energy harvester and electronics is possible. However, there is currently no directly interlinked system analytical model. It is still to use FE analysis first and then equivalent circuit model for the analyses. Due to the generally low harvested power, it is crucial for the power management circuit to consume as little power as possible. This is usually achieved by designing circuits that are bespoke to the energy harvester with almost no adaptation capability to different applications.[519] Given the uniqueness of every single design, the lack of transferable design parameters would make the whole system design process even more tedious.

4. Future directions

For real-world applications, it would be necessary to understand environmental conditions and requirements to design a system using the whole system approach. For example, a system that uses MFC as its energy harvester to harvest strain energy from structures has been developed. Although the MFC is operating at a very low frequency that is far from its resonance, hundreds of microwatts to a few milliwatts of power can be generated when the strain is exerted on the MFC at a couple of hundred microstrain.[487] The whole system was then designed by applying a number of novel methods and techniques, such as coupled system modeling, MPPT, and EAI, as discussed earlier. The capability to characterize different parts of the complete whole system simultaneously using an online multichannel characterization testbed is also crucial to give a full understanding and appreciation of the synergetic link among them.[482,487] Furthermore, continuous research effort in the creation of novel energy harvesting materials and structures to increase energy density output is crucial for successful applications of energy harvesting powered systems. A significant breakthrough in the energy conversion efficiency of the active materials of energy harvesters is necessary to generate sufficiently high power for useful applications. Also, continuous research effort in the electronic to further reduce the power consumption of the power management circuit and the wireless sensor system is necessary to reduce the gap between the generation and demand. Innovation in the circuit topology that makes the circuit self-adaptive and self-configurable to a wide range of different energy harvesters and operating conditions but still consumes extremely low power would significantly reduce the time required to design an energy harvesting powered wireless sensor system as such a circuit is versatile for different applications.[520] It is clear that relying solely on the expertise in a single domain may still generate inspiring innovations for a particular subsystem of the energy harvesting technologies. However, they may not be compatible with other subsystems and cannot be implemented as a complete system. A complete whole energy harvesting powered wireless sensor system approach is essential and requires a multidisciplinary and cross-sector joint effort that includes academia and industry. Understanding of the energy harvesting technology capability and challenging bottleneck of the technology among technology solution providers and the end-users will drive the research on its path for real-world applications.

D. Nanogenerators and sensors for E-textiles

S. P. Beeby (*spb@ecs.soton.ac.uk)

1. Abstract

Electronic textiles (e-textiles) concern the integration of electronic and sensing functionality within an otherwise conventional textile resulting in smart, functional fabrics. Achieving invisible integration, reliable operation and powering e-textiles systems are current barriers to the development of the technology and its wider adoption in practical applications. The current status of textile-based triboelectric and piezoelectric nanogenerators and sensors is briefly reviewed. While several examples are presented in the literature demonstrating the feasibility of these technologies, these are far from practical solutions and significant challenges remain in the practical and robust implementation suitable for real world applications.

Electronic textile technology (e-textiles) whereby electronic and sensing functionality is embedded invisibly within an otherwise conventional textile has the potential to revolutionize wearable technologies. While great strides are being made in the integration of discrete electronics and sensors[521,522] within a textile, there is currently no alternative to powering e-textile systems other than by using conventional rigid batteries that are incompatible with the feel and nature of a fabric. Energy harvesting technologies convert ambient energy from, for example, physical movement into electrical energy, and by using suitable nanomaterials, both triboelectric and piezoelectric, electrochemical harvesting and sensing have been demonstrated to be incorporated into the textile itself. This offers the potential to recharge textile integrated batteries[523] and supercapacitors[524] or even directly power the e-textile system itself.

2. State-of-the-art

The triboelectric effect can be used for both energy harvesting and sensing and the coupling between the physical movement associated with human motion and the associated displacement of a textile garment is well suited to this transduction mechanism. Furthermore, textile based triboelectric devices can be implemented without compromising the feel of the textile. The triboelectric effect

can be achieved either by functionalizing the surface of a complete textile or the yarn itself, which may be subsequently woven or knitted into a fabric or embroidered onto an existing fabric.

Capturing human motion in the form of a smart glove has been demonstrated by sewing the sensing yarn into patterns on certain parts of the fingers of the glove.[525] The all-textile triboelectric sensor (ATTS) smart yarn is formed from a stainless steel fiber surrounded by polyester fibers resulting in a diameter of around 200 μm (see Fig. 22). The sensing yarn is sewn into a knitted nylon fabric with the interaction between the polyester and nylon fibers forming the triboelectric combination with the stainless steel core collecting the electrical signal (Fig. 22). Compressive forces cause contact and separation between the fibers resulting in signals of around 1.8 V and 5 nA and it also functions when the textile is deformed, such as from the finger bending. This represents an elegant approach to sensing a range of gestures and grips. Wash testing did show some deterioration in the output signal and was limited to only ten washes and repeatability of sensing signal across a range of forces was not demonstrated.

Textile pressure sensors based on triboelectric nanogenerators (TENGs) have also been demonstrated using Cu-coated polyacrylonitrile (Cu-PAN) yarns and parylene coated Cu-PAN (parylene-Cu-PAN) yarns suitable for weaving, knitting, or sewing.[526] The Cu coating is 300 nm thick, and the parylene coating is 5 μm, resulting in a resistance along the length of the yarn of 0.15 Ω/cm. While the suitability of the yarns for different textile manufacturing approaches is good and yields an interesting insight into the effect of the different structures on the output of the TENGs, the yarn coating processes are based on polymer-assisted metal deposition and chemical vapor deposition, which are not ideal for low cost mass manufacture of the yarns itself.

Fibers based upon a piezoelectric nanowire composite of Polyvinylidene fluoride (PVDF)/Antimony sulfoiodide (SbSI) have also been embedded in a textile for energy harvesting and sensing applications.[527] The piezoelectric fibers were produced using an extrusion process that was capable for producing 2.5 km formed at a velocity of up to 500 m/min, which indicates excellent potential for industrial scale production. The piezoelectric activity of the fibers was demonstrated, but the actual energy harvested or electrical signals obtained in use case scenarios have not been quantified.

The vertically aligned ZnO nanorods have been deposited on to the surface of a nylon fabric using a novel hydrothermal method forming a piezoelectric nanogenerator (PENG).[528] The nylon fabric is first coated with a screen printed silver electrode layer after which a ZnO seed layer and hexagonal ZnO nanorods were formed by immersion in a precursor solution at a controlled temperature. The final textile device is achieved by adding a second Ag coated nylon fabric on top forming the second electrode with the ZnO nanorods sandwiched between the fabric/electrode layers (see Fig. 23). The textile structure produces clear electrical signals from palm clapping and finger bending with output voltages and currents of about 4 V, 20 nA, and 0.8 V, 5 nA, respectively. Energy harvesting performance is again not meaningfully quantified.

Electrochemical based transduction has also been demonstrated for sensing and energy harvesting from yarns. Biocompatible

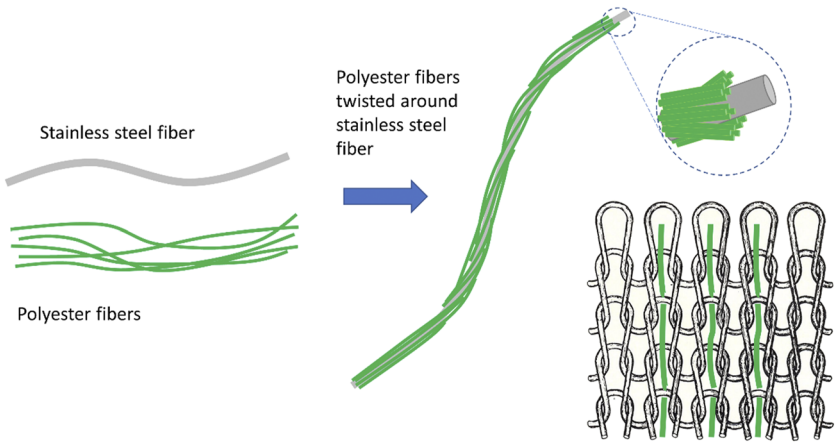

FIG. 22. Schematic illustration of the ATTS fabrication process. (a) Yarn assembly. (b) Sensing yarn sewn into knitted nylon textile.

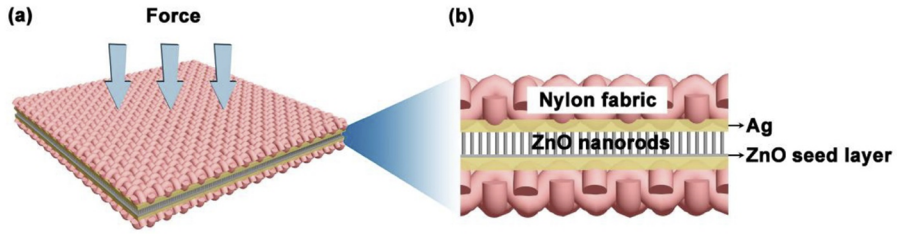

FIG. 23. (a) The structure of the fully assembled PENG. (b) PENG cross section. Taken with permission from Zhang *et al.*, Physica E **105**, 212 (2019). Copyright 2019 Elsevier B.V. All rights reserved.

Prussian blue (PB) active coatings on polyester–carbon nanotube (CNT) threads demonstrate a mechanical–electrochemical coupling effect that results in area power densities of up to 3.8 μW/cm^2 at low frequencies associated with human motion using aqueous or polymer gel electrolytes.[529] Forest-drawn carbon multiwalled nanotubes (MWNTs) formed into high-strength twisted yarns have also been shown to convert torsional and tensile mechanical motion into electrical energy.[530] Stretching these twisted yarns has generated up to 250 W/kg of peak electrical power at 30 Hz cycling frequency.

Further examples can be found in more comprehensive reviews of textile-based triboelectric and piezoelectric nanogenerators.[68,108,531]

3. Future challenges

Textiles are challenging materials to work with given their physical characteristics (flexible, stretchable, breathable, etc.), the nature of the mass manufacturing processed used within the textile industry and the rigors of actual use typified by machine wash cycles. Textiles are incredibly robust and the transduction mechanisms must achieve the same level of robustness without compromising the feel of the textile. While current research is successfully demonstrating the feasibility of different energy harvesting and sensing approaches, insufficient attention is being paid to the issue of robustness and ensuring that potential solutions are practical. Achieving the required level of robustness will influence implementation of the technologies and this must be considered at the outset in order to minimize the overall impact on the feel of the textile.

The flexible and compliant nature of textiles also represents a challenge with respect to the force/strain/displacements that are coupled to the transducer. The compliant nature of a textile makes it comfortable for the wearer, but this reduces the mechanical energy coupled into the energy harvesting/sensing transducer, which in turn reduces the energy that can be harvested. Most wearable applications involve bending or straining the textile or have some sliding between two separate textiles, and this makes triboelectric harvesting an attractive approach. Piezoelectric harvesting relies on the active material being strained and this may require engineering methods to increase the strain coupled to the piezoelectric element. This may involve, for example, designing a garment in such a way that strain is concentrated through the energy harvester. Further materials research to improve the performance of the energy harvesters and achieve improved levels of flexibility also remains an important requirement.

4. Concluding remarks

There are considerable opportunities for application in a wide range of application domains, including consumer electronics, human–machine interfaces, robotics, and healthcare. It is unlikely a one-size fits all solution will be identified given the very different use case scenarios, expected activity levels, and sensing requirements. However, it is clear energy harvesting and sensing technologies that can be integrated seamlessly and invisibly within a textile and can survive the rigors of use will revolutionize e-textiles and their use in wearable technology applications.

E. Triboelectric nanogenerators as highly sensitive sensors for human–machine interface

Xianjie Pu, Hengyu Guo, Chenguo Hu (*hucg@cqu.edu.cn)

1. Abstract

Human–machine interface (HMI) is an indispensable part of our lives. In the past few years, the triboelectric nanogenerator (TENG) becomes not only an energy harvesting technology but also an advanced sensor technology in various areas, including HMIs. As a highly sensitive and self-powered sensor, TENG can detect the mechanical micro-motion of the skin around the corners of eyes, respond to acoustic vibration in a wide broadband, quantify the rotations of a hinge model via mechanical displacements, and position the touch point on a flexible interface, which enable TENG to be used in HMI control nowadays including eye-movement, voice, gesture, and touch. Besides, the TENG can also play a role in the feedback stage of HMIs in visual, auditory, or tactile modes worthy of further investigations. This paper gives a brief review of the current status of TENG-based sensors in HMIs, with focus on several works of our group around the control-feedback loop, together with discussion of the current challenges and future prospects.

2. State-of-the-art

Human–machine interface (HMI) has become an indispensable part of our lives. From the original keyboards to the virtual reality today, the goal of HMI is to make life more convenient and fascinating. In recent years, the fast development of nanotechnology provides theory basis and techniques to improve HMIs.[419,532,533] Among these technologies, triboelectric nanogenerator (TENG)[28]—based on the contact electrification and electrostatic induction[4,61]—was invented for energy harvesting with unique advantages of high outpulifhtedt, light weight, low cost, applicability of design, stability, and robustness.[50,534–536] Since TENGs can generate electricity from almost all mechanical motions, including vibration, rotation, sliding, touching, etc., they can also act as self-powered sensors for these kinds of mechanical motions usually used in HMIs.[537–544] In this review, four general types of TENG-based HMIs are introduced, mainly focusing on our four works aiming at intuitive interfaces through eye movement,[419] voice,[545] gesture,[546] and touch,[547] as illustrated in Fig. 24. From HMIs in certain scenarios to HMIs in daily applications, these four types of work are reviewed successively.

As a communication channel between humans and external devices, HMI is one way to turn a virtual thought into realistic action, which plays a unique role in helping the disabled, such as the patients suffering from amyotrophic lateral sclerosis (ALS).[548] That is precisely what brain–computer interface (BCI) stands out from HMI for Ref. 549. However, BCIs based on noninvasive bioelectrical signals, including electroencephalogram (EEG)[550] and similar electromyogram (EMG)[551] and electro-oculogram (EOG),[552] have inherent disadvantages of low signal-to-noise ratio (SNR), lack of efficient resolution, poor stability, and durability.[550,551,553] These drawbacks limit its wide use in daily life. With TENG technology, a non-invasive, sensitive, stable, reusable, comfortable, and aesthetical sensor is developed based on bionic membrane sensors exquisitely designed by the early researchers to replace these bioelectrical-based

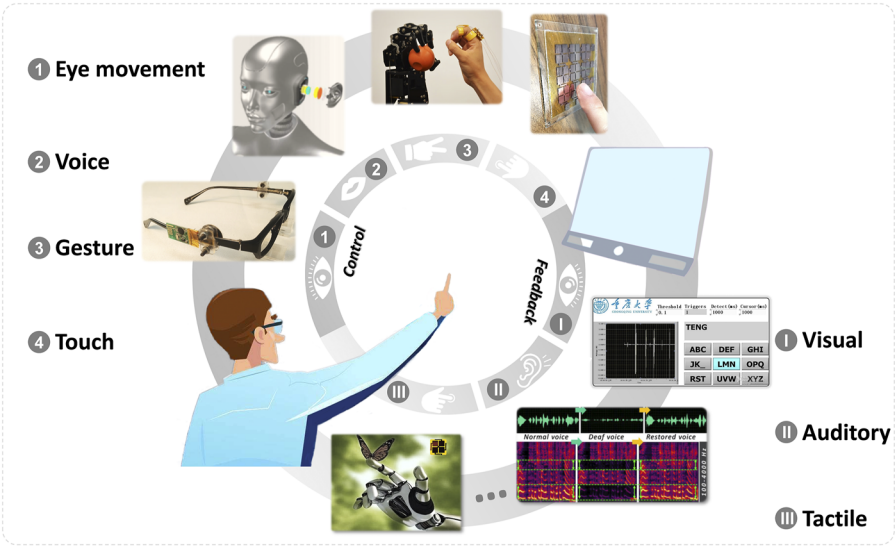

FIG. 24. TENG-based sensors in the control-feedback loop of HMIs. Reproduced with permission from Pu *et al.*, Sci. Adv. **3**, e1700694 (2017). Copyright 2017 American Association for the Advancement of Science. Reproduced with permission from Guo *et al.*, Sci. Rob. **3**, eaat2516 (2018). Copyright 2018 American Association for the Advancement of Science. Reproduced with permission from Pu *et al.*, Nano Energy **54**, 453 (2018). Copyright 2018 Elsevier. Reproduced with permission from Pu *et al.*, Nano Energy **76**, 105047 (2020). Copyright 2020 Elsevier.

HMI sensors.[419,554] This sensor is named mechnosensational TENG (msTENG),[419] as shown in Fig. 25(a). It is designed with a multi-film structure based on a single-electrode mode and thus could be flexibly mounted and hidden behind a pair of glasses to form a wearable sensor. An acrylic thin annulus is tightly attached as a spacer between the two tribo-layers to realize vertical contact/separation driven by eye-blink and other mechnosensational movements. The synchronous measurement illustrates that the voltage amplitude from the msTENG is significantly larger (~750 times) than that of EOG. Through threshold sets, the voluntary and involuntary eye-blink can be easily distinguished. Based on this distinct advantage, with a simple signal processing circuit, the msTENG glasses are adopted in the control of household appliances. Furthermore, via a wireless module, a hand-free virtual keyboard typing system is developed to help the ALS patients. This study realizes applying the TENG to the field of mechnosensational HMIs and will greatly help people achieving a convenient and colorful life.

Besides eye movement, voice communication is another important and effective channel with the outside world. For mature social mobile robotics, a sensitive and energy efficient auditory sensor should be equipped to listen to our instructions and even perceive our vocal intonations.[555] For people with impaired hearing served by the robotics, reconstructing the normal hearing via such kind of auditory sensor is also necessary, as illustrated in Fig. 24. Several research groups have developed this kind of self-powered auditory sensor based on piezoelectric effect, which is different from the traditional ones based on electromagnetic effect, capacitive sensing, and piezo-resistive effect.[377,556–559] However, the piezoelectric auditory sensor[377,556] has a relatively low signal output, and its response range is always higher than frequency ranges of human voice, while a TENG-based auditory sensor can induce a much higher output and can easily realize a selective response range via adjusting structural parameters.[545,560] As shown in Fig. 25(b), this circular type TENG is called triboelectric acoustic sensor (TAS).[545] Similar to the msTENG, the inner film (blue) attached on the acrylic thin annulus will vibrate under air flow. Then, the electrode (yellow) induces signal. This tiny, thin, and even transparent TAS shows ultra-high sensitivity up to 110 mV/dB. Through the design of the annular or sectorial inner boundary architecture, the TAS achieves the broadband response from 100 to 5000 Hz, which almost covers the whole frequency range of the human voice.[561] Furthermore, the characteristics of tunable resonant frequency make itself a single channel hearing aid with selected frequency bands, which matches the lost bands of the impaired hearing. This device achieves a complete human–robotic voice communication efficiently with low energy consumption.

In scenarios of manufacturing industry, deep-sea exploration, telesurgery, and disaster salvation, HMIs via gesture control can help bring about an intuitive interface instead of operation based on careful learning and training,[555,562] as illustrated in Fig. 24. Current technologies about gesture control robotic hands include visual tracking, physiological signal collection, and mechanical signal collection, which have the problems of poor wearability, low SNR, complex algorithms, or nonlinearity.[533,563–565] In recent years, epidermal electronics, stretchable polymer semiconductor films, piezoelectric nanodevices, and TENGs provide several possible strategies.[533,566–568] In TENG methods, to realize quantization of fingers' movement, a micro-grated displacement mode is adopted.[546,569] This sensor worn on a finger joint is called joint motion triboelectric quantization sensor (jmTQS),[546] as shown in Fig. 25(c). Verifying by a hinge model,[570] the rotation angle is linear to the tensile displacement at the finger joint. When the slider moves forward/backward under finger's flexion/extension, the relative displacement between slider and fixed interdigitated electrodes induce pulses. Both the slider and the fixed electrodes have the corresponding block part and finer grating part, which induce wide pulses representing the direction and narrow pulses representing the degree, respectively. These two signals constitute the signals shown in Fig. 25(c). For these coupling signals, through calculating the narrow pulses in unit time, the rotation angle and speed can be determined; through judging the positive or negative direction of the coupling signal, the rotation direction can also be determined. Therefore, the jmTQS can directly

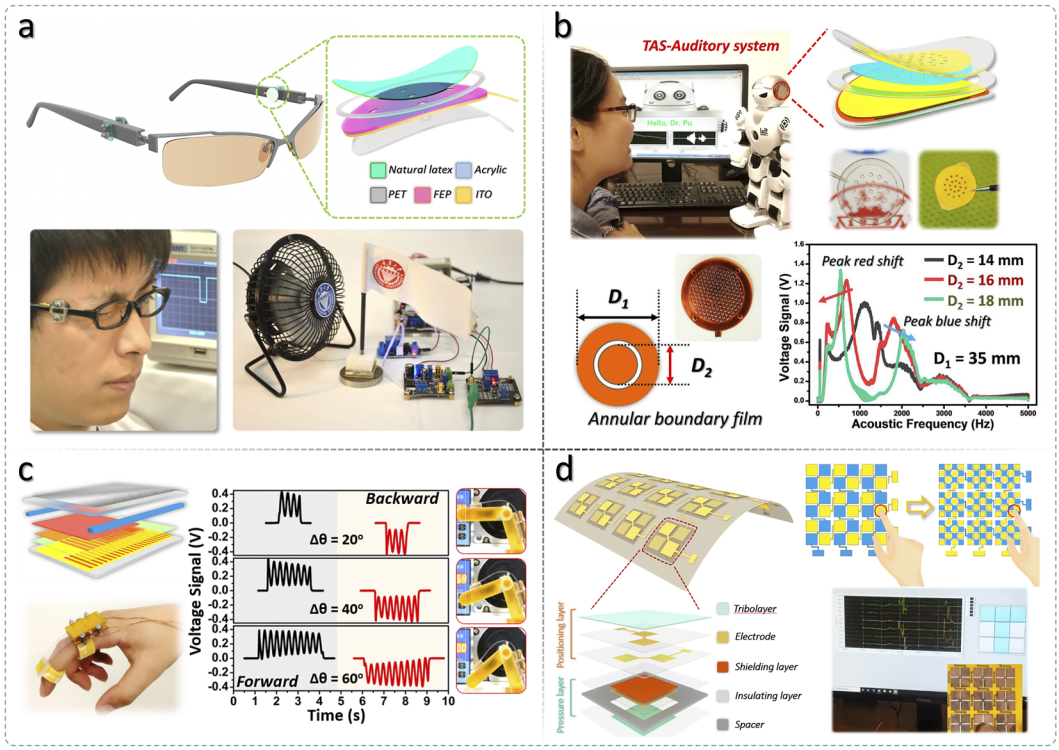

FIG. 25. TENG-based sensors in HMIs of eye-movement, voice, gesture, and touch. (a) The mechnosensational TENG (msTENG) for controlling the equipment via eye-blink. Reproduced with permission from Pu *et al.*, Sci. Adv. **3**, e1700694 (2017). Copyright 2017 American Association for the Advancement of Science. (b) The triboelectric auditory sensor (TAS) for interacting with the robotic via voice. Reproduced with permission from Guo *et al.*, Sci. Rob. **3**, eaat2516 (2018). Copyright 2018 American Association for the Advancement of Science. (c) The joint motion triboelectric quantization sensor (jmTQS) for constructing a robotic hand synchronous control system. Reproduced with permission from Pu *et al.*, Nano Energy **54**, 453 (2018). Copyright 2018 Elsevier. (d) The 3D triboelectric touch pad (3D-TTP) for an effective and efficient touch-screen graphical user interface. Reproduced with permission from Pu *et al.*, Nano Energy **76**, 105047 (2020). Copyright 2020 Elsevier.

quantify finger joint's flexion-extension degree/speed and this has been verified on a hinge model test. Based on sensing these intermediate states of finger movement, a robotic hand synchronous control system has been constructed.

In daily life, some traditional interactive modes, such as keyboards and touch pads, still have a strong vitality and practical value.[179,571–573] Based on different physical transduction mechanisms, these keyboards or touch pads are essentially tactile sensors that transduce the physical touches into electrical signals and map them to corresponding positioning units.[572,574,575] Converting physical movement into electrical signal is the original intention of TENG, which addresses the power/energy challenges of devices with powerful sensors nowadays.[555] Therefore, the self-powered TENG technology is exactly a good solution for developing a tactile sensor equipped on these devices.[538,540,574,576–578] In these applications, XY matrix scheme greatly reduces the number of channels and is conducive to high resolution wiring layout.[575,578] In this scheme, crosstalk and target sensing resolution are the problems. To address these problems, a 3D triboelectric touch pad (3D-TTP) with XY Complementary Subdivision Pattern (XYCSP) is developed,[547] as shown in Fig. 25(d). The upper three layers constitute the XY positioning layer, and the lower three layers construct the pressure sensing layer. The XYCSP is designed to suppress the crosstalk through reducing the overlap between XY electrodes as well as make object positioning robust in object size and contact point. It provides a paradigm of successive subdivision for regulating the object sensing resolution and demonstrates its use in trajectory. Furthermore, with the attached pressure sensing layer, password-based authentication is demonstrated. These two composite functional layers have the potential for tactile sensors for motion monitoring, electronic skin, robotics, and other traditional human–machine interactions.

3. Challenges and future prospects

With the rapid development of sensor technology, the increase of various precision sensors poses a challenge to the power source of HMI systems. As self-powered sensors, TENGs transform the various mechanical motions into target signals without power supply, which greatly reduce the energy consumption. However, the back-end data collection devices and signal processing devices still need power supply. To realize a fully self-powered mobile HMI system, it needs to draw support from the TENG's power generating nature and the corresponding power management technique to power the essential back-end devices or at least to meet the wireless transmission of the sensing signal.[419,535,579–582] For signal processing progress,

advanced algorithms based on machine learning and big data are essential for robust HMIs in daily applications.

Taking advantages of various functional materials and advanced fabrication techniques, the TENG sensors can be developed to be more flexible, stretchable, even washable and multifunctional to meet the portable or wearable requirements of HMIs.[583–585] Meanwhile, these improved TENG sensors are also beneficial to collecting environment energy for the back-end equipment.

Besides the illustrated applications in the control stage of HMIs, in the feedback phase of HMI, TENG as a highly sensitive sensor transforming mechanic movements into electric signals can also be used in visual, auditory, and tactile modes. Take the TAS study above, for example, it demonstrates that this resonant frequency-tunable auditory sensor is also a hearing aid for people with impaired hearing in the feedback stage between robotics and them.[545] Furthermore, the 3D-TTP tactile sensor can be another kind of electronic skin of the robotics for perception of various parameters of objects.[547,586,587] Integrated with more other technologies, such as near-field transmission, nanophotonic readout, and electroluminescence, the multiparameter system can be found based on advanced packaging and optimized modularization. With these attempts, we may foresee more potential for TENG-based sensors in the control-feedback loop of HMIs.

4. Concluding remarks

In this paper, TENG-based HMIs, including eye-movement, voice, gesture, and touch, are reviewed. Due to their unique characteristics, TENG sensors display advantages of high sensitivity, low cost, light weight, feasible structure design, stability, and robustness and have potential applications in the feedback stage of HMIs. Thus, TENG sensors will surely play a more important role in the control-feedback loop of universal HMIs.

5. Acknowledgments

This work was supported by the National Natural Science Foundation of China (NSFC) (Grant Nos. 51902035 and 52073037), the Natural Science Foundation of Chongqing (Grant No. cstc2020jcyj-msxmX0807), and the Fundamental Research Funds for the Central Universities (Grant Nos. 2019CDXZWL001, 2020CDCGJ005, and 2020CDJ-LHSS-001).

F. Powering body-implantable medical devices with triboelectric nanogenerators

Sumanta Kumar Karan, Sang-Woo Kim (*kimsw1@skku.edu)

1. Abstract

Body-implantable medical devices (BIMDs) play a crucial role in early clinical diagnosis and treatment of diseases in the modern world.[588,589] However, they require a power source, such as a battery, and conventional IMDs are powered with primary batteries that demand frequent surgeries for replacement. In order to minimize the problems associated with repeated surgeries, powering various kinds of low power-consuming IMDs with triboelectric energy harvesters is of great concern. In this short review, we explore recent improvements in methods of powering IMDs with triboelectric nanogenerators (TENGs), which improve patients' quality of life and lower the risks associated with replacement of batteries implanted in the human body. In most of the research, internal biomechanical energy is an important energy source for TENGs used to power IMDs. Alternatively, ultrasound-assisted TENG is emerging as a new technology to power IMDs. We also analyze the challenges that remain in the field and discuss recent developments in TENGs used to power IMDs for *in vivo* healthcare applications.

2. Introduction

a. Significance of TENGs for powering IMDs. Body-implantable medical devices (BIMDs) are essential for observing, defining, and recording physical actions *in vivo*. Unfortunately, repeated surgery is necessary to replace the battery in such devices after it has expired, which may cause physical and mental damage to patients. In addition, although the surgical procedures involved are believed to be safe, any surgery comes with a risk of infection.[590] Modern IMDs (e.g., pacemakers) require internal power sources but have mechanical parts that need to be repaired or replaced after some years.[591] Continuous operation of IMDs with the help of either power transferred from external energy sources in a wireless manner or energy harvested from within the body is required for early clinic diagnosis and treatment of some diseases. One method of charging secondary batteries inside IMDs, wireless electromagnetic power transmission, has been proposed as an innovative powering system, but it has several critical issues that need to be resolved, such as excessive tissue heating, which can affect the patient's metabolism.[592] On the other hand nanogenerators (NGs), have been proposed to harvest the mechanical energy produced by the human body. Triboelectric nanogenerators (TENGs) can generate electricity if there is a physical contact or rubbing.[593] Unlike piezoelectric NGs (PENGs) depend on restricted group of noncentrosymmetric materials [e.g., ZnO, GaN, $Pb(Zr,Ti)O_3$, $BaTiO_3$, and PVDF],[589,594] TENG has emerged as a promising technology that may bring about self-powered IMDs and healthcare monitoring systems with low power consumption as shown in Fig. 26.

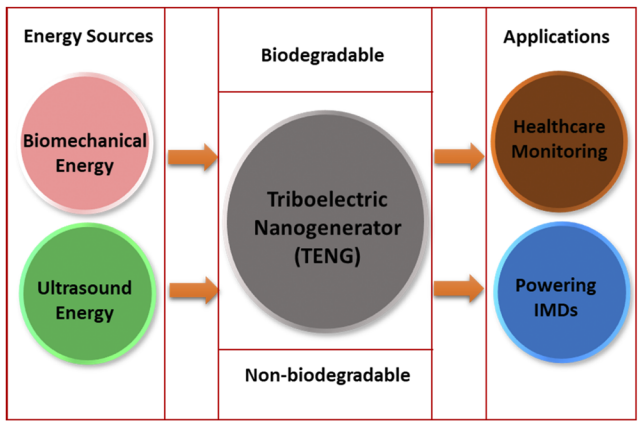

FIG. 26. Graphical overview of mechanical energy sources and TENG-based devices, and applications of TENGs in IMDs and self-powered healthcare monitoring systems.

3. Energy sources, device types, and TENGs-based IMDs for biomedical applications

TENGs have been explored as a means of converting mechanical energy into electrical energy. TENGs that provide reliable and sustainable energy conversion have gained significant attention, with many options for available materials, compatibility with modern IMDs, flexibility in structural design, and prominent mechanical durability. To power body-implanted devices with TENGs, either biomechanical energy (from various types of muscular movements) or ultrasound energy transferred into the body are excellent mechanical energy sources that can generate electricity. Potential applications of such TENGs include IMDs and self-powered healthcare monitoring systems (Fig. 26). Some important biomedical applications of TENGs include IMDs, cardiac monitoring sensors, laser curing systems for osteogenesis, nerve cell stimulation devices, and real-time monitoring sensors of respiratory rate, heart rate, and blood pressure.[591,595] Zheng *et al.*[596] explored a self-powered wireless transmission system using a TENG (1.2 × 1.2 cm^2) that demonstrated its feasibility for real-time remote cardiac monitoring by transferring an electrical signal obtained from an *in vivo* heartbeat of rat. The PDMS film (100 μm thick) with pyramid arrays and nanostructured Al foil used as the friction layers. Kapton and gold (Au) film utilized as the supporting substrate and back electrode, respectively. Tang *et al.*[597] demonstrated the ability of a self-energized laser treatment method by fixing a TENG (1.5 × 1.0 cm^2) to the arm of a living rat. The system significantly accelerated the mouse embryonic osteoblasts proliferation and differentiation. Pyramid array patterned PDMS and indium–tin oxide (ITO) films were acted as the friction materials. A self-powered ultrasensitive TENG (20 × 10 × 0.1 mm^3) based pulse sensor is used to monitor heart rate in the *in vivo* conditions investigated by Ouyang *et al.*[598] Nanostructured Kapton and Cu thin films were employed as the two triboelectric layers. Zheng *et al.*[596] used a TENG placed in the diaphragm to sense the movement of the lungs. Apart from the above-mentioned works, many recent research has been done concentrating on human–machine interactions (HMI)[599] and IMDs applications.[600,601] The TENG device is capable of recognizing the minute behaviors associated with breathing, which is an essential feature of a medical sensor. Thus, TENGs are regarded as one of the most promising energy solutions for powering BIMDs.

The energy-harvesting performance of TENGs depends upon a given level of biomechanical energy.[589,602] TENGs intended to charge lithium (Li)-ion secondary batteries in IMDs have inherent shortcomings due to a low level of input biomechanical energy. The inherently small amount of mechanical energy available in the body and the limited size of implanted devices present technical challenges for TENGs used to power IMDs. Human body motion from various organs and parts is a rich source of energy and has been utilized to develop self-powered TENG healthcare devices.[603–605] TENG has introduced multiple non-invasive methods to monitor and analyze medical parameters in real-time. Its applications have extended to the biomechanical energy-based application such as heart and respiration monitoring heart, sleep monitoring, sweat sensor respiration, fall detection, Parkinson's disease tremor sensor, and many other circumstances.[606–609] Accordingly, there is a need to secure non-invasive and sustainable TENG-based powering technology apart from organ motion-driven TENG systems. Ultrasound, which has been approved by the US Food and Drug Administration (FDA) for various medical treatments, can trigger a TENG device to generate a large electrical power output into water; this method can achieve an output power of 0.362 W/cm^2 at an ultrasonic wave frequency of 80 kHz.[610] In addition to typical non-biodegradable TENGs, a fully biodegradable TENG was demonstrated as an implantable power sources with time-transient functionality.[611] The device is fabricated using of biodegradable polymers and resorbable metals. The TENG device is degradable and resorbed in an animal body after the work cycle without any long-term effects. The device can generate an open-circuit voltage up to ~40 V and the corresponding short-circuit current up to ~1 μA. The selection of materials used to fabricate the biodegradable TENG is based on the biomaterials point of view, such as biodegradable and biocompatibility. However, the biodegradable TENG was fabricated mostly using biodegradable polymer due the above property as well as it has different tendency to gain/lose electrons when polymer used as the friction part of the TENG.[6] Furthermore, the polymers used in biodegradable in TENG are low-cost, commercially available, and soluble in suitable solvent systems to promote facile processing methods, including spin coating and solution casting. From the above properties, the best polymers, such poly(L-lactide-*co*-glycolide) (PLGA), poly(3-hydroxybutyric acid-*co*-3-hydroxyvaleric acid) (PHB/V), poly(caprolactone) (PCL), and poly(vinyl alcohol) (PVA), have been used in fabricating biodegradable TENG.[611]

4. Powering IMDs using TENGs

a. TENGs driven by biomechanical energy. Zheng *et al.*[596] utilized an implantable TENG to power *in vivo* biomedical electronics and form a self-powered system [Fig. 27(a)]. The TENG was inserted beneath the left chest membrane of a rat and generated an output voltage and current of ~3.73 V and ~0.14 μA, respectively. They explored a self-powered pacemaker model; the output of a particular stimulation pulse of the developed pacemaker model was almost 25 μA, and the pulse width was about 2 ms, which is analogous to those of commercial pacemakers. Furthermore, Ouyang *et al.*[427] explored an implantable TENG with an output power of ~10 μW/cm^2 [Fig. 27(b)]. It is noteworthy that RFID tags and wireless sensors can be driven with 1–10 μW/cm^2. The amount of energy generated solely depends on the function of the heart, which may raise concerns regarding the effectiveness and safety of TENGs in powered devices. Unlike various external movements, the movement of different parts inside the body is so small that a TENG needs to be finely tuned in order to work. Hence, the research community is looking forward to non-invasive and sustainable TENG-based powering systems with high power-generating performance.

b. TENG driven by ultrasound. Ultrasound is an important instrument for diagnosis and treatment in various medical applications approved by FDA. A sound wave can effectively travel through biological tissue and cause oscillation in a specific region. The ultrasound technology has been made using inverse piezoelectric principle and possibility to achieve high energy harvesting performance using advanced piezoelectric materials, designing device, and choosing resonance frequency.[612] The ultrasound based piezoelectric energy harvesting strategy is to use propagating ultrasound waves to carry the available energy, which is essentially a

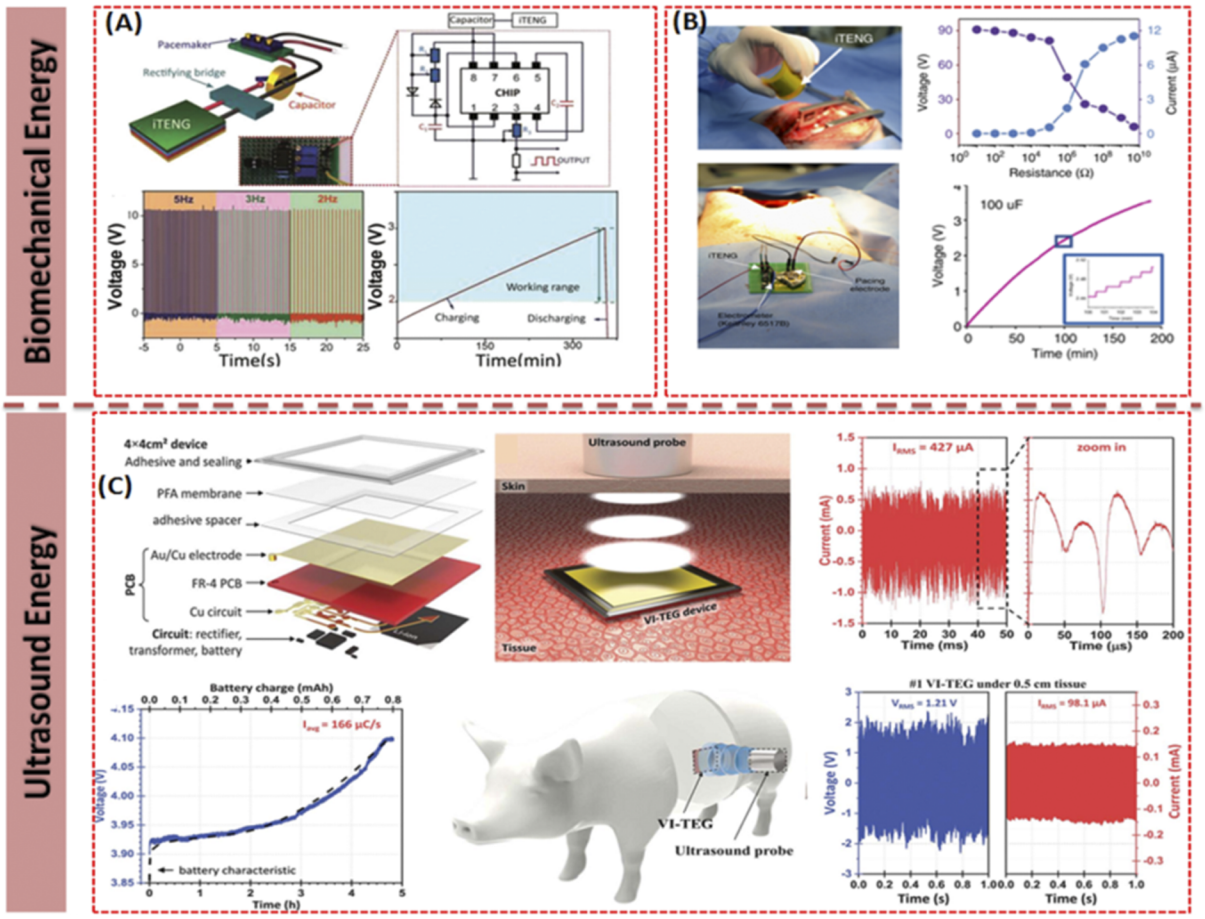

FIG. 27. (a)–(c) Powering IMDs with energy generated from TENGs with different mechanical vibration energy sources. Reproduced with permission from Ouyang *et al.*, Nat. Commun. **10**, 1821 (2019). Copyright 2019 Springer Nature. Reproduced with permission from Zheng *et al.*, Adv. Mater. **26**, 5851 (2014). Copyright 2014 Wiley-VCH Verlag GmbH & Co. KGaA. Reproduced with permission from Hinchet *et al.*, Science **365**, 491 (2019). Copyright 2019 AAAS.

mechanical vibration that propagates in a host medium. The structure of piezoelectric materials (such as PZT, $BaTiO_3$, and ZnO) structure is deformed by ultrasonic waves, and the charge separation process generates a piezoelectric potential in that will induce a current to drive electronics.[613] Thus, the electrical signal flowing through the external circuit is consecutively produced as the piezo-potential under dynamic pressure. The microelectromechanical system-based piezoelectric ultrasound energy can be used for IMDs explored by Shi *et al.*[614,615] where they used PZT diaphragm array with a resonance frequency of 240–250 kHz capable to generate 3.75 $\mu W/cm^2$ at distance of 1 cm and 1 mW/cm^2 of ultrasound intensity. In case of TENG, under ultrasound energy, the two different materials with different surface potential can contact together and generate electrical signal via external circuit similar to the conventional triboelectric mechanism, such as contacting/sliding of two different materials layers under ultrasound pressure. Ultrasound pressure can be measured by a hydrophone placed at 1 cm distance from the bulk PZT, and then ultrasound intensity can be calculated using formula $I = P^2/2Z$, where I is the ultrasound intensity, P is the ultrasound pressure, and Z is the acoustic impedance (for water medium, Z is 1.48×10^6 kg/m^2 s).[615] Recently, TENGs have begun to be regarded as a back-up alternative energy technology for powering IMDs due to their powering capability, wide materials selection, etc.[616] Recently, Hinchet *et al.*[592] reported transcutaneous ultrasound energy harvesting using a TENG technology for powering IMDs. An ultrasound-based TENG was triggered by application of a 20 kHz ultrasound at 3 W/cm^2 and reached 9.71 V (output voltage) and 427 μA (output current) (root mean square value). The ultrasound induced μm-scale displacement of a polymer thin membrane to generate electrical energy through contact electrification. For *in vivo* applications, researchers have experimentally simulated clinical conditions that are closer to those seen in humans in order to predict the TENG's ability to power an IMD. The implanted TENG produced a voltage and current from ultrasound energy transfer of 2.4 V and 156 μA, respectively, under porcine tissue, which could charge a rechargeable Li-ion battery

with a capacity of 0.7 mA h. Hence, the amount of power generated is high enough to recharge secondary batteries in smart IMDs, such as neurostimulators, insulin pumps, cochlear implants, artificial organs, and pacemakers, which only need 1–100 mW of power to run.

5. Remarks and future challenges

This review discussed recent advances in implantable TENGs for biomechanical energy harvesting and powering IMDs. The fabrication process of TENG devices is relatively simple and convenient, with low cost. In addition, TENG provides enough output power with high efficiency to power low power-consuming IMDs. Moreover, TENGs can produce continuous electricity using kinetic motion and triboelectric materials (generally polymers) in wearable platforms that can interface with biological systems. However, there are some limitations regarding the powering of IMDs using TENGs. For example, the output power generated is not constant and depends on consistent cyclic movement of the device. A cavity must form between two contact layers. Furthermore, during long-term operation of a TENG, its performance may deteriorate due to unwanted misallocation of the spacers between triboelectric materials.

The research community is expecting substantial improvements in methods of powering IMDs using TENGs in the coming days. The energy-harvesting property of TENGs is an indispensable aspect of IMD application, and a non-invasive solution would be a remarkable advancement. It is difficult for biomechanical energy-driven TENGs to generate enough electrical power to fully charge the batteries in IMDs. In this respect, transcutaneous ultrasound has been proposed in an attempt to enhance the output power of a TENG. This advancement promises the ability to generate higher power levels than traditional methods. Still, miniaturization, higher power output, and a proper power management system for TENGs used to power IMDs are necessary.

In order to develop sustainable implantable TENGs to run IMDs, from a commercial viewpoint, some essential features must be developed and additional efforts are required. (i) Fundamental studies on triboelectrification must be fully supported to increase the power conversion efficiency, flexibility, and sustainability of TENGs for long-term *in vivo* applications. (ii) Researchers must be deeply concerned about the toxicity, biocompatibility, and biodegradability of TENGs, which are essential for the safe implementation of TENGs inside the body. (iii) Strategies for encapsulating TENGs should be developed that prolong the devices' lifespans under implantable environments. (iv) The input ultrasound energy of ultrasound-mediated TENGs needs to be studied as a function of the depth of the device. (v) To improve interfacial adhesion and strain relief for long-lasting couplings, the interface between body tissue and implanted TENGs must be well controlled.

6. Acknowledgments

This work was financially Nano Material Technology Development Program (Grant No. 2020M3H4A1A03084600) through the National Research Foundation of Korea (NRF) funded by Ministry of Science and ICT and the GRRC Program of Gyeonggi Province (GRRC Sungkyunkwan 2017-B05).

VI. SUMMARY OF CHALLENGES

Qingshen Jing (*qj214@cam.ac.uk), Sohini Kar-Narayan (*sk568@cam.ac.uk)

The field of nanogenerators and piezotronics has witnessed an exponential growth within the last decade, and has ushered in innovative technologies for energy harvesting and sensing in a variety of different settings and applications, as has been highlighted in this roadmap. Progress in this field has been spurred on through advances in materials science and engineering that have led to novel functional materials and devices, as well as the development of new theoretical and computational frameworks that have provided a better understanding of the piezoelectric, piezotronic, photopiezotronic, and triboelectric phenomena that underpin this fast-moving field of research. This roadmap has sought to capture key advances and challenges in the field of nanogenerators and piezotronics, with a view to stimulate further research and innovation in what is undoubtedly a scientifically exciting and technologically relevant area. For example, there still remain open questions about the charge species involved in the operation of triboelectric nanogenerators, or indeed the charge transfer dynamics. Recent studies have indicated that electron transfer is the dominant mechanism for triboelectrification between solid–solid pairs. The same mechanism can be extended to liquid–solid, liquid–gas, and even liquid–liquid pairs, where the interaction is mediated via molecules.[61] While these topics have been researched intensively, a conclusive model is still being developed, and therefore establishing a solid theoretical framework remains an important challenge in the field.

One of the most promising application areas of nanogenerators and piezotronics devices is in wearables and smart textile applications.[617] As discussed in this roadmap, there remain challenges in the integration of such devices into textiles and fibers. For example, in the case of TENGs, the porous structure of fibers reduces charge density, hence energy output, and also absorbed moisture lowers power generation. Therefore, a structural design with complex geometric configuration for multiple TENG working models is required, taking into account decreased performance due to the increase of resistance and decrease of flexibility when fibers are woven together into textiles. Dimensional and output stability related to washability also needs to be improved in order to be compatible with textile-based applications. It is also important to note that while the compliant nature of a textile makes it comfortable for the wearer, it also reduces the mechanical energy coupled into the energy harvesting/sensing transducer, which in turn reduces the energy that can be harvested. This may involve, for example, designing a garment in such a way that strain is concentrated through the energy harvester itself.

However, increased porosity may actually be desirable as in the case of piezoelectric ceramics. There are still challenges related to the flexibility of these materials and in the ability to maintain compositional homogeneity and stability of properties particularly for applications in large-scale energy harvesting. There is plenty of scope in this area to further develop materials and systems that suit broadband mechanical energy sources through optimization of materials and devices, including through the development of new ferroelectret materials.

Another class of materials that has generated significant interest in the community is functional 2D materials, such as those exhibiting piezoelectric properties. However, the difficulty in exploring the known 2D piezoelectric materials for practical applications is in achieving consistent piezoelectric response using current fabrication processes. The symmetry in most 2D piezoelectrics results in thickness-dependent piezoelectric properties that impose formidable challenges for the process control. Also, unintentional environmental doping of 2D materials affects the carrier concentration and, hence, the performance. There is therefore a need to develop a sound understanding of the mechanism governing piezoelectricity at the atomic scale, and from a more practical point of view, there is a need to improve and up-scale the fabrication and device integration methods.

In terms of architected material for energy harvesting, innovative metamaterial design schemes that increase the degree of input wave energy amplification are expected to be well-suited to a wide range of frequencies. While significant progress has been made in this area, there are still challenges associated with size reduction required to match the wavelength of acoustic and elastic waves present in ambient mechanical vibrations. Machine learning-based design algorithms could prove to be highly beneficial specific target applications. Also, improvement of impedance matching at the interface between the metamaterials-amplified wave energy and energy harvesting devices needs to be considered in more detail.

An interesting development in the field of nanogenerators has been the emergence of organo-halide perovskites in multimodal piezoelectric generators. In terms of challenges, the intrinsic structural instability of halide perovskites, such as phase instability, and their extrinsic instability (thermal/optical/ambient) need to be considered and addressed. At the same time, novel material architectures need to be explored based on the wide tunability of the perovskite. Decoupling the effect among multiple energetic stimuli to gain fundamental understanding of the mechanisms at play is required, as well as demonstrations of applicability of these materials in sensors and energy generators.

There has been continued interest in the use of polymers for nanogenerators and piezotronics in the field.[618] In this regard, smart polymer materials (SPM) have generated significant interest; however, the improvement in certain properties of SPM device tends to be accompanied with a trade-off in other properties. For example, current SPMs used in TENGs are not necessarily situated at extreme positions in the triboelectric series, or they may need advanced fabrication approaches for micro- or nanopatterning.[619] When SPM-based TENGs are used as sensors, the output can be easily affected by various factors that reduce the reliability. At the same time, polymer-based PENGs are limited by their low piezoelectric coefficients and thermostability compared to piezoelectric ceramics. This points toward the development of robust polymer–ceramic composites with reproducible and reliable piezoelectric performance. In any case, the conflict between narrow power bandwidth of many piezoelectric energy harvesters and real-world energy sources with broadband spectrum is one of the biggest challenges in the field. Output power is often limited due to the size constraint on the system. There is no general energy harvester design method that suits different applications due to factors such as narrow bandwidth of the transducer and different environmental conditions. Thus, the lack of real-world environmental data makes it challenging to design a working system for a given application.

In terms of applications of piezoelectric acoustic sensors, the resonant frequencies of the acoustic sensors need to be properly designed for the spectrum range, especially when the dimension of the sensor is downscaled. Going forward, the sensitivity of resonant acoustic sensors could be enhanced for modularization, which requires robust characteristics under noisy conditions, for instance. The combination of an acoustic sensor with optimized machine learning algorithms could pave the way for accurate voice recognition and speech processing. Similarly, nanogenerators could pave the way for closed-loop electrostimulation in biomedical applications. One of the challenges is how to generate stable and sufficiently large electric pulses from small biomechanical motions *in vivo*. Flexible nanogenerators and packaged devices need to be designed with specific motion and softness configurations, without burdening the organ or muscle to which they are to be attached. Importantly, further in-depth cellular level understanding is required to quantify the relationship between electrostimulation from nanogenerators and the targeted biological processes.

When it comes to biological and biomedical applications, TENGs have proven to be highly promising candidates, both as energy harvesters and as sensors. For example, they can be deployed as highly sensitive sensors for human–machine interface. Although the sensor can actively generate electrical signals without being powered, the associated back-end device still needs an additional power supply. At the same time, more flexibility, stretchability, washability and multi-functionality is desired to meet the portable or wearable requirements of human machine interfaces, thus requiring further development of functional materials and advanced fabrication techniques. Even greater challenges exist in the use of TENGs to power body-implantable medical devices, for example, the output power generated is not constant and depends on consistent cyclic movement of the device. As it is extremely difficult for biomechanical energy-driven TENGs to generate enough electrical power for implantable devices, transcutaneous ultrasound can deployed to improve TENG output power. More generally, there is a lot of scope for fundamental studies for "body-energy" conversion efficiency, flexibility and sustainability for *in vivo* applications. Issues related to toxicity, biocompatibility, and biodegradability of TENGs for safe implantation still need to be addressed.

In summary, there is great potential in the field of nanogenerators and piezotronics across many application areas, but there also remain open questions in our understanding of the fundamentals of this field, and challenges in the practical implementation. This roadmap serves to highlight key developments and directions in the field, in order to stimulate further research and innovation that may lead to successful commercial technologies across energy, healthcare, communications, wearables, robotics, and other industries.

AUTHOR DECLARATIONS

Conflict of Interest

The authors have no conflicts to disclose.

Author Contributions

Philippe Basset: Conceptualization (equal); Funding acquisition (lead); Supervision (lead); Writing – original draft (equal); Writing – review & editing (equal). **Stephen Paul Beeby**: Conceptualization (equal); Funding acquisition (lead); Supervision (lead); Writing – original draft (equal); Writing – review & editing (equal). **Chris Bowen**: Conceptualization (equal); Funding acquisition (lead); Supervision (lead); Writing – original draft (equal); Writing – review & editing (equal). **Zheng Jun Chew**: Conceptualization (equal); Writing – original draft (equal); Writing – review & editing (equal). **Ahmad Delbani**: Conceptualization (equal); Writing – original draft (equal); Writing – review & editing (equal). **R. D. Ishara G. Dharmasena**: Conceptualization (equal); Writing – original draft (equal); Writing – review & editing (equal). **Bhaskar Dudem**: Conceptualization (equal); Writing – original draft (equal); Writing – review & editing (equal). **Feng Ru Fan**: Conceptualization (equal); Funding acquisition (lead); Supervision (lead); Writing – original draft (equal); Writing – review & editing (equal). **Dimitri Galayko**: Conceptualization (equal); Writing – original draft (equal); Writing – review & editing (equal). **Hengyu Guo**: Conceptualization (equal); Writing – original draft (equal); Writing – review & editing (equal). **Jianhua Hao**: Conceptualization (equal); Funding acquisition (lead); Supervision (lead); Writing – original draft (equal); Writing – review & editing (equal). **Yuchen Hou**: Conceptualization (equal); Writing – original draft (equal); Writing – review & editing (equal). **Chenguo Hu**: Conceptualization (equal); Funding acquisition (lead); Supervision (lead); Writing – original draft (equal); Writing – review & editing (equal). **Qingshen Jing**: Conceptualization (equal); Project administration (lead); Supervision (lead); Writing – original draft (equal); Writing – review & editing (equal). **Young Hoon Jung**: Conceptualization (equal) Writing – original draft, Writing – review & editing. **Sumanta Kumar Karan**: Conceptualization (equal) Writing – original draft (equal); Writing – review & editing (equal). **Sohini Kar-Narayan**: Conceptualization (equal); Funding acquisition (lead); Supervision (lead); Writing – original draft (equal); Writing – review & editing (equal). **Miso Kim**: Conceptualization (equal); Funding acquisition (lead); Supervision (lead); Writing – original draft (equal); Writing – review & editing (equal). **Sang-Woo Kim**: Conceptualization (equal); Funding acquisition (lead); Supervision (lead); Writing – original draft (equal); Writing – review & editing (equal). **Yang Kuang**: Conceptualization (equal); Writing – original draft (equal); Writing – review & editing (equal). **Keon Jae Lee**: Conceptualization (equal); Funding acquisition (lead); Supervision (lead); Writing – original draft (equal); Writing – review & editing (equal). **Jialu Li**: Conceptualization (equal); Writing – original draft (equal); Writing – review & editing (equal). **Zhaoling Li**: Conceptualization (equal); Funding acquisition (lead); Supervision (lead) Writing – original draft (equal); Writing – review & editing (equal). **Yin Long**: Conceptualization (equal); Writing – original draft (equal); Writing – review & editing (equal). **Shashank Priya**: Conceptualization (equal); Funding acquisition (lead); Supervision (lead); Writing – original draft (equal); Writing – review & editing (equal). **Xianjie Pu**: Conceptualization (equal); Writing – original draft (equal); Writing – review & editing (equal). **Tingwen Ruan**: Conceptualization (equal); Writing – original draft (equal); Writing – review & editing (equal). **S. Ravi P. Silva**: Conceptualization (equal); Funding acquisition (lead); Supervision (lead); Writing – original draft (equal); Writing – review & editing (equal). **Hee Seung Wang**: Conceptualization (equal); Writing – original draft (equal); Writing – review & editing (equal). **Kai Wang**: Conceptualization (equal); Writing – original draft (equal); Writing – review & editing (equal). **Xudong Wang**: Conceptualization (equal); Funding acquisition (lead); Supervision (lead); Writing – original draft (equal); Writing – review & editing (equal). **Zhong Lin Wang**: Conceptualization (equal); Funding acquisition (lead); Supervision (lead); Writing – original draft (equal); Writing – review & editing (equal). **Wenzhuo Wu**: Conceptualization (equal); Funding acquisition (lead); Supervision (lead); Writing – original draft (equal); Writing – review & editing (equal). **Wei Xu**: Conceptualization (equal); Writing – original draft (equal); Writing – review & editing (equal). **Hemin Zhang**: Conceptualization (equal); Writing – original draft (equal); Writing – review & editing (equal). **Yan Zhang**: Conceptualization (equal); Writing – original draft (equal); Writing – review & editing (equal). **Meiling Zhu**: Conceptualization (equal); Funding acquisition (lead); Supervision (lead); Writing – original draft (equal); Writing – review & editing (equal).

DATA AVAILABILITY

Data sharing is not applicable to this article as no new data were created or analyzed in this study.

REFERENCES

[1] Z. L. Wang and J. Song, Science **312**, 242 (2006).
[2] F.-R. Fan, Z.-Q. Tian, and Z. Lin Wang, Nano Energy **1**, 328 (2012).
[3] F.-R. Fan, L. Lin, G. Zhu, W. Wu, R. Zhang, and Z. L. Wang, Nano Lett. **12**, 3109 (2012).
[4] Z. L. Wang, Mater. Today **20**, 74 (2017).
[5] Z. L. Wang, Nano Energy **68**, 104272 (2020).
[6] Z. L. Wang, ACS Nano **7**, 9533 (2013).
[7] X. Zhao, Z. Kang, Q. Liao, Z. Zhang, M. Ma, Q. Zhang, and Y. Zhang, Nano Energy **48**, 312 (2018).
[8] X. Zhao, H. Askari, and J. Chen, Joule **5**, 1391 (2021).
[9] J. Luo, W. Gao, and Z. L. Wang, Adv. Mater. **33**, 2004178 (2021).
[10] Z. L. Wang, Nano Energy **58**, 669 (2019).
[11] Z. L. Wang, Nano Today **5**, 512 (2010).
[12] Z. Zhou, X. Li, Y. Wu, H. Zhang, Z. Lin, K. Meng, Z. Lin, Q. He, C. Sun, J. Yang, and Z. L. Wang, Nano Energy **53**, 501 (2018).
[13] Y. Zhou, M. Shen, X. Cui, Y. Shao, L. Li, and Y. Zhang, Nano Energy **84**, 105887 (2021).
[14] Z. L. Wang, Adv. Energy Mater. **10**, 2000137 (2020).
[15] C. Wu, A. C. Wang, W. Ding, H. Guo, and Z. L. Wang, Adv. Energy Mater. **9**, 1802906 (2019).
[16] Z. L. Wang, T. Jiang, and L. Xu, Nano Energy **39**, 9 (2017).
[17] J. Chen, J. Yang, Z. Li, X. Fan, Y. Zi, Q. Jing, H. Guo, Z. Wen, K. C. Pradel, S. Niu, and Z. L. Wang, ACS Nano **9**, 3324 (2015).
[18] Y. S. Choi and S. Kar-Narayan, EcoMat **2**, e12063 (2020).
[19] Y. S. Choi, S. W. Kim, and S. Kar-Narayan, Adv. Energy Mater. **11**, 2003802 (2021).
[20] Q. Jing and S. Kar-Narayan, J. Phys. D: Appl. Phys. **51**, 303001 (2018).
[21] Z. L. Wang, Adv. Mater. **19**, 889 (2007).
[22] J. Zhou, P. Fei, Y. Gu, W. Mai, Y. Gao, R. Yang, G. Bao, and Z. L. Wang, Nano Lett. **8**, 3973 (2008).
[23] Y. Hu, Y. Chang, P. Fei, R. L. Snyder, and Z. L. Wang, ACS Nano **4**, 1234 (2010).

[24]Q. Yang, X. Guo, W. Wang, Y. Zhang, S. Xu, D. H. Lien, and Z. L. Wang, ACS Nano **4**, 6285 (2010).
[25]Y. Yang, L. Lin, Y. Zhang, Q. Jing, T.-C. Hou, and Z. L. Wang, ACS Nano **6**, 10378 (2012).
[26]S. Wang, L. Lin, and Z. L. Wang, Nano Lett. **12**, 6339 (2012).
[27]B. Dudem, Y. H. Ko, J. W. Leem, S. H. Lee, and J. S. Yu, ACS Appl. Mater. Interfaces **7**, 20520 (2015).
[28]Z. L. Wang, Faraday Discuss. **176**, 447 (2014).
[29]S. Niu, Y. Liu, S. Wang, L. Lin, Y. S. Zhou, Y. Hu, and Z. L. Wang, Adv. Mater. **25**, 6184 (2013).
[30]S. Niu, S. Wang, L. Lin, Y. Liu, Y. S. Zhou, Y. Hu, and Z. L. Wang, Energy Environ. Sci. **6**, 3576 (2013).
[31]S. Niu, Y. Liu, S. Wang, L. Lin, Y. S. Zhou, Y. Hu, and Z. L. Wang, Adv. Funct. Mater. **24**, 3332 (2014).
[32]S. Niu, S. Wang, Y. Liu, Y. S. Zhou, L. Lin, Y. Hu, K. C. Pradel, and Z. L. Wang, Energy Environ. Sci. **7**, 2339 (2014).
[33]S. Niu, Y. Liu, X. Chen, S. Wang, Y. S. Zhou, L. Lin, Y. Xie, and Z. L. Wang, Nano Energy **12**, 760 (2015).
[34]S. Niu and Z. L. Wang, Nano Energy **14**, 161 (2014).
[35]R. D. I. G. Dharmasena, K. D. G. I. Jayawardena, C. A. Mills, J. H. B. Deane, J. V. Anguita, R. A. Dorey, and S. R. P. Silva, Energy Environ. Sci. **10**, 1801 (2017).
[36]B. Dudem, N. D. Huynh, W. Kim, D. H. Kim, H. J. Hwang, D. Choi, and J. S. Yu, Nano Energy **42**, 269 (2017).
[37]I.-W. Tcho, W.-G. Kim, S.-B. Jeon, S.-J. Park, B. J. Lee, H.-K. Bae, D. Kim, and Y.-K. Choi, Nano Energy **42**, 34 (2017).
[38]R. D. I. G. Dharmasena, J. H. B. Deane, and S. R. P. Silva, Adv. Energy Mater. **8**, 1802190 (2018).
[39]R. D. I. G. Dharmasena, K. D. G. I. Jayawardena, C. A. Mills, R. A. Dorey, and S. R. P. Silva, Nano Energy **48**, 391 (2018).
[40]C. Xu, Y. Zi, A. C. Wang, H. Zou, Y. Dai, X. He, P. Wang, Y.-C. Wang, P. Feng, D. Li, and Z. L. Wang, Adv. Mater. **30**, 1706790 (2018).
[41]J. Wu, X. Wang, H. Li, F. Wang, W. Yang, and Y. Hu, Nano Energy **48**, 607 (2018).
[42]S. Lin, L. Xu, L. Zhu, X. Chen, and Z. L. Wang, Adv. Mater. **31**, 1901418 (2019).
[43]X. Li, T. H. Lau, D. Guan, and Y. Zi, J. Mater. Chem. A **7**, 19485 (2019).
[44]R. D. I. G. Dharmasena and S. R. P. Silva, Nano Energy **62**, 530 (2019).
[45]J. H. B. Deane, R. D. I. G. Dharmasena, and G. Gentile, Nano Energy **54**, 39 (2018).
[46]J. Shao, M. Willatzen, and Z. L. Wang, J. Appl. Phys. **128**, 111101 (2020).
[47]S.-H. Shin, Y. H. Kwon, Y.-H. Kim, J.-Y. Jung, M. H. Lee, and J. Nah, ACS Nano **9**, 4621 (2015).
[48]B. Meng, W. Tang, Z.-h. Too, X. Zhang, M. Han, W. Liu, and H. Zhang, Energy Environ. Sci. **6**, 3235 (2013).
[49]S. Wang, Y. Xie, S. Niu, L. Lin, C. Liu, Y. S. Zhou, and Z. L. Wang, Adv. Mater. **26**, 6720 (2014).
[50]Y. Zi, S. Niu, J. Wang, Z. Wen, W. Tang, and Z. L. Wang, Nat. Commun. **6**, 8376 (2015).
[51]X. Xia, J. Fu, and Y. Zi, Nat. Commun. **10**, 4428 (2019).
[52]J. Shao, T. Jiang, W. Tang, X. Chen, L. Xu, and Z. L. Wang, Nano Energy **51**, 688 (2018).
[53]J. Shao, M. Willatzen, T. Jiang, W. Tang, X. Chen, J. Wang, and Z. L. Wang, Nano Energy **59**, 380 (2019).
[54]J.-G. Sun, T. N. Yang, I.-S. Kuo, J.-M. Wu, C.-Y. Wang, and L.-J. Chen, Nano Energy **32**, 180 (2017).
[55]L. Zhao, Q. Zheng, H. Ouyang, H. Li, L. Yan, B. Shi, and Z. Li, Nano Energy **28**, 172 (2016).
[56]B. Dudem, A. R. Mule, H. R. Patnam, and J. S. Yu, Nano Energy **55**, 305 (2019).
[57]B. Dudem, D. H. Kim, A. R. Mule, and J. S. Yu, ACS Appl. Mater. Interfaces **10**, 24181 (2018).
[58]D. Kim, S. Lee, Y. Ko, C. H. Kwon, and J. Cho, Nano Energy **44**, 228 (2018).
[59]J. Chun, J. W. Kim, W.-s. Jung, C.-Y. Kang, S.-W. Kim, Z. L. Wang, and J. M. Baik, Energy Environ. Sci. **8**, 3006 (2015).
[60]G. Xu, X. Li, X. Xia, J. Fu, W. Ding, and Y. Zi, Nano Energy **59**, 154 (2019).
[61]Z. L. Wang and A. C. Wang, Mater. Today **30**, 34 (2019).
[62]C.-y. Liu and A. J. Bard, Chem. Phys. Lett. **480**, 145 (2009).
[63]A. F. Diaz, D. Wollmann, and D. Dreblow, Chem. Mater. **3**, 997 (1991).
[64]L. S. McCarty and G. M. Whitesides, Angew. Chem., Int. Ed. **47**, 2188 (2008).
[65]H. T. Baytekin, A. Z. Patashinski, M. Branicki, B. Baytekin, S. Soh, and B. A. Grzybowski, Science **333**, 308 (2011).
[66]A. C. Wang, B. Zhang, C. Xu, H. Zou, Z. Lin, and Z. L. Wang, Adv. Funct. Mater. **30**, 1909384 (2020).
[67]K. R. S. Gunawardhana, N. D. Wanasekara, K. G. Wijayantha, and R. D. I. Dharmasena, ACS Appl. Electron. Mater. **4**, 678 (2022).
[68]W. Paosangthong, R. Torah, and S. Beeby, Nano Energy **55**, 401 (2019).
[69]Y. Yao, T. Jiang, L. Zhang, X. Chen, Z. Gao, and Z. L. Wang, ACS Appl. Mater. Interfaces **8**, 21398 (2016).
[70]K. Dong, X. Peng, J. An, A. C. Wang, J. Luo, B. Sun, J. Wang, and Z. L. Wang, Nat. Commun. **11**, 2868 (2020).
[71]R. D. I. G. Dharmasena and K. G. U. Wijayantha, Nano Energy **90**, 106511 (2021).
[72]X. Guo, J. Shao, M. Willatzen, Y. Yang, and Z. L. Wang, Nano Energy **92**, 106762 (2022).
[73]J. Shao, Y. Yang, O. Yang, J. Wang, M. Willatzen, and Z. L. Wang, Adv. Energy Mater. **11**, 2100065 (2021).
[74]D. Zhang, J. Fuel Chem. Technol. **33**, 399 (2005).
[75]Y. He, Y. Xu, Y. Pang, H. Tian, and R. Wu, Renewable Energy **89**, 695 (2016).
[76]W. Liu, Z. Wang, and C. Hu, Mater. Today **45**, 93 (2021).
[77]T. Huang, J. Zhang, B. Yu, H. Yu, H. Long, H. Wang, Q. Zhang, and M. Zhu, Nano Energy **58**, 375 (2019).
[78]Y. Su, T. Yang, X. Zhao, Z. Cai, G. Chen, M. Yao, K. Chen, M. Bick, J. Wang, S. Li, G. Xie, H. Tai, X. Du, Y. Jiang, and J. Chen, Nano Energy **74**, 104941 (2020).
[79]Y. Su, J. Wang, B. Wang, T. Yang, B. Yang, G. Xie, Y. Zhou, S. Zhang, H. Tai, Z. Cai, G. Chen, Y. Jiang, L.-Q. Chen, and J. Chen, ACS Nano **14**, 6067 (2020).
[80]T. Sun, B. Zhou, Q. Zheng, L. Wang, W. Jiang, and G. J. Snyder, Nat. Commun. **11**, 572 (2020).
[81]Y. Guo, X.-S. Zhang, Y. Wang, W. Gong, Q. Zhang, H. Wang, and J. Brugger, Nano Energy **48**, 152 (2018).
[82]Y. Zhou, J. He, H. Wang, K. Qi, N. Nan, X. You, W. Shao, L. Wang, B. Ding, and S. Cui, Sci. Rep. **7**, 12949 (2017).
[83]S. S. Kwak, H. Kim, W. Seung, J. Kim, R. Hinchet, and S.-W. Kim, ACS Nano **11**, 10733 (2017).
[84]Z. Zhao, C. Yan, Z. Liu, X. Fu, L.-M. Peng, Y. Hu, and Z. Zheng, Adv. Mater. **28**, 10267 (2016).
[85]Y. Guo, K. Li, C. Hou, Y. Li, Q. Zhang, and H. Wang, ACS Appl. Mater. Interfaces **8**, 4676 (2016).
[86]X. Pu, L. Li, H. Song, C. Du, Z. Zhao, C. Jiang, G. Cao, W. Hu, and Z. L. Wang, Adv. Mater. **27**, 2472 (2015).
[87]W. Gong, C. Hou, J. Zhou, Y. Guo, W. Zhang, Y. Li, Q. Zhang, and H. Wang, Nat. Commun. **10**, 868 (2019).
[88]W. Seung, M. K. Gupta, K. Y. Lee, K.-S. Shin, J.-H. Lee, T. Y. Kim, S. Kim, J. Lin, J. H. Kim, and S.-W. Kim, ACS Nano **9**, 3501 (2015).
[89]Y. Yang, L. Xie, Z. Wen, C. Chen, X. Chen, A. Wei, P. Cheng, X. Xie, and X. Sun, ACS Appl. Mater. Interfaces **10**, 42356 (2018).
[90]X. He, Y. Zi, H. Guo, H. Zheng, Y. Xi, C. Wu, J. Wang, W. Zhang, C. Lu, and Z. L. Wang, Adv. Funct. Mater. **27**, 1604378 (2017).
[91]J. Liu, N. Cui, T. Du, G. Li, S. Liu, Q. Xu, Z. Wang, L. Gu, and Y. Qin, Nanoscale Adv. **2**, 4482 (2020).
[92]J. Zhong, Y. Zhang, Q. Zhong, Q. Hu, B. Hu, Z. L. Wang, and J. Zhou, ACS Nano **8**, 6273 (2014).
[93]Z. Li, J. Shen, I. Abdalla, J. Yu, and B. Ding, Nano Energy **36**, 341 (2017).
[94]T. Zhou, C. Zhang, C. B. Han, F. R. Fan, W. Tang, and Z. L. Wang, ACS Appl. Mater. Interfaces **6**, 14695 (2014).
[95]Z. Zhao, X. Pu, C. Du, L. Li, C. Jiang, W. Hu, and Z. L. Wang, ACS Nano **10**, 1780 (2016).
[96]S. Li, J. Wang, W. Peng, L. Lin, Y. Zi, S. Wang, G. Zhang, and Z. L. Wang, Adv. Energy Mater. **7**, 1602832 (2017).
[97]K. Dong, J. Deng, Y. Zi, Y.-C. Wang, C. Xu, H. Zou, W. Ding, Y. Dai, B. Gu, B. Sun, and Z. L. Wang, Adv. Mater. **29**, 1702648 (2017).

[98]Q. Qiu, M. Zhu, Z. Li, K. Qiu, X. Liu, J. Yu, and B. Ding, Nano Energy **58**, 750 (2019).
[99]R. Cheng, K. Dong, L. Liu, C. Ning, P. Chen, X. Peng, D. Liu, and Z. L. Wang, ACS Nano **14**, 15853 (2020).
[100]B. Liu, A. Libanori, Y. Zhou, X. Xiao, G. Xie, X. Zhao, Y. Su, S. Wang, Z. Yuan, Z. Duan, J. Liang, Y. Jiang, H. Tai, and J. Chen, ACS Appl. Mater. Interfaces **14**, 7301 (2022).
[101]X. Li, Z.-H. Lin, G. Cheng, X. Wen, Y. Liu, S. Niu, and Z. L. Wang, ACS Nano **8**, 10674 (2014).
[102]B. Shi, Q. Zheng, W. Jiang, L. Yan, X. Wang, H. Liu, Y. Yao, Z. Li, and Z. L. Wang, Adv. Mater. **28**, 846 (2016).
[103]M. Han, X.-S. Zhang, B. Meng, W. Liu, W. Tang, X. Sun, W. Wang, and H. Zhang, ACS Nano **7**, 8554 (2013).
[104]W.-S. Jung, M.-G. Kang, H. G. Moon, S.-H. Baek, S.-J. Yoon, Z.-L. Wang, S.-W. Kim, and C.-Y. Kang, Sci. Rep. **5**, 9309 (2015).
[105]X. Chen, Y. Song, Z. Su, H. Chen, X. Cheng, J. Zhang, M. Han, and H. Zhang, Nano Energy **38**, 43 (2017).
[106]G. Chen, Y. Li, M. Bick, and J. Chen, Chem. Rev. **120**, 3668 (2020).
[107]Y. Su, C. Chen, H. Pan, Y. Yang, G. Chen, X. Zhao, W. Li, Q. Gong, G. Xie, Y. Zhou, S. Zhang, H. Tai, Y. Jiang, and J. Chen, Adv. Funct. Mater. **31**, 2010962 (2021).
[108]K. Dong, X. Peng, and Z. L. Wang, Adv. Mater. **32**, 1902549 (2020).
[109]Q. Wei, G. Chen, H. Pan, Z. Ye, C. Au, C. Chen, X. Zhao, Y. Zhou, X. Xiao, H. Tai, Y. Jiang, G. Xie, Y. Su, and J. Chen, Small Methods **6**, 2101051 (2022).
[110]J. Xiong, P. Cui, X. Chen, J. Wang, K. Parida, M.-F. Lin, and P. S. Lee, Nat. Commun. **9**, 4280 (2018).
[111]Z. Yang, S. Zhou, J. Zu, and D. Inman, Joule **2**, 642 (2018).
[112]J. I. Roscow, H. Pearce, H. Khanbareh, S. Kar-Narayan, and C. R. Bowen, Eur. Phys. J.: Spec. Top. **228**, 1537 (2019).
[113]J. I. Roscow, Y. Zhang, M. J. Kraśny, R. W. C. Lewis, J. Taylor, and C. R. Bowen, J. Phys. D: Appl. Phys. **51**, 225301 (2018).
[114]R. A. Islam and S. Priya, Appl. Phys. Lett. **88**, 032903 (2006).
[115]X. Yu, Y. Hou, M. Zheng, J. Yan, W. Jia, and M. Zhu, J. Am. Ceram. Soc. **102**, 275 (2019).
[116]C. Sun, L. Qin, F. Li, and Q.-M. Wang, J. Intell. Mater. Syst. Struct. **20**, 559 (2009).
[117]F. Li, M. J. Cabral, B. Xu, Z. Cheng, E. C. Dickey, J. M. LeBeau, J. Wang, J. Luo, S. Taylor, W. Hackenberger, L. Bellaiche, Z. Xu, L.-Q. Chen, T. R. Shrout, and S. Zhang, Science **364**, 264 (2019).
[118]Y. Zhang, M. Xie, J. Roscow, Y. Bao, K. Zhou, D. Zhang, and C. R. Bowen, J. Mater. Chem. A **5**, 6569 (2017).
[119]M. Yan, Z. Xiao, J. Ye, X. Yuan, Z. Li, C. Bowen, Y. Zhang, and D. Zhang, Energy Environ. Sci. **14**, 6158 (2021).
[120]W. Qian, K. Zhao, D. Zhang, C. R. Bowen, Y. Wang, and Y. Yang, ACS Appl. Mater. Interfaces **11**, 27862 (2019).
[121]Y. Zhang, J. Roscow, R. Lewis, H. Khanbareh, V. Y. Topolov, M. Xie, and C. R. Bowen, Acta Mater. **154**, 100 (2018).
[122]T. Xu and C.-A. Wang, Mater. Des. **91**, 242 (2016).
[123]J. E. Smay, J. Cesarano, B. A. Tuttle, and J. A. Lewis, J. Appl. Phys. **92**, 6119 (2002).
[124]G. Zhang, P. Zhao, X. Zhang, K. Han, T. Zhao, Y. Zhang, C. K. Jeong, S. Jiang, S. Zhang, and Q. Wang, Energy Environ. Sci. **11**, 2046 (2018).
[125]W. Liu, J. Xu, Y. Wang, H. Xu, X. Xi, and J. Yang, J. Am. Ceram. Soc. **96**, 1827 (2013).
[126]B. P. Kumar, H. H. Kumar, and D. K. Kharat, J. Mater. Sci.: Mater. Electron. **16**, 681 (2005).
[127]J. I. Roscow, J. Taylor, and C. R. Bowen, Ferroelectrics **498**, 40 (2016).
[128]R. E. Newnham, D. P. Skinner, K. A. Klicker, A. S. Bhalla, B. Hardiman, and T. R. Gururaja, Ferroelectrics **27**, 49 (1980).
[129]N. Sharifi Olyaei, M. M. Mohebi, and R. Kaveh, J. Am. Ceram. Soc. **100**, 1432 (2017).
[130]H. Dommati, S. S. Ray, J.-C. Wang, and S.-S. Chen, RSC Adv. **9**, 16869 (2019).
[131]D.-J. Shin, D.-H. Lim, B.-K. Koo, M.-S. Kim, I.-S. Kim, and S.-J. Jeong, J. Alloys Compd. **831**, 154792 (2020).
[132]J. I. Roscow, R. W. C. Lewis, J. Taylor, and C. R. Bowen, Acta Mater. **128**, 207 (2017).
[133]Y. Zhang, M. Xie, J. Roscow, and C. Bowen, Mater. Res. Bull. **112**, 426 (2019).
[134]F. F. Abdullah, A. Nemati, and R. Bagheri, Mater. Lett. **151**, 85 (2015).
[135]T. Zeng, X. L. Dong, H. Chen, and Y. L. Wang, Mater. Sci. Eng., B **131**, 181 (2006).
[136]T. Zeng, X. Dong, S. Chen, and H. Yang, Ceram. Int. **33**, 395 (2007).
[137]J. Tan and Z. Li, Ceram. Int. **41**, S414 (2015).
[138]T. Zeng, X. Dong, C. Mao, S. Chen, and H. Chen, Mater. Sci. Eng., B **135**, 50 (2006).
[139]A. N. Reznichenko, M. A. Lugovaya, E. I. Petrova, N. A. Shvetsova, and A. N. Rybyanets, Ferroelectrics **539**, 93 (2019).
[140]A. Yang, C.-A. Wang, R. Guo, Y. Huang, and C.-W. Nan, J. Am. Ceram. Soc. **93**, 1427 (2010).
[141]R. Guo, C.-A. Wang, and A. Yang, J. Am. Ceram. Soc. **94**, 1794 (2011).
[142]S.-H. Lee, S.-H. Jun, H.-E. Kim, and Y.-H. Koh, J. Am. Ceram. Soc. **91**, 1912 (2008).
[143]S.-H. Lee, S.-H. Jun, H.-E. Kim, and Y.-H. Koh, J. Am. Ceram. Soc. **90**, 2807 (2007).
[144]P. Dixit, S. Seth, B. Rawal, B. P. Kumar, and H. S. Panda, J. Mater. Sci.: Mater. Electron. **32**, 5393 (2021).
[145]Y.-Y. Li, L.-T. Li, and B. Li, J. Alloys Compd. **620**, 125 (2015).
[146]Y. Li, L. Li, and B. Li, Materials **8**, 1729 (2015).
[147]Y. Zhang, C. R. Bowen, S. K. Ghosh, D. Mandal, H. Khanbareh, M. Arafa, and C. Wan, Nano Energy **57**, 118 (2019).
[148]M. Xie, Y. Zhang, M. J. Kraśny, C. Bowen, H. Khanbareh, and N. Gathercole, Energy Environ. Sci. **11**, 2919 (2018).
[149]Y. Zhang, C. R. Bowen, and S. Deville, Soft Matter **15**, 825 (2019).
[150]K. Mistewicz, M. Jesionek, H. J. Kim, S. Hajra, M. Kozioł, Ł. Chrobok, and X. Wang, Ultrason. Sonochem. **78**, 105718 (2021).
[151]W. Yang, Y. Wang, Z. Hou, and C. Li, Nanotechnology **30**, 505402 (2019).
[152]F. Li, D. Lin, Z. Chen, Z. Cheng, J. Wang, C. Li, Z. Xu, Q. Huang, X. Liao, L.-Q. Chen, T. R. Shrout, and S. Zhang, Nat. Mater. **17**, 349 (2018).
[153]F. Bouville, E. Portuguez, Y. Chang, G. L. Messing, A. J. Stevenson, E. Maire, L. Courtois, and S. Deville, J. Am. Ceram. Soc. **97**, 1736 (2014).
[154]Y. Zi, J. Wang, S. Wang, S. Li, Z. Wen, H. Guo, and Z. L. Wang, Nat. Commun. **7**, 10987 (2016).
[155]H. Qin, G. Cheng, Y. Zi, G. Gu, B. Zhang, W. Shang, F. Yang, J. Yang, Z. Du, and Z. L. Wang, Adv. Funct. Mater. **28**, 1805216 (2018).
[156]H. Samaali, Y. Perrin, A. Galisultanov, H. Fanet, G. Pillonnet, and P. Basset, Nano Energy **55**, 277 (2019).
[157]R. Hinchet, A. Ghaffarinejad, Y. Lu, J. Y. Hasani, S.-W. Kim, and P. Basset, Nano Energy **47**, 401 (2018).
[158]P. Basset, E. Blokhina, and D. Galayko, *Electrostatic Kinetic Energy Harvesting* (Wiley-ISTE, 2016).
[159]P. Basset, A. Kaiser, B. Legrand, D. Collard, and L. Buchaillot, IEEE/ASME Trans. Mechatron. **12**, 23 (2007).
[160]W. Liu, Z. Wang, G. Wang, G. Liu, J. Chen, X. Pu, Y. Xi, X. Wang, H. Guo, C. Hu, and Z. L. Wang, Nat. Commun. **10**, 1426 (2019).
[161]A. Ghaffarinejad, J. Yavand Hasani, D. Galayko, and P. Basset, Nano Energy **66**, 104137 (2019).
[162]A. C. M. De Queiroz and M. Domingues, IEEE Trans. Circuits Syst. II: Express Briefs **58**, 797 (2011).
[163]A. Ghaffarinejad, J. Y. Hasani, R. Hinchet, Y. Lu, H. Zhang, A. Karami, D. Galayko, S.-W. Kim, and P. Basset, Nano Energy **51**, 173 (2018).
[164]E. Lefeuvre, S. Risquez, J. Wei, M. Woytasik, and F. Parrain, J. Phys.: Conf. Ser. **557**, 012052 (2014).
[165]A. Karami, D. Galayko, and P. Basset, IEEE Trans. Circuits Syst. I: Regular Pap. **64**, 227 (2017).
[166]X. Xia, H. Wang, P. Basset, Y. Zhu, and Y. Zi, ACS Appl. Mater. Interfaces **12**, 5892 (2020).
[167]A. Brenes, A. Morel, J. Juillard, E. Lefeuvre, and A. Badel, Smart Mater. Struct. **29**, 033001 (2020).

[168]E. Lefeuvre, A. Badel, C. Richard, and D. Guyomar, J. Intell. Mater. Syst. Struct. **16**, 865 (2005).
[169]A. Badel, D. Guyomar, E. Lefeuvre, and C. Richard, J. Intell. Mater. Syst. Struct. **16**, 889 (2005).
[170]X. Cheng, L. Miao, Y. Song, Z. Su, H. Chen, X. Chen, J. Zhang, and H. Zhang, Nano Energy **38**, 438 (2017).
[171]F. Xi, Y. Pang, W. Li, T. Jiang, L. Zhang, T. Guo, G. Liu, C. Zhang, and Z. L. Wang, Nano Energy **37**, 168 (2017).
[172]J. Yang, F. Yang, L. Zhao, W. Shang, H. Qin, S. Wang, X. Jiang, G. Cheng, and Z. Du, Nano Energy **46**, 220 (2018).
[173]G. K. Ottman, H. F. Hofmann, A. C. Bhatt, and G. A. Lesieutre, IEEE Trans. Power Electron. **17**, 669 (2002).
[174]S. Niu, X. Wang, F. Yi, Y. S. Zhou, and Z. L. Wang, Nat. Commun. **6**, 8975 (2015).
[175]W. Harmon, D. Bamgboje, H. Guo, T. Hu, and Z. L. Wang, Nano Energy **71**, 104642 (2020).
[176]H. Zhang, F. Marty, X. Xia, Y. Zi, T. Bourouina, D. Galayko, and P. Basset, Nat. Commun. **11**, 3221 (2020).
[177]P. Bonato, IEEE Eng. Med. Biol. Mag. **29**, 25 (2010).
[178]D.-H. Kim, N. Lu, R. Ma, Y.-S. Kim, R.-H. Kim, S. Wang, J. Wu, S. M. Won, H. Tao, A. Islam, K. J. Yu, T.-i. Kim, R. Chowdhury, M. Ying, L. Xu, M. Li, H.-J. Chung, H. Keum, M. McCormick, P. Liu, Y.-W. Zhang, F. G. Omenetto, Y. Huang, T. Coleman, and J. A. Rogers, Science **333**, 838 (2011).
[179]W. Wu, X. Wen, and Z. L. Wang, Science **340**, 952 (2013).
[180]A. Chortos, J. Liu, and Z. Bao, Nat. Mater. **15**, 937 (2016).
[181]P. D. Marasco, K. Kim, J. E. Colgate, M. A. Peshkin, and T. A. Kuiken, Brain **134**, 747 (2011).
[182]B. J. Kane, M. R. Cutkosky, and G. T. A. Kovacs, J. Microelectromech. Syst. **9**, 425 (2000).
[183]E.-S. Hwang, J.-h. Seo, and Y.-J. Kim, J. Microelectromech. Syst. **16**, 556 (2007).
[184]W. Wu and Z. L. Wang, Nat. Rev. Mater. **1**, 16031 (2016).
[185]D. Akinwande, C. J. Brennan, J. S. Bunch, P. Egberts, J. R. Felts, H. Gao, R. Huang, J.-S. Kim, T. Li, Y. Li, K. M. Liechti, N. Lu, H. S. Park, E. J. Reed, P. Wang, B. I. Yakobson, T. Zhang, Y.-W. Zhang, Y. Zhou, and Y. Zhu, Extreme Mech. Lett. **13**, 42 (2017).
[186]K.-A. N. Duerloo, M. T. Ong, and E. J. Reed, J. Phys. Chem. Lett. **3**, 2871 (2012).
[187]M. N. Blonsky, H. L. Zhuang, A. K. Singh, and R. G. Hennig, ACS Nano **9**, 9885 (2015).
[188]C. Cui, F. Xue, W.-J. Hu, and L.-J. Li, npj 2D Mater. Appl. **2**, 18 (2018).
[189]W. Wu, L. Wang, Y. Li, F. Zhang, L. Lin, S. Niu, D. Chenet, X. Zhang, Y. Hao, T. F. Heinz, J. Hone, and Z. L. Wang, Nature **514**, 470 (2014).
[190]H. Zhu, Y. Wang, J. Xiao, M. Liu, S. Xiong, Z. J. Wong, Z. Ye, Y. Ye, X. Yin, and X. Zhang, Nat. Nanotechnol. **10**, 151 (2015).
[191]J. Qi, Y.-W. Lan, A. Z. Stieg, J.-H. Chen, Y.-L. Zhong, L.-J. Li, C.-D. Chen, Y. Zhang, and K. L. Wang, Nat. Commun. **6**, 7430 (2015).
[192]Y. Zhou, D. Wu, Y. Zhu, Y. Cho, Q. He, X. Yang, K. Herrera, Z. Chu, Y. Han, M. C. Downer, H. Peng, and K. Lai, Nano Lett. **17**, 5508 (2017).
[193]X. Wang, X. He, H. Zhu, L. Sun, W. Fu, X. Wang, L. C. Hoong, H. Wang, Q. Zeng, W. Zhao, J. Wei, Z. Jin, Z. Shen, J. Liu, T. Zhang, and Z. Liu, Sci. Adv. **2**, e1600209 (2016).
[194]W. Wu, L. Wang, R. Yu, Y. Liu, S.-H. Wei, J. Hone, and Z. L. Wang, Adv. Mater. **28**, 8463 (2016).
[195]S. K. Kim, R. Bhatia, T.-H. Kim, D. Seol, J. H. Kim, H. Kim, W. Seung, Y. Kim, Y. H. Lee, and S.-W. Kim, Nano Energy **22**, 483 (2016).
[196]A. R. Rezk, B. Carey, A. F. Chrimes, D. W. M. Lau, B. C. Gibson, C. Zheng, M. S. Fuhrer, L. Y. Yeo, and K. Kalantar-zadeh, Nano Lett. **16**, 849 (2016).
[197]J.-H. Lee, J. Y. Park, E. B. Cho, T. Y. Kim, S. A. Han, T.-H. Kim, Y. Liu, S. K. Kim, C. J. Roh, H.-J. Yoon, H. Ryu, W. Seung, J. S. Lee, J. Lee, and S.-W. Kim, Adv. Mater. **29**, 1606667 (2017).
[198]R. Fei, W. Li, J. Li, and L. Yang, Appl. Phys. Lett. **107**, 173104 (2015).
[199]W. Li and J. Li, Nano Res. **8**, 3796 (2015).
[200]A.-Y. Lu, H. Zhu, J. Xiao, C.-P. Chuu, Y. Han, M.-H. Chiu, C.-C. Cheng, C.-W. Yang, K.-H. Wei, Y. Yang, Y. Wang, D. Sokaras, D. Nordlund, P. Yang, D. A. Muller, M.-Y. Chou, X. Zhang, and L.-J. Li, Nat. Nanotechnol. **12**, 744 (2017).
[201]W. Ma, J. Lu, B. Wan, D. Peng, Q. Xu, G. Hu, Y. Peng, C. Pan, and Z. L. Wang, Adv. Mater. **32**, 1905795 (2020).
[202]H. Khan, N. Mahmood, A. Zavabeti, A. Elbourne, M. A. Rahman, B. Y. Zhang, V. Krishnamurthi, P. Atkin, M. B. Ghasemian, J. Yang, G. Zheng, A. R. Ravindran, S. Walia, L. Wang, S. P. Russo, T. Daeneke, Y. Li, and K. Kalantar-Zadeh, Nat. Commun. **11**, 3449 (2020).
[203]M. Zelisko, Y. Hanlumyuang, S. Yang, Y. Liu, C. Lei, J. Li, P. M. Ajayan, and P. Sharma, Nat. Commun. **5**, 4284 (2014).
[204]L. Wang, S. Liu, Z. Zhang, X. Feng, L. Zhu, H. Guo, W. Ding, L. Chen, Y. Qin, and Z. L. Wang, Nano Energy **60**, 724 (2019).
[205]K. F. Mak, D. Xiao, and J. Shan, Nat. Photonics **12**, 451 (2018).
[206]W. Han, APL Mater. **4**, 032401 (2016).
[207]J. R. Schaibley, H. Yu, G. Clark, P. Rivera, J. S. Ross, K. L. Seyler, W. Yao, and X. Xu, Nat. Rev. Mater. **1**, 16055 (2016).
[208]P. Lin, C. Pan, and Z. L. Wang, Mater. Today Nano **4**, 17 (2018).
[209]J. M. Wu, W. E. Chang, Y. T. Chang, and C. K. Chang, Adv. Mater. **28**, 3718 (2016).
[210]S. Kim, M. K. Gupta, K. Y. Lee, A. Sohn, T. Y. Kim, K.-S. Shin, D. Kim, S. K. Kim, K. H. Lee, H.-J. Shin, D.-W. Kim, and S.-W. Kim, Adv. Mater. **26**, 3918 (2014).
[211]C. Wu, T. W. Kim, J. H. Park, H. An, J. Shao, X. Chen, and Z. L. Wang, ACS Nano **11**, 8356 (2017).
[212]M. Seol, S. Kim, Y. Cho, K.-E. Byun, H. Kim, J. Kim, S. K. Kim, S.-W. Kim, H.-J. Shin, and S. Park, Adv. Mater. **30**, 1801210 (2018).
[213]M. S. Majdoub, P. Sharma, and T. Cagin, Phys. Rev. B **77**, 125424 (2008).
[214]L. Wang, S. Liu, X. Feng, C. Zhang, L. Zhu, J. Zhai, Y. Qin, and Z. L. Wang, Nat. Nanotechnol. **15**, 661 (2020).
[215]J. Kang, W. Liu, D. Sarkar, D. Jena, and K. Banerjee, Phys. Rev. X **4**, 031005 (2014).
[216]Y. Zhao, K. Xu, F. Pan, C. Zhou, F. Zhou, and Y. Chai, Adv. Funct. Mater. **27**, 1603484 (2017).
[217]Y. Gong, H. Yuan, C.-L. Wu, P. Tang, S.-Z. Yang, A. Yang, G. Li, B. Liu, J. Van De Groep, M. L. Brongersma, M. F. Chisholm, S.-C. Zhang, W. Zhou, and Y. Cui, Nat. Nanotechnol. **13**, 294 (2018).
[218]C. Wang, Q. He, U. Halim, Y. Liu, E. Zhu, Z. Lin, H. Xiao, X. Duan, Z. Feng, R. Cheng, N. O. Weiss, G. Ye, Y.-C. Huang, H. Wu, H.-C. Cheng, I. Shakir, L. Liao, X. Chen, W. A. Goddard III, Y. Huang, and X. Duan, Nature **555**, 231 (2018).
[219]S. Kumar, A. Kaczmarczyk, and B. D. Gerardot, Nano Lett. **15**, 7567 (2015).
[220]C. R. Dean, A. F. Young, I. Meric, C. Lee, L. Wang, S. Sorgenfrei, K. Watanabe, T. Taniguchi, P. Kim, K. L. Shepard, and J. Hone, Nat. Nanotechnol. **5**, 722 (2010).
[221]H. Liu, K. Xu, X. Zhang, and P. D. Ye, Appl. Phys. Lett. **100**, 152115 (2012).
[222]M. Kim, S. Lee, and Y.-i. Kim, APL Mater. **8**, 071109 (2020).
[223]M. Kim, M. Hoegen, J. Dugundji, and B. L. Wardle, Smart Mater. Struct. **19**, 045023 (2010).
[224]D. R. Smith, J. B. Pendry, and M. C. K. Wiltshire, Science **305**, 788 (2004).
[225]M.-H. Lu, L. Feng, and Y.-F. Chen, Mater. Today **12**, 34 (2009).
[226]G. Ma and P. Sheng, Sci. Adv. **2**, e1501595 (2016).
[227]T. Gorishnyy, M. Maldovan, C. Ullal, and E. Thomas, Phys. World **18**, 24 (2005).
[228]Z. Chen, B. Guo, Y. Yang, and C. Cheng, Physica B **438**, 1 (2014).
[229]T. Tan, Z. Yan, H. Zou, K. Ma, F. Liu, L. Zhao, Z. Peng, and W. Zhang, Appl. Energy **254**, 113717 (2019).
[230]W. S. Gan, *Gauge Invariance Approach to Acoustic Fields* (Springer, Singapore, 2019), pp. 125–169.
[231]H. Lv, X. Tian, M. Y. Wang, and D. Li, Appl. Phys. Lett. **102**, 034103 (2013).
[232]L.-Y. Wu, L.-W. Chen, and C.-M. Liu, Appl. Phys. Lett. **95**, 013506 (2009).
[233]W.-C. Wang, L.-Y. Wu, L.-W. Chen, and C.-M. Liu, Smart Mater. Struct. **19**, 045016 (2010).
[234]M. Carrara, M. R. Cacan, J. Toussaint, M. J. Leamy, M. Ruzzene, and A. Erturk, Smart Mater. Struct. **22**, 065004 (2013).
[235]S.-H. Jo, H. Yoon, Y. C. Shin, W. Choi, C.-S. Park, M. Kim, and B. D. Youn, Int. J. Mech. Sci. **179**, 105670 (2020).
[236]C.-S. Park, Y. C. Shin, S.-H. Jo, H. Yoon, W. Choi, B. D. Youn, and M. Kim, Nano Energy **57**, 327 (2019).

[237]S. Gonella, A. C. To, and W. K. Liu, J. Mech. Phys. Solids **57**, 621 (2009).
[238]Y. C. Shin, H. Yoon, S.-H. Jo, W. Choi, C.-S. Park, M. Kim, and B. D. Youn, Int. J. Mech. Sci. **189**, 106003 (2021).
[239]S.-H. Jo, H. Yoon, Y. C. Shin, M. Kim, and B. D. Youn, J. Appl. Phys. **127**, 164901 (2020).
[240]A. Yang, P. Li, Y. Wen, C. Lu, X. Peng, J. Zhang, and W. He, Appl. Phys. Express **6**, 127101 (2013).
[241]A. Yang, P. Li, Y. Wen, C. Lu, X. Peng, J. Zhang, and W. He, Appl. Phys. Lett. **104**, 151904 (2014).
[242]A. Yang, P. Li, Y. Wen, C. Yang, D. Wang, F. Zhang, and J. Zhang, Appl. Phys. Express **8**, 057101 (2015).
[243]Y. L. Xu, X. G. Tian, and C. Q. Chen, Physica B **407**, 1995 (2012).
[244]J. S. Lee, S. Yoo, Y. K. Ahn, and Y. Y. Kim, J. Acoust. Soc. Am. **138**, EL217 (2015).
[245]A. Shakouri, F. Xu, and Z. Fan, Appl. Phys. Lett. **111**, 054103 (2017).
[246]Z. Chen, Y. Yang, Z. Lu, and Y. Luo, Physica B **410**, 5 (2013).
[247]D. Cao, W. Hu, Y. Gao, and X. Guo, Smart Mater. Struct. **28**, 085014 (2019).
[248]Y. Li, E. Baker, T. Reissman, C. Sun, and W. K. Liu, Appl. Phys. Lett. **111**, 251903 (2017).
[249]J. Hyun, W.-H. Cho, C.-S. Park, J. Chang, and M. Kim, Appl. Phys. Lett. **116**, 234102 (2020).
[250]J. Hyun, C.-S. Park, J. Chang, W.-H. Cho, and M. Kim, Appl. Phys. Lett. **116**, 234101 (2020).
[251]S. Tol, F. L. Degertekin, and A. Erturk, Appl. Phys. Lett. **109**, 063902 (2016).
[252]S. Tol, F. L. Degertekin, and A. Erturk, Appl. Phys. Lett. **111**, 013503 (2017).
[253]J. Hyun, W. Choi, and M. Kim, Appl. Phys. Lett. **115**, 173901 (2019).
[254]J. Hyun, M. Kim, and W. Choi, Sci. Rep. **10**, 14630 (2020).
[255]L. Zhao, S. C. Conlon, and F. Semperlotti, Smart Mater. Struct. **23**, 065021 (2014).
[256]L. Zhao, S. C. Conlon, and F. Semperlotti, Smart Mater. Struct. **24**, 065039 (2015).
[257]A. Zareei, A. Darabi, M. J. Leamy, and M.-R. Alam, Appl. Phys. Lett. **112**, 023901 (2018).
[258]F. Maugan, S. Chesne, M. Monteil, M. Collet, and K. Yi, Smart Mater. Struct. **28**, 075015 (2019).
[259]Z. Liu, X. Zhang, Y. Mao, Y. Y. Zhu, Z. Yang, C. T. Chan, and P. Sheng, Science **289**, 1734 (2000).
[260]N. Fang, D. Xi, J. Xu, M. Ambati, W. Srituravanich, C. Sun, and X. Zhang, Nat. Mater. **5**, 452 (2006).
[261]Y. Wu, Y. Lai, and Z.-Q. Zhang, Phys. Rev. Lett. **107**, 105506 (2011).
[262]Y. Jin, R. Kumar, O. Poncelet, O. Mondain-Monval, and T. Brunet, Nat. Commun. **10**, 143 (2019).
[263]T. Brunet, A. Merlin, B. Mascaro, K. Zimny, J. Leng, O. Poncelet, C. Aristégui, and O. Mondain-Monval, Nat. Mater. **14**, 384 (2015).
[264]S. Qi, M. Oudich, Y. Li, and B. Assouar, Appl. Phys. Lett. **108**, 263501 (2016).
[265]G. Ma, M. Yang, S. Xiao, Z. Yang, and P. Sheng, Nat. Mater. **13**, 873 (2014).
[266]J. Li, X. Zhou, G. Huang, and G. Hu, Smart Mater. Struct. **25**, 045013 (2016).
[267]M. Yuan, Z. Cao, J. Luo, and R. Ohayon, J. Low Freq. Noise, Vib. Act. Control **37**, 1015 (2018).
[268]K. H. Sun, J. E. Kim, J. Kim, and K. Song, Smart Mater. Struct. **26**, 075011 (2017).
[269]M. Yuan, Z. Cao, J. Luo, and Z. Pang, Rev. Sci. Instrum. **89**, 055002 (2018).
[270]M. Yuan, X. Sheng, Z. Cao, Z. Pang, and G. Huang, Smart Mater. Struct. **29**, 035012 (2020).
[271]X. Wang, J. Xu, J. Ding, C. Zhao, and Z. Huang, Smart Mater. Struct. **28**, 025035 (2019).
[272]C. Sugino and A. Erturk, J. Phys. D: Appl. Phys. **51**, 215103 (2018).
[273]B. Assouar, B. Liang, Y. Wu, Y. Li, J.-C. Cheng, and Y. Jing, Nat. Rev. Mater. **3**, 460 (2018).
[274]H. Ge, M. Yang, C. Ma, M.-H. Lu, Y.-F. Chen, N. Fang, and P. Sheng, Natl. Sci. Rev. **5**, 159 (2018).
[275]Y. Xie, W. Wang, H. Chen, A. Konneker, B.-I. Popa, and S. A. Cummer, Nat. Commun. **5**, 5553 (2014).
[276]J. Zhao, B. Li, Z. N. Chen, and C.-W. Qiu, Appl. Phys. Lett. **103**, 151604 (2013).
[277]H. Lee, J. K. Lee, H. M. Seung, and Y. Y. Kim, J. Mech. Phys. Solids **112**, 577 (2018).
[278]Y. Li and B. M. Assouar, Appl. Phys. Lett. **108**, 063502 (2016).
[279]S. Huang, X. Fang, X. Wang, B. Assouar, Q. Cheng, and Y. Li, Appl. Phys. Lett. **113**, 233501 (2018).
[280]S. Qi and B. Assouar, Appl. Phys. Lett. **111**, 243506 (2017).
[281]M. Jin, B. Liang, J. Yang, J. Yang, and J.-c. Cheng, Sci. Rep. **9**, 11152 (2019).
[282]T. Frenzel, M. Kadic, and M. Wegener, Science **358**, 1072 (2017).
[283]S. Babaee, J. Shim, J. C. Weaver, E. R. Chen, N. Patel, and K. Bertoldi, Adv. Mater. **25**, 5044 (2013).
[284]Z. Zhai, Y. Wang, and H. Jiang, Proc. Natl. Acad. Sci. U. S. A. **115**, 2032 (2018).
[285]J. T. B. Overvelde, T. A. de Jong, Y. Shevchenko, S. A. Becerra, G. M. Whitesides, J. C. Weaver, C. Hoberman, and K. Bertoldi, Nat. Commun. **7**, 10929 (2016).
[286]B. Haghpanah, L. Salari-Sharif, P. Pourrajab, J. Hopkins, and L. Valdevit, Adv. Mater. **28**, 7915 (2016).
[287]X. Ren, R. Das, P. Tran, T. D. Ngo, and Y. M. Xie, Smart Mater. Struct. **27**, 023001 (2018).
[288]M. Kadic, T. Bückmann, N. Stenger, M. Thiel, and M. Wegener, Appl. Phys. Lett. **100**, 191901 (2012).
[289]T. Bückmann, M. Thiel, M. Kadic, R. Schittny, and M. Wegener, Nat. Commun. **5**, 4130 (2014).
[290]J. L. Silverberg, A. A. Evans, L. McLeod, R. C. Hayward, T. Hull, C. D. Santangelo, and I. Cohen, Science **345**, 647 (2014).
[291]K. Bertoldi, V. Vitelli, J. Christensen, and M. van Hecke, Nat. Rev. Mater. **2**, 17066 (2017).
[292]J. U. Surjadi, L. Gao, H. Du, X. Li, X. Xiong, N. X. Fang, and Y. Lu, Adv. Eng. Mater. **21**, 1800864 (2019).
[293]S. Shan, S. H. Kang, J. R. Raney, P. Wang, L. Fang, F. Candido, J. A. Lewis, and K. Bertoldi, Adv. Mater. **27**, 4296 (2015).
[294]H. Tao and J. Gibert, Adv. Funct. Mater. **30**, 2001720 (2020).
[295]M. Yang, Y. Li, C. Meng, C. Fu, J. Mei, Z. Yang, and P. Sheng, C. R. Mec. **343**, 635 (2015).
[296]M. Yang, S. Chen, C. Fu, and P. Sheng, Mater. Horizons **4**, 673 (2017).
[297]W. Ma, F. Cheng, and Y. Liu, ACS Nano **12**, 6326 (2018).
[298]J. K. Wilt, C. Yang, and G. X. Gu, Adv. Eng. Mater. **22**, 1901266 (2020).
[299]S. So, J. Mun, and J. Rho, ACS Appl. Mater. Interfaces **11**, 24264 (2019).
[300]T.-G. Lee, S.-H. Jo, H. M. Seung, S.-W. Kim, E.-J. Kim, B. D. Youn, S. Nahm, and M. Kim, Nano Energy **78**, 105226 (2020).
[301]M. Coll, A. Gomez, E. Mas-Marza, O. Almora, G. Garcia-Belmonte, M. Campoy-Quiles, and J. Bisquert, J. Phys. Chem. Lett. **6**, 1408 (2015).
[302]Y. Kutes, L. Ye, Y. Zhou, S. Pang, B. D. Huey, and N. P. Padture, J. Phys. Chem. Lett. **5**, 3335 (2014).
[303]S. Liu, F. Zheng, I. Grinberg, and A. M. Rappe, J. Phys. Chem. Lett. **7**, 1460 (2016).
[304]S. Govinda, B. P. Kore, M. Bokdam, P. Mahale, A. Kumar, S. Pal, B. Bhattacharyya, J. Lahnsteiner, G. Kresse, C. Franchini, A. Pandey, and D. D. Sarma, J. Phys. Chem. Lett. **8**, 4113 (2017).
[305]A. García-Fernández, J. M. Bermúdez-García, S. Castro-García, A. L. Llamas-Saiz, R. Artiaga, J. López-Beceiro, S. Hu, W. Ren, A. Stroppa, M. Sánchez-Andújar, and M. A. Señarís-Rodríguez, Inorg. Chem. **56**, 4918 (2017).
[306]Y.-M. You, W.-Q. Liao, D. Zhao, H.-Y. Ye, Y. Zhang, Q. Zhou, X. Niu, J. Wang, P.-F. Li, D.-W. Fu, Z. Wang, S. Gao, K. Yang, J.-M. Liu, J. Li, Y. Yan, and R.-G. Xiong, Science **357**, 306 (2017).
[307]H.-Y. Ye, Y. Zhang, D.-W. Fu, and R.-G. Xiong, Angew. Chem., Int. Ed. **53**, 11242 (2014).
[308]Q. Dong, J. Song, Y. Fang, Y. Shao, S. Ducharme, and J. Huang, Adv. Mater. **28**, 2816 (2016).
[309]J. Song, Z. Xiao, B. Chen, S. Prockish, X. Chen, A. Rajapitamahuni, L. Zhang, J. Huang, and X. Hong, ACS Appl. Mater. Interfaces **10**, 19218 (2018).
[310]S. Ippili, V. Jella, J. Kim, S. Hong, and S.-G. Yoon, Nano Energy **49**, 247 (2018).
[311]S. Huang, G. Tang, H. Huang, X.-g. Wu, P. Zhou, L. Zou, L. Xie, J. Deng, X. Wang, H. Zhong, and J. Hong, Sci. Bull. **63**, 1254 (2018).

[312]D. Wang, M. Wright, N. K. Elumalai, and A. Uddin, Sol. Energy Mater. Sol. Cells **147**, 255 (2016).
[313]B. Li, Y. Kawakita, Y. Liu, M. Wang, M. Matsuura, K. Shibata, S. Ohira-Kawamura, T. Yamada, S. Lin, K. Nakajima, and S. Liu, Nat. Commun. **8**, 16086 (2017).
[314]Y.-J. Kim, T.-V. Dang, H.-J. Choi, B.-J. Park, J.-H. Eom, H.-A. Song, D. Seol, Y. Kim, S.-H. Shin, J. Nah, and S.-G. Yoon, J. Mater. Chem. A **4**, 756 (2016).
[315]J.-H. Eom, H.-J. Choi, S. V. N. Pammi, V.-D. Tran, Y.-J. Kim, H.-J. Kim, and S.-G. Yoon, J. Mater. Chem. C **6**, 2786 (2018).
[316]V. Jella, S. Ippili, J.-H. Eom, Y.-J. Kim, H.-J. Kim, and S.-G. Yoon, Nano Energy **52**, 11 (2018).
[317]R. Ding, H. Liu, X. Zhang, J. Xiao, R. Kishor, H. Sun, B. Zhu, G. Chen, F. Gao, X. Feng, J. Chen, X. Chen, X. Sun, and Y. Zheng, Adv. Funct. Mater. **26**, 7708 (2016).
[318]J. Dhar, S. Sil, N. A. Hoque, A. Dey, S. Das, P. P. Ray, and D. Sanyal, ChemistrySelect **3**, 5304 (2018).
[319]R. Ding, X. Zhang, G. Chen, H. Wang, R. Kishor, J. Xiao, F. Gao, K. Zeng, X. Chen, X. W. Sun, and Y. Zheng, Nano Energy **37**, 126 (2017).
[320]A. Sultana, M. M. Alam, P. Sadhukhan, U. K. Ghorai, S. Das, T. R. Middya, and D. Mandal, Nano Energy **49**, 380 (2018).
[321]V. Jella, S. Ippili, J.-H. Eom, J. Choi, and S.-G. Yoon, Nano Energy **53**, 46 (2018).
[322]Z. L. Wang, J. Chen, and L. Lin, Energy Environ. Sci. **8**, 2250 (2015).
[323]Y. S. Choi, Q. Jing, A. Datta, C. Boughey, and S. Kar-Narayan, Energy Environ. Sci. **10**, 2180 (2017).
[324]L.-B. Huang, W. Xu, C. Zhao, Y.-L. Zhang, K.-L. Yung, D. Diao, K. H. Fung, and J. Hao, ACS Appl. Mater. Interfaces **12**, 24030 (2020).
[325]M. C. Wong, W. Xu, and J. Hao, Adv. Funct. Mater. **29**, 1904090 (2019).
[326]L.-B. Huang, W. Xu, and J. Hao, Small **13**, 1701820 (2017).
[327]W. Xu, L.-B. Huang, M.-C. Wong, L. Chen, G. Bai, and J. Hao, Adv. Energy Mater. **7**, 1601529 (2017).
[328]A. Kumar, A. Srivastava, I. Y. Galaev, and B. Mattiasson, Prog. Polym. Sci. **32**, 1205 (2007).
[329]J. Hu, H. Meng, G. Li, and S. I. Ibekwe, Smart Mater. Struct. **21**, 053001 (2012).
[330]W. Seung, H.-J. Yoon, T. Y. Kim, H. Ryu, J. Kim, J.-H. Lee, J. H. Lee, S. Kim, Y. K. Park, Y. J. Park, and S.-W. Kim, Adv. Energy Mater. **7**, 1600988 (2017).
[331]P. Bai, G. Zhu, Y. S. Zhou, S. Wang, J. Ma, G. Zhang, and Z. L. Wang, Nano Res. **7**, 990 (2014).
[332]W. Xu, M.-C. Wong, and J. Hao, Nano Energy **55**, 203 (2019).
[333]G. I. Dzhardimalieva, B. C. Yadav, I. E. Uflyand, C. M. Oliva González, B. I. Kharisov, O. V. Kharissova, and B. O. García, J. Mater. Res. **36**, 1225 (2021).
[334]G. I. Dzhardimalieva, B. C. Yadav, S. E. Kudaibergenov, and I. E. Uflyand, Polymers **12**, 2594 (2020).
[335]Y. Yang and M. W. Urban, Chem. Soc. Rev. **42**, 7446 (2013).
[336]Y. C. Yuan, T. Yin, M. Z. Rong, and M. Q. Zhang, eXPRESS Polym. Lett. **2**, 238 (2008).
[337]V. K. Thakur and M. R. Kessler, Polymer **69**, 369 (2015).
[338]W. Xu, L.-B. Huang, and J. Hao, Nano Energy **40**, 399 (2017).
[339]K. Parida, G. Thangavel, G. Cai, X. Zhou, S. Park, J. Xiong, and P. S. Lee, Nat. Commun. **10**, 2158 (2019).
[340]J. H. Park, K. J. Park, T. Jiang, Q. Sun, J.-H. Huh, Z. L. Wang, S. Lee, and J. H. Cho, Nano Energy **38**, 412 (2017).
[341]W. Xu, M.-C. Wong, Q. Guo, T. Jia, and J. Hao, J. Mater. Chem. A **7**, 16267 (2019).
[342]K. Parida, J. Xiong, X. Zhou, and P. S. Lee, Nano Energy **59**, 237 (2019).
[343]K. Parida, V. Kumar, W. Jiangxin, V. Bhavanasi, R. Bendi, and P. S. Lee, Adv. Mater. **29**, 1702181 (2017).
[344]J. Sun, X. Pu, M. Liu, A. Yu, C. Du, J. Zhai, W. Hu, and Z. L. Wang, ACS Nano **12**, 6147 (2018).
[345]Y. C. Lai, H. M. Wu, H. C. Lin, C. L. Chang, H. H. Chou, Y. C. Hsiao, and Y. C. Wu, Adv. Funct. Mater. **29**, 1904626 (2019).
[346]Y. Chen, X. Pu, M. Liu, S. Kuang, P. Zhang, Q. Hua, Z. Cong, W. Guo, W. Hu, and Z. L. Wang, ACS Nano **13**, 8936 (2019).
[347]X. Dai, L. B. Huang, Y. Du, J. Han, Q. Zheng, J. Kong, and J. Hao, Adv. Funct. Mater. **30**, 1910723 (2020).
[348]Y. Du, X. Wang, X. Dai, W. Lu, Y. Tang, and J. Kong, J. Mater. Sci. Technol. **100**, 1 (2022).
[349]H. Chen, J. J. Koh, M. Liu, P. Li, X. Fan, S. Liu, J. C. C. Yeo, Y. Tan, B. C. K. Tee, and C. He, ACS Appl. Mater. Interfaces **12**, 31975 (2020).
[350]Q. Guan, G. Lin, Y. Gong, J. Wang, W. Tan, D. Bao, Y. Liu, Z. You, X. Sun, Z. Wen, and Y. Pan, J. Mater. Chem. A **7**, 13948 (2019).
[351]P. Liu, N. Sun, Y. Mi, X. Luo, X. Dong, J. Cai, X. Jia, M. A. Ramos, T. S. Hu, and Q. Xu, Compos. Sci. Technol. **208**, 108733 (2021).
[352]G. Li, L. Li, P. Zhang, C. Chang, F. Xu, and X. Pu, RSC Adv. **11**, 17437 (2021).
[353]Q. Guan, Y. Dai, Y. Yang, X. Bi, Z. Wen, and Y. Pan, Nano Energy **51**, 333 (2018).
[354]J. Deng, X. Kuang, R. Liu, W. Ding, A. C. Wang, Y.-C. Lai, K. Dong, Z. Wen, Y. Wang, L. Wang, H. J. Qi, T. Zhang, and Z. L. Wang, Adv. Mater. **30**, 1705918 (2018).
[355]T. Patel, M. P. Kim, J. Park, T. H. Lee, P. Nellepalli, S. M. Noh, H. W. Jung, H. Ko, and J. K. Oh, ACS Nano **14**, 11442 (2020).
[356]J. H. Lee, R. Hinchet, S. K. Kim, S. Kim, and S.-W. Kim, Energy Environ. Sci. **8**, 3605 (2015).
[357]R. Liu, X. Kuang, J. Deng, Y.-C. Wang, A. C. Wang, W. Ding, Y.-C. Lai, J. Chen, P. Wang, Z. Lin, H. J. Qi, B. Sun, and Z. L. Wang, Adv. Mater. **30**, 1705195 (2018).
[358]L.-B. Huang, G. Bai, M.-C. Wong, Z. Yang, W. Xu, and J. Hao, Adv. Mater. **28**, 2744 (2016).
[359]L.-b. Huang, W. Xu, G. Bai, M.-C. Wong, Z. Yang, and J. Hao, Nano Energy **30**, 36 (2016).
[360]J. Xiong, H. Luo, D. Gao, X. Zhou, P. Cui, G. Thangavel, K. Parida, and P. S. Lee, Nano Energy **61**, 584 (2019).
[361]S. Qi, H. Guo, J. Chen, J. Fu, C. Hu, M. Yu, and Z. L. Wang, Nanoscale **10**, 4745 (2018).
[362]Z. Ren, Y. Ding, J. Nie, F. Wang, L. Xu, S. Lin, X. Chen, and Z. L. Wang, ACS Appl. Mater. Interfaces **11**, 6143 (2019).
[363]S. Cui, Y. Zheng, T. Zhang, D. Wang, F. Zhou, and W. Liu, Nano Energy **49**, 31 (2018).
[364]D. Yang, X. Kong, Y. Ni, Z. Ren, S. Li, J. Nie, X. Chen, and L. Zhang, Nano Energy **66**, 104139 (2019).
[365]J. Nie, X. Chen, and Z. L. Wang, Adv. Funct. Mater. **29**, 1806351 (2019).
[366]H.-J. Park, S. Kim, J. H. Lee, H. T. Kim, W. Seung, Y. Son, T. Y. Kim, U. Khan, N.-M. Park, and S.-W. Kim, ACS Appl. Mater. Interfaces **11**, 5200 (2019).
[367]L. Zheng, S. Dong, J. Nie, S. Li, Z. Ren, X. Ma, X. Chen, H. Li, and Z. L. Wang, ACS Appl. Mater. Interfaces **11**, 42504 (2019).
[368]Z. He, B. Gao, T. Li, J. Liao, B. Liu, X. Liu, C. Wang, Z. Feng, and Z. Gu, ACS Sustainable Chem. Eng. **7**, 1745 (2019).
[369]S. Mishra, L. Unnikrishnan, S. K. Nayak, and S. Mohanty, Macromol. Mater. Eng. **304**, 1800463 (2019).
[370]B. Bera and M. D. Sarkar, IOSR J. Appl. Phys. **09**, 95 (2017).
[371]R. A. Whiter, V. Narayan, and S. Kar-Narayan, Adv. Energy Mater. **4**, 1400519 (2014).
[372]S. K. Ghosh, T. K. Sinha, B. Mahanty, S. Jana, and D. Mandal, J. Appl. Phys. **120**, 174501 (2016).
[373]X. Wang, Q. Liu, X. Hu, M. You, Q. Zhang, K. Hu, Q. Zhang, and Y. Xiang, Nano Energy **97**, 107176 (2022).
[374]M. Yang, J. Liu, D. Liu, J. Jiao, N. Cui, S. Liu, Q. Xu, L. Gu, and Y. Qin, Research **2021**, 9793458.
[375]Y. Yanagisawa, Y. Nan, K. Okuro, and T. Aida, Science **359**, 72 (2018).
[376]H. Shintaku, T. Nakagawa, D. Kitagawa, H. Tanujaya, S. Kawano, and J. Ito, Sens. Actuators, A **158**, 183 (2010).
[377]H. S. Lee, J. Chung, G.-T. Hwang, C. K. Jeong, Y. Jung, J.-H. Kwak, H. Kang, M. Byun, W. D. Kim, S. Hur, S.-H. Oh, and K. J. Lee, Adv. Funct. Mater. **24**, 6914 (2014).
[378]S. Park, X. Guan, Y. Kim, F. X. Creighton, E. Wei, I. Kymissis, H. H. Nakajima, and E. S. Olson, Trends Hear. **22**, 2331216518774450 (2018).
[379]C. Lang, J. Fang, H. Shao, X. Ding, and T. Lin, Nat. Commun. **7**, 11108 (2016).

[380]J. Jang, J. Lee, S. Woo, D. J. Sly, L. J. Campbell, J.-H. Cho, S. J. O'Leary, M.-H. Park, S. Han, J.-W. Choi, J. Hun Jang, and H. Choi, Sci. Rep. **5**, 12447 (2015).
[381]J. H. Han, J.-H. Kwak, D. J. Joe, S. K. Hong, H. S. Wang, J. H. Park, S. Hur, and K. J. Lee, Nano Energy **53**, 198 (2018).
[382]J. H. Han, K. M. Bae, S. K. Hong, H. Park, J.-H. Kwak, H. S. Wang, D. J. Joe, J. H. Park, Y. H. Jung, S. Hur, C. D. Yoo, and K. J. Lee, Nano Energy **53**, 658 (2018).
[383]Y. H. Jung, S. K. Hong, H. S. Wang, J. H. Han, T. X. Pham, H. Park, J. Kim, S. Kang, C. D. Yoo, and K. J. Lee, Adv. Mater. **32**, 1904020 (2020).
[384]G. Von Békésy, Nature **225**, 1207 (1970).
[385]S. Walser, C. Siegel, M. Winter, G. Feiertag, M. Loibl, and A. Leidl, Sens. Actuators, A **247**, 663 (2016).
[386]E. Sillero, O. A. Williams, V. Lebedev, V. Cimalla, C.-C. Röhlig, C. E. Nebel, and F. Calle, J. Micromech. Microeng. **19**, 115016 (2009).
[387]K.-I. Park, M. Lee, Y. Liu, S. Moon, G.-T. Hwang, G. Zhu, J. E. Kim, S. O. Kim, D. K. Kim, Z. L. Wang, and K. J. Lee, Adv. Mater. **24**, 2999 (2012).
[388]C. K. Jeong, I. Kim, K.-I. Park, M. H. Oh, H. Paik, G.-T. Hwang, K. No, Y. S. Nam, and K. J. Lee, ACS Nano **7**, 11016 (2013).
[389]K.-I. Park, C. K. Jeong, J. Ryu, G.-T. Hwang, and K. J. Lee, Adv. Energy Mater. **3**, 1539 (2013).
[390]C. K. Jeong, K.-I. Park, J. Ryu, G.-T. Hwang, and K. J. Lee, Adv. Funct. Mater. **24**, 2620 (2014).
[391]C. Baek, J. H. Yun, J. E. Wang, C. K. Jeong, K. J. Lee, K.-I. Park, and D. K. Kim, Nanoscale **8**, 17632 (2016).
[392]K.-I. Park, C. K. Jeong, N. K. Kim, and K. J. Lee, Nano Convergence **3**, 12 (2016).
[393]K.-I. Park, S. Xu, Y. Liu, G.-T. Hwang, S.-J. L. Kang, Z. L. Wang, and K. J. Lee, Nano Lett. **10**, 4939 (2010).
[394]K.-I. Park, J. H. Son, G.-T. Hwang, C. K. Jeong, J. Ryu, M. Koo, I. Choi, S. H. Lee, M. Byun, Z. L. Wang, and K. J. Lee, Adv. Mater. **26**, 2514 (2014).
[395]H. E. Lee, J. Choi, S. H. Lee, M. Jeong, J. H. Shin, D. J. Joe, D. Kim, C. W. Kim, J. H. Park, J. H. Lee, D. Kim, C.-S. Shin, and K. J. Lee, Adv. Mater. **30**, 1800649 (2018).
[396]D. J. Joe, S. Kim, J. H. Park, D. Y. Park, H. E. Lee, T. H. Im, I. Choi, R. S. Ruoff, and K. J. Lee, Adv. Mater. **29**, 1606586 (2017).
[397]J. H. Park, H. E. Lee, C. K. Jeong, D. H. Kim, S. K. Hong, K.-I. Park, and K. J. Lee, Nano Energy **56**, 531 (2019).
[398]T. Jeon, H. M. Jin, S. H. Lee, J. M. Lee, H. I. Park, M. K. Kim, K. J. Lee, B. Shin, and S. O. Kim, ACS Nano **10**, 7907 (2016).
[399]I. Choi, H. Y. Jeong, D. Y. Jung, M. Byun, C.-G. Choi, B. H. Hong, S.-Y. Choi, and K. J. Lee, ACS Nano **8**, 7671 (2014).
[400]I. Choi, H. Y. Jeong, H. Shin, G. Kang, M. Byun, H. Kim, A. M. Chitu, J. S. Im, R. S. Ruoff, S.-Y. Choi, and K. J. Lee, Nat. Commun. **7**, 13562 (2016).
[401]M. B. Khan, D. H. Kim, J. H. Han, H. Saif, H. Lee, Y. Lee, M. Kim, E. Jang, S. K. Hong, D. J. Joe, T.-I. Lee, T.-S. Kim, K. J. Lee, and Y. Lee, Nano Energy **58**, 211 (2019).
[402]C. K. Jeong, S. B. Cho, J. H. Han, D. Y. Park, S. Yang, K.-I. Park, J. Ryu, H. Sohn, Y.-C. Chung, and K. J. Lee, Nano Res. **10**, 437 (2017).
[403]G.-T. Hwang, H. Park, J.-H. Lee, S. Oh, K.-I. Park, M. Byun, H. Park, G. Ahn, C. K. Jeong, K. No, H. Kwon, S.-G. Lee, B. Joung, and K. J. Lee, Adv. Mater. **26**, 4880 (2014).
[404]G.-T. Hwang, J. Yang, S. H. Yang, H.-Y. Lee, M. Lee, D. Y. Park, J. H. Han, S. J. Lee, C. K. Jeong, J. Kim, K.-I. Park, and K. J. Lee, Adv. Energy Mater. **5**, 1500051 (2015).
[405]G.-T. Hwang, Y. Kim, J.-H. Lee, S. Oh, C. K. Jeong, D. Y. Park, J. Ryu, H. Kwon, S.-G. Lee, B. Joung, D. Kim, and K. J. Lee, Energy Environ. Sci. **8**, 2677 (2015).
[406]X. Wang, J. Song, J. Liu, and Z. L. Wang, Science **316**, 102 (2007).
[407]X. Wang, Nano Energy **1**, 13 (2012).
[408]Y. Wang, Y. Yang, and Z. L. Wang, npj Flexible Electron. **1**, 10 (2017).
[409]C. Yao, X. Yin, Y. Yu, Z. Cai, and X. Wang, Adv. Funct. Mater. **27**, 1700794 (2017).
[410]J. Li, Y. Long, F. Yang, and X. Wang, Curr. Opin. Solid State Mater. Sci. **24**, 100806 (2020).
[411]S. Li, D. Liu, Z. Zhao, L. Zhou, X. Yin, X. Li, Y. Gao, C. Zhang, Q. Zhang, J. Wang, and Z. L. Wang, ACS Nano **14**, 2475 (2020).
[412]M. Xu, P. Wang, Y.-C. Wang, S. L. Zhang, A. C. Wang, C. Zhang, Z. Wang, X. Pan, and Z. L. Wang, Adv. Energy Mater. **8**, 1702432 (2018).
[413]M. Wang, J. Zhang, Y. Tang, J. Li, B. Zhang, E. Liang, Y. Mao, and X. Wang, ACS Nano **12**, 6156 (2018).
[414]Y. Feng, L. Zhang, Y. Zheng, D. Wang, F. Zhou, and W. Liu, Nano Energy **55**, 260 (2019).
[415]Y. Mao, D. Geng, E. Liang, and X. Wang, Nano Energy **15**, 227 (2015).
[416]T. Guo, G. Liu, Y. Pang, B. Wu, F. Xi, J. Zhao, T. Bu, X. Fu, X. Li, C. Zhang, and Z. L. Wang, Extreme Mech. Lett. **18**, 1 (2018).
[417]Y. Long, Y. Yu, X. Yin, J. Li, C. Carlos, X. Du, Y. Jiang, and X. Wang, Nano Energy **57**, 558 (2019).
[418]L. Xu, T. Jiang, P. Lin, J. J. Shao, C. He, W. Zhong, X. Y. Chen, and Z. L. Wang, ACS Nano **12**, 1849 (2018).
[419]X. Pu, H. Guo, J. Chen, X. Wang, Y. Xi, C. Hu, and Z. L. Wang, Sci. Adv. **3**, e1700694 (2017).
[420]T.-C. Hou, Y. Yang, H. Zhang, J. Chen, L.-J. Chen, and Z. Lin Wang, Nano Energy **2**, 856 (2013).
[421]A. Yu, X. Pu, R. Wen, M. Liu, T. Zhou, K. Zhang, Y. Zhang, J. Zhai, W. Hu, and Z. L. Wang, ACS Nano **11**, 12764 (2017).
[422]R. Yang, Y. Qin, C. Li, G. Zhu, and Z. L. Wang, Nano Lett. **9**, 1201 (2009).
[423]Z. Li, G. Zhu, R. Yang, A. C. Wang, and Z. L. Wang, Adv. Mater. **22**, 2534 (2010).
[424]S. Khadtare, E. J. Ko, Y. H. Kim, H. S. Lee, and D. K. Moon, Sens. Actuators, A **299**, 111575 (2019).
[425]B. Lu, Y. Chen, D. Ou, H. Chen, L. Diao, W. Zhang, J. Zheng, W. Ma, L. Sun, and X. Feng, Sci. Rep. **5**, 16065 (2015).
[426]J. Li, L. Kang, Y. Long, H. Wei, Y. Yu, Y. Wang, C. A. Ferreira, G. Yao, Z. Zhang, C. Carlos, L. German, X. Lan, W. Cai, and X. Wang, ACS Appl. Mater. Interfaces **10**, 42030 (2018).
[427]H. Ouyang, Z. Liu, N. Li, B. Shi, Y. Zou, F. Xie, Y. Ma, Z. Li, H. Li, Q. Zheng, X. Qu, Y. Fan, Z. L. Wang, H. Zhang, and Z. Li, Nat. Commun. **10**, 1821 (2019).
[428]T. Starner, IBM Syst. J. **35**, 618 (1996).
[429]F. Invernizzi, S. Dulio, M. Patrini, G. Guizzetti, and P. Mustarelli, Chem. Soc. Rev. **45**, 5455 (2016).
[430]Z. Yi, F. Xie, Y. Tian, N. Li, X. Dong, Y. Ma, Y. Huang, Y. Hu, X. Xu, D. Qu, X. Lang, Z. Xu, J. Liu, H. Zhang, and B. Yang, Adv. Funct. Mater. **30**, 2000477 (2020).
[431]J. Li, Y. Long, and X. Wang, Chem. Res. Chin. Univ. **36**, 41 (2020).
[432]M. Levin and C. G. Stevenson, Annu. Rev. Biomed. Eng. **14**, 295 (2012).
[433]C. Ribeiro, V. Sencadas, D. M. Correia, and S. Lanceros-Méndez, Colloids Surf., B **136**, 46 (2015).
[434]G. Moncada and J. Black, Plast. Surg. Nurs. **6**, 124 (1986).
[435]M. Piccolino, Trends Neurosci. **20**, 443 (1997).
[436]M. Vöröslakos, Y. Takeuchi, K. Brinyiczki, T. Zombori, A. Oliva, A. Fernández-Ruiz, G. Kozák, Z. T. Kincses, B. Iványi, G. Buzsáki, and A. Berényi, Nat. Commun. **9**, 483 (2018).
[437]A. Antal, I. Alekseichuk, M. Bikson, J. Brockmöller, A. R. Brunoni, R. Chen, L. G. Cohen, G. Dowthwaite, J. Ellrich, A. Flöel, F. Fregni, M. S. George, R. Hamilton, J. Haueisen, C. S. Herrmann, F. C. Hummel, J. P. Lefaucheur, D. Liebetanz, C. K. Loo, C. D. McCaig, C. Miniussi, P. C. Miranda, V. Moliadze, M. A. Nitsche, R. Nowak, F. Padberg, A. Pascual-Leone, W. Poppendieck, A. Priori, S. Rossi, P. M. Rossini, J. Rothwell, M. A. Rueger, G. Ruffini, K. Schellhorn, H. R. Siebner, Y. Ugawa, A. Wexler, U. Ziemann, M. Hallett, and W. Paulus, Clin. Neurophysiol. **128**, 1774 (2017).
[438]S. Bauer, H. Baier, C. Baumgartner, K. Bohlmann, S. Fauser, W. Graf, B. Hillenbrand, M. Hirsch, C. Last, H. Lerche, T. Mayer, A. Schulze-Bonhage, B. J. Steinhoff, Y. Weber, A. Hartlep, F. Rosenow, and H. M. Hamer, Brain Stimul. **9**, 356 (2016).
[439]K. Chakravarthy, A. Nava, P. J. Christo, and K. Williams, Curr. Pain Headache Rep. **20**, 60 (2016).
[440]A. P. de Silva Salazar, C. Stein, R. R. Marchese, R. Della Méa Plentz, and A. De Souza Pagnussat, Pain Physician **20**, 15 (2017).
[441]G. Yao, L. Kang, J. Li, Y. Long, H. Wei, C. A. Ferreira, J. J. Jeffery, Y. Lin, W. Cai, and X. Wang, Nat. Commun. **9**, 5349 (2018).
[442]J. Aberle, P. Busch, J. Veigel, A. Duprée, T. Roesch, C. zu Eulenburg, B. Paschen, B. M. Scholz, S. Wolter, N. Sauer, K. Ludwig, J. Izbicki, and O. Mann, Obes. Surg. **26**, 369 (2016).
[443]J. M. Khalifeh, Z. Zohny, M. MacEwan, M. Stephen, W. Johnston, P. Gamble, Y. Zeng, Y. Yan, and W. Z. Ray, IEEE Rev. Biomed. Eng. **11**, 217 (2018).

[444]J. Hunckler and A. de Mel, J. Multidiscip. Healthcare **10**, 179 (2017).
[445]P. Gargiulo, B. Vatnsdal, P. Ingvarsson, S. Knútsdóttir, V. Gudmundsdóttir, S. Yngvason, and T. Helgason, Artif. Organs **32**, 609 (2008).
[446]S. Ikramuddin, R. P. Blackstone, A. Brancatisano, J. Toouli, S. N. Shah, B. M. Wolfe, K. Fujioka, J. W. Maher, J. Swain, F. G. Que, J. M. Morton, D. B. Leslie, R. Brancatisano, L. Kow, R. W. O'Rourke, C. Deveney, M. Takata, C. J. Miller, M. B. Knudson, K. S. Tweden, S. A. Shikora, M. G. Sarr, and C. J. Billington, JAMA, J. Am. Med. Assoc. **312**, 915 (2014).
[447]D. Val-Laillet, A. Biraben, G. Randuineau, and C. H. Malbert, Appetite **55**, 245 (2010).
[448]C. M. Apovian, S. N. Shah, B. M. Wolfe, S. Ikramuddin, C. J. Miller, K. S. Tweden, C. J. Billington, and S. A. Shikora, Obes. Surg. **27**, 169 (2017).
[449]T. Hampton, JAMA, J. Am. Med. Assoc. **313**, 785 (2015).
[450]A. Priori, A. Berardelli, M. Inghilleri, N. Accornero, and M. Manfredi, Brain **117**, 317 (1994).
[451]S. C. Kabay, S. Kabay, M. Yucel, and H. Ozden, Neurourol. Urodyn. **28**, 62 (2009).
[452]A. Q. Farrand, K. L. Helke, R. A. Gregory, M. Gooz, V. K. Hinson, and H. A. Boger, Brain Stimul. **10**, 1045 (2017).
[453]R. Pahwa, R. Dhall, J. Ostrem, R. Gwinn, K. Lyons, S. Ro, C. Dietiker, N. Luthra, P. Chidester, S. Hamner, E. Ross, and S. Delp, Neuromodulation **22**, 537 (2019).
[454]A. Handforth, W. G. Ondo, S. Tatter, G. W. Mathern, R. K. Simpson, F. Walker, J. P. Sutton, J. P. Hubble, and J. Jankovic, Neurology **61**, 1401 (2003).
[455]A. Berényi, M. Belluscio, D. Mao, and G. Buzsáki, Science **337**, 735 (2012).
[456]R. S. Fisher and A. L. Velasco, Nat. Rev. Neurol. **10**, 261 (2014).
[457]H. S. Mayberg, A. M. Lozano, V. Voon, H. E. McNeely, D. Seminowicz, C. Hamani, J. M. Schwalb, and S. H. Kennedy, Neuron **45**, 651 (2005).
[458]F. Jiménez, F. Velasco, R. Salin-Pascual, J. A. Hernández, M. Velasco, J. L. Criales, and H. Nicolini, Neurosurgery **57**, 585 (2005).
[459]A. M. Lozano, N. Lipsman, H. Bergman, P. Brown, S. Chabardes, J. W. Chang, K. Matthews, C. C. McIntyre, T. E. Schlaepfer, M. Schulder, Y. Temel, J. Volkmann, and J. K. Krauss, Nat. Rev. Neurol. **15**, 148 (2019).
[460]M. J. Russell, T. Goodman, R. Pierson, S. Shepherd, Q. Wang, B. Groshong, and D. F. Wiley, J. Biomed. Res. **27**, 495 (2013).
[461]S. Ohki, *Comprehensive Treatise of Electrochemistry* (Springer US, Boston, MA, 1985), pp. 1–130.
[462]X. Cheng, W. Tang, Y. Song, H. Chen, H. Zhang, and Z. L. Wang, Nano Energy **61**, 517 (2019).
[463]S. Ud-Din, N. Greaves, M. Baguneid, and A. Bayat, Wound Repair Regener. **22**, A64 (2014).
[464]G. D. Gentzkow, J. Dermatol. Surg. Oncol. **19**, 753 (1993).
[465]Y. Long, H. Wei, J. Li, G. Yao, B. Yu, D. Ni, A. L. Gibson, X. Lan, Y. Jiang, W. Cai, and X. Wang, ACS Nano **12**, 12533 (2018).
[466]M. B. Starr, J. Shi, and X. Wang, Angew. Chem., Int. Ed. **51**, 5962 (2012).
[467]M. Lei and C.-M. Chuong, Science **351**, 559 (2016).
[468]H. Matsumura, Y. Mohri, N. T. Binh, H. Morinaga, M. Fukuda, M. Ito, S. Kurata, J. Hoeijmakers, and E. K. Nishimura, Science **351**, aad4395 (2016).
[469]B. Benjamin, D. Ziginskas, J. Harman, and T. Meakin, Psychooncology **11**, 244 (2002).
[470]W. S. Maddin, P. W. Bell, and J. H. M. James, Int. J. Dermatol. **29**, 446 (1990).
[471]W. S. Maddin, I. Amara, and W. A. Sollecito, Int. J. Dermatol. **31**, 878 (1992).
[472]G. Yao, D. Jiang, J. Li, L. Kang, S. Chen, Y. Long, Y. Wang, P. Huang, Y. Lin, W. Cai, and X. Wang, ACS Nano **13**, 12345 (2019).
[473]E. Fukada and I. Yasuda, J. Phys. Soc. Jpn. **12**, 1158 (1957).
[474]M. D. Mattei, N. Gagliano, C. Moscheni, C. Dellavia, C. Calastrini, A. Pellati, M. Gioia, A. Caruso, and G. Stabellini, Bioelectromagnetics **26**, 207 (2005).
[475]R. A. Luben, C. D. Cain, M. C.-Y. Chen, D. M. Rosen, and W. R. Adey, Proc. Natl. Acad. Sci. U. S. A. **79**, 4180 (1982).
[476]J. A. Spadaro and W. H. Bergstrom, Calcif. Tissue Int. **70**, 496 (2002).
[477]Z. Schwartz, B. J. Simon, M. A. Duran, G. Barabino, R. Chaudhri, and B. D. Boyan, J. Orthop. Res. **26**, 1250 (2008).
[478]J. Tian, R. Shi, Z. Liu, H. Ouyang, M. Yu, C. Zhao, Y. Zou, D. Jiang, J. Zhang, and Z. Li, Nano Energy **59**, 705 (2019).
[479]C. Dagdeviren, B. D. Yang, Y. Su, P. L. Tran, P. Joe, E. Anderson, J. Xia, V. Doraiswamy, B. Dehdashti, X. Feng, B. Lu, R. Poston, Z. Khalpey, R. Ghaffari, Y. Huang, M. J. Slepian, and J. A. Rogers, Proc. Natl. Acad. Sci. U. S. A. **111**, 1927 (2014).
[480]Y. Li, R. L. Z. Hoye, H.-H. Gao, L. Yan, X. Zhang, Y. Zhou, J. L. MacManus-Driscoll, and J. Gan, ACS Appl. Mater. Interfaces **12**, 7135 (2020).
[481]Y. Kuang and M. Zhu, Sens. Actuators, A **263**, 510 (2017).
[482]Z. J. Chew, T. Ruan, and M. Zhu, IEEE Trans. Power Electron. **34**, 8671 (2019).
[483]M. Sami, N. K. Noordin, and M. Khabazian, IEEE Commun. Lett. **20**, 808 (2016).
[484]C. K. Jeong, D. Y. Hyeon, G.-T. Hwang, G.-J. Lee, M.-K. Lee, J.-J. Park, and K.-I. Park, J. Mater. Chem. A **7**, 25481 (2019).
[485]S. Roundy, P. K. Wright, and J. Rabaey, Comput. Commun. **26**, 1131 (2003).
[486]H. A. Sodano, D. J. Inman, and G. Park, Shock Vib. Dig. **36**, 197 (2004).
[487]Z. J. Chew, T. Ruan, and M. Zhu, IEEE Trans. Ind. Inf. **13**, 3006 (2017).
[488]A. Ahmed, I. Hassan, A. S. Helal, V. Sencadas, A. Radhi, C. K. Jeong, and M. F. El-Kady, iScience **23**, 101286 (2020).
[489]M. Zhu and E. Worthington, in *2009 IEEE Sensors* (IEEE, 2009), pp. 699–702.
[490]M. Zhu, E. Worthington, and A. Tiwari, IEEE Trans. Ultrason., Ferroelectr., Freq. Control **57**, 427 (2010).
[491]Y. Kuang, A. Daniels, and M. Zhu, J. Phys. D: Appl. Phys. **50**, 345501 (2017).
[492]Y. Kuang, Z. J. Chew, and M. Zhu, Energy Convers. Manage. **213**, 112855 (2020).
[493]C. Cheng, Z. Chen, H. Shi, Z. Liu, and Y. Xiong, Shock Vib. **2016**, 2413578.
[494]Y. Kuang and M. Zhu, Composites, Part B **158**, 189 (2019).
[495]A. J. Schönecker, T. Daue, B. Brückner, C. Freytag, L. Hähne, and T. Rödig, Proc. SPIE **6170**, 61701K (2006).
[496]S. Sreenivasa Prasath and A. Arockiarajan, Sens. Actuators, A **214**, 31 (2014).
[497]M. A. Trindade and A. Benjeddou, Compos. Struct. **151**, 47 (2016).
[498]H. Xia, R. Chen, L. Ren, and Q. Zhou, J. Intell. Mater. Syst. Struct. **28**, 1105 (2017).
[499]N. Kong and D. S. Ha, IEEE Trans. Power Electron. **27**, 2298 (2012).
[500]Z. J. Chew and M. Zhu, IEEE Trans. Power Electron. **33**, 8164 (2018).
[501]J. Sankman and D. Ma, IEEE Trans. Power Electron. **30**, 632 (2015).
[502]Z. J. Chew, T. Ruan, M. Zhu, M. Bafleur, and J.-M. Dilhac, IEEE Trans. Ind. Electron. **64**, 9646 (2017).
[503]M. Shim, J. Kim, J. Jeong, S. Park, and C. Kim, IEEE J. Solid-State Circuits **50**, 2367 (2015).
[504]R. Torah, P. Glynne-Jones, M. Tudor, T. O'Donnell, S. Roy, and S. Beeby, Meas. Sci. Technol. **19**, 125202 (2008).
[505]M. Minami, T. Morito, H. Morikawa, and T. Aoyama, in 2nd International Conference on Embedded Networked Sensor Systems, 2005.
[506]B. H. Stark, G. D. Szarka, and E. D. Rooke, IET Circuits, Devices Syst. **5**, 267 (2011).
[507]T. Ruan, Z. J. Chew, and M. Zhu, IEEE Sens. J. **17**, 2165 (2017).
[508]Z. J. Chew and M. Zhu, Proceedings **2**, 1052 (2018).
[509]Y. Kuang, T. Ruan, Z. J. Chew, and M. Zhu, Sens. Actuators, A **254**, 69 (2017).
[510]A. S. Weddell, D. Zhu, G. V. Merrett, S. P. Beeby, and B. M. Al-Hashimi, In Proceedings of the 1st International Workshop on Energy Neutral Sensing Systems (ENSSys '13), Article **18**, 1–2 (2013).
[511]D. Zhu and S. P. Beeby, Proc. SPIE **9517**, 95170P (2015).
[512]Z. J. Chew and M. Zhu, in *2016 IEEE Sensors* (IEEE, 2016), pp. 1–3.
[513]I. C. Lien, Y. C. Shu, W. J. Wu, S. M. Shiu, and H. C. Lin, Smart Mater. Struct. **19**, 125009 (2010).
[514]A. Morel, A. Badel, Y. Wanderoild, and G. Pillonnet, Smart Mater. Struct. **27**, 084002 (2018).
[515]A. Morel, G. Pillonnet, P. Gasnier, E. Lefeuvre, and A. Badel, Smart Mater. Struct. **28**, 025009 (2019).
[516]Y. Wu, A. Badel, F. Formosa, W. Liu, and A. E. Agbossou, J. Intell. Mater. Syst. Struct. **24**, 1445 (2013).
[517]Y. Wu, A. Badel, F. Formosa, W. Liu, and A. Agbossou, J. Intell. Mater. Syst. Struct. **25**, 2165 (2014).
[518]Z. J. Chew, T. Ruan, and M. Zhu, IEEE Trans. Ind. Inf. **17**, 1505 (2021).

[519]S. Fan, R. Wei, L. Zhao, X. Yang, L. Geng, and P. X.-L. Feng, IEEE Trans. Power Electron. **33**, 7326 (2018).
[520]Z. J. Chew and M. Zhu, IEEE Trans. Ind. Electron. **67**, 3267 (2020).
[521]A. Komolafe, R. Torah, Y. Wei, H. Nunes-Matos, M. Li, D. Hardy, T. Dias, M. Tudor, and S. Beeby, Adv. Mater. Technol. **4**, 1900176 (2019).
[522]I. Wicaksono, C. I. Tucker, T. Sun, C. A. Guerrero, C. Liu, W. M. Woo, E. J. Pence, and C. Dagdeviren, npj Flexible Electron. **4**, 5 (2020).
[523]Y. Zhu, M. Yang, Q. Huang, D. Wang, R. Yu, J. Wang, Z. Zheng, and D. Wang, Adv. Mater. **32**, 1906205 (2020).
[524]S. Yong, J. Owen, and S. Beeby, Adv. Eng. Mater. **20**, 1700860 (2018).
[525]Q. He, Y. Wu, Z. Feng, W. Fan, Z. Lin, C. Sun, Z. Zhou, K. Meng, W. Wu, and J. Yang, J. Mater. Chem. A **7**, 26804 (2019).
[526]Z. Zhao, Q. Huang, C. Yan, Y. Liu, X. Zeng, X. Wei, Y. Hu, and Z. Zheng, Nano Energy **70**, 104528 (2020).
[527]M. Jesionek, B. Toroń, P. Szperlich, W. Biniaś, D. Biniaś, S. Rabiej, A. Starczewska, M. Nowak, M. Kępińska, and J. Dec, Polymer **180**, 121729 (2019).
[528]Z. Zhang, Y. Chen, and J. Guo, Physica E **105**, 212 (2019).
[529]M. Zohair, K. Moyer, J. Eaves-Rathert, C. Meng, J. Waugh, and C. L. Pint, ACS Nano **14**, 2308 (2020).
[530]S. H. Kim, C. S. Haines, N. Li, K. J. Kim, T. J. Mun, C. Choi, J. Di, Y. J. Oh, J. P. Oviedo, J. Bykova, S. Fang, N. Jiang, Z. Liu, R. Wang, P. Kumar, R. Qiao, S. Priya, K. Cho, M. Kim, M. S. Lucas, L. F. Drummy, B. Maruyama, D. Y. Lee, X. Lepró, E. Gao, D. Albarq, R. Ovalle-Robles, S. J. Kim, and R. H. Baughman, Science **357**, 773 (2017).
[531]Y. Hu and Z. Zheng, Nano Energy **56**, 16 (2019).
[532]T. Someya, Z. Bao, and G. G. Malliaras, Nature **540**, 379 (2016).
[533]J.-W. Jeong, W.-H. Yeo, A. Akhtar, J. J. S. Norton, Y.-J. Kwack, S. Li, S.-Y. Jung, Y. Su, W. Lee, J. Xia, H. Cheng, Y. Huang, W.-S. Choi, T. Bretl, and J. A. Rogers, Adv. Mater. **25**, 6839 (2013).
[534]D. Liu, X. Yin, H. Guo, L. Zhou, X. Li, C. Zhang, J. Wang, and Z. L. Wang, Sci. Adv. **5**, eaav6437 (2019).
[535]Q. Tang, X. Pu, Q. Zeng, H. Yang, J. Li, Y. Wu, H. Guo, Z. Huang, and C. Hu, Nano Energy **66**, 104087 (2019).
[536]H. Guo, J. Chen, M.-H. Yeh, X. Fan, Z. Wen, Z. Li, C. Hu, and Z. L. Wang, ACS Nano **9**, 5577 (2015).
[537]G. Zhu, W. Q. Yang, T. Zhang, Q. Jing, J. Chen, Y. S. Zhou, P. Bai, and Z. L. Wang, Nano Lett. **14**, 3208 (2014).
[538]J. Chen, G. Zhu, J. Yang, Q. Jing, P. Bai, W. Yang, X. Qi, Y. Su, and Z. L. Wang, ACS Nano **9**, 105 (2015).
[539]S. Wang, L. Lin, and Z. L. Wang, Nano Energy **11**, 436 (2015).
[540]Q. Shi, T. He, and C. Lee, Nano Energy **57**, 851 (2019).
[541]H. Guo, J. Wan, H. Wang, H. Wu, C. Xu, L. Miao, M. Han, and H. Zhang, Research **2021**, 4689869.
[542]M. Zhu, Z. Yi, B. Yang, and C. Lee, Nano Today **36**, 101016 (2021).
[543]X. Pu, S. An, Q. Tang, H. Guo, and C. Hu, iScience **24**, 102027 (2021).
[544]J. Han, C. Xu, J. Zhang, N. Xu, Y. Xiong, X. Cao, Y. Liang, L. Zheng, J. Sun, J. Zhai, Q. Sun, and Z. L. Wang, ACS Nano **15**, 1597 (2021).
[545]H. Guo, X. Pu, J. Chen, Y. Meng, M.-H. Yeh, G. Liu, Q. Tang, B. Chen, D. Liu, S. Qi, C. Wu, C. Hu, J. Wang, and Z. L. Wang, Sci. Rob. **3**, eaat2516 (2018).
[546]X. Pu, H. Guo, Q. Tang, J. Chen, L. Feng, G. Liu, X. Wang, Y. Xi, C. Hu, and Z. L. Wang, Nano Energy **54**, 453 (2018).
[547]X. Pu, Q. Tang, W. Chen, Z. Huang, G. Liu, Q. Zeng, J. Chen, H. Guo, L. Xin, and C. Hu, Nano Energy **76**, 105047 (2020).
[548]L. R. Hochberg, D. Bacher, B. Jarosiewicz, N. Y. Masse, J. D. Simeral, J. Vogel, S. Haddadin, J. Liu, S. S. Cash, P. Van Der Smagt, and J. P. Donoghue, Nature **485**, 372 (2012).
[549]M. A. Lebedev and M. A. L. Nicolelis, Trends Neurosci. **29**, 536 (2006).
[550]N. Birbaumer, N. Ghanayim, T. Hinterberger, I. Iversen, B. Kotchoubey, A. Kübler, J. Perelmouter, E. Taub, and H. Flor, Nature **398**, 297 (1999).
[551]R. Okuno, M. Yoshida, and K. Akazawa, IEEE Eng. Med. Biol. Mag. **24**, 48 (2005).
[552]A. B. Usakli and S. Gurkan, IEEE Trans. Instrum. Meas. **59**, 2099 (2010).
[553]X. Guo, W. Pei, Y. Wang, Y. Chen, H. Zhang, X. Wu, X. Yang, H. Chen, Y. Liu, and R. Liu, Biomed. Signal Process. Control **30**, 98 (2016).
[554]J. Yang, J. Chen, Y. Su, Q. Jing, Z. Li, F. Yi, X. Wen, Z. Wang, and Z. L. Wang, Adv. Mater. **27**, 1316 (2015).
[555]G.-Z. Yang, J. Bellingham, P. E. Dupont, P. Fischer, L. Floridi, R. Full, N. Jacobstein, V. Kumar, M. McNutt, R. Merrifield, B. J. Nelson, B. Scassellati, M. Taddeo, R. Taylor, M. Veloso, Z. L. Wang, and R. Wood, Sci. Rob. **3**, eaar7650 (2018).
[556]J. Jang, S. Kim, D. J. Sly, S. J. O'leary, and H. Choi, Sens. Actuators, A **203**, 6 (2013).
[557]J. C. Isaacs and N. A. Strakhov, Bell Syst. Tech. J. **52**, 101 (1973).
[558]S. C. B. Mannsfeld, B. C.-K. Tee, R. M. Stoltenberg, C. V. H.-H. Chen, S. Barman, B. V. O. Muir, A. N. Sokolov, C. Reese, and Z. Bao, Nat. Mater. **9**, 859 (2010).
[559]M. Li, H. X. Tang, and M. L. Roukes, Nat. Nanotechnol. **2**, 114 (2007).
[560]X. Fan, J. Chen, J. Yang, P. Bai, Z. Li, and Z. L. Wang, ACS Nano **9**, 4236 (2015).
[561]J. Jang, J. Lee, J. H. Jang, and H. Choi, Adv. Healthcare Mater. **5**, 2481 (2016).
[562]N. Jacobstein, J. Bellingham, and G.-Z. Yang, Sci. Rob. **2**, eaan5594 (2017).
[563]T. D'Orazio, R. Marani, V. Renò, and G. Cicirelli, Image Vision Comput. **52**, 56 (2016).
[564]P. G. Jung, G. Lim, S. Kim, and K. Kong, IEEE Trans. Ind. Inf. **11**, 485 (2015).
[565]S. Alavi, D. Arsenault, and A. Whitehead, Sensors **16**, 605 (2016).
[566]J. Xu, S. Wang, G.-J. N. Wang, C. Zhu, S. Luo, L. Jin, X. Gu, S. Chen, V. R. Feig, J. W. F. To, S. Rondeau-Gagné, J. Park, B. C. Schroeder, C. Lu, J. Y. Oh, Y. Wang, Y.-H. Kim, H. Yan, R. Sinclair, D. Zhou, G. Xue, B. Murmann, C. Linder, W. Cai, J. B.-H. Tok, J. W. Chung, and Z. Bao, Science **355**, 59 (2017).
[567]K. C. Pradel, W. Wu, Y. Ding, and Z. L. Wang, Nano Lett. **14**, 6897 (2014).
[568]F. Yi, X. Wang, S. Niu, S. Li, Y. Yin, K. Dai, G. Zhang, L. Lin, Z. Wen, H. Guo, J. Wang, M.-H. Yeh, Y. Zi, Q. Liao, Z. You, Y. Zhang, and Z. L. Wang, Sci. Adv. **2**, e1501624 (2016).
[569]Y. S. Zhou, G. Zhu, S. Niu, Y. Liu, P. Bai, Q. Jing, and Z. L. Wang, Adv. Mater. **26**, 1719 (2014).
[570]G. Figliolini and M. Ceccarelli, Robotica **20**, 13 (2002).
[571]C. O'Madagain, G. Kachel, and B. Strickland, Sci. Adv. **5**, eaav2558 (2019).
[572]S. Takamatsu, T. Lonjaret, E. Ismailova, A. Masuda, T. Itoh, and G. G. Malliaras, Adv. Mater. **28**, 4485 (2016).
[573]C. Qiu, B. Wang, N. Zhang, S. Zhang, J. Liu, D. Walker, Y. Wang, H. Tian, T. R. Shrout, Z. Xu, L.-Q. Chen, and F. Li, Nature **577**, 350 (2020).
[574]Y. Chen, Y.-C. Wang, Y. Zhang, H. Zou, Z. Lin, G. Zhang, C. Zou, and Z. L. Wang, Adv. Energy Mater. **8**, 1802159 (2018).
[575]Q. Zhang, T. Jiang, D. Ho, S. Qin, X. Yang, J. H. Cho, Q. Sun, and Z. L. Wang, ACS Nano **12**, 254 (2018).
[576]X. Wang, H. Zhang, L. Dong, X. Han, W. Du, J. Zhai, C. Pan, and Z. L. Wang, Adv. Mater. **28**, 2896 (2016).
[577]X. Wang, M. Que, M. Chen, X. Han, X. Li, C. Pan, and Z. L. Wang, Adv. Mater. **29**, 1605817 (2017).
[578]X. X. Zhu, Z. B. Li, X. S. Li, L. Su, X. Y. Wei, S. Y. Kuang, B. W. Su, J. Yang, Z. L. Wang, and G. Zhu, Nano Energy **50**, 497 (2018).
[579]J. Wang, S. Li, F. Yi, Y. Zi, J. Lin, X. Wang, Y. Xu, and Z. L. Wang, Nat. Commun. **7**, 12744 (2016).
[580]H. Guo, M.-H. Yeh, Y.-C. Lai, Y. Zi, C. Wu, Z. Wen, C. Hu, and Z. L. Wang, ACS Nano **10**, 10580 (2016).
[581]Z. Wen, M.-H. Yeh, H. Guo, J. Wang, Y. Zi, W. Xu, J. Deng, L. Zhu, X. Wang, C. Hu, L. Zhu, X. Sun, and Z. L. Wang, Sci. Adv. **2**, e1600097 (2016).
[582]S. S. K. Mallineni, Y. Dong, H. Behlow, A. M. Rao, and R. Podila, Adv. Energy Mater. **8**, 1702736 (2018).
[583]R. Cao, X. Pu, X. Du, W. Yang, J. Wang, H. Guo, S. Zhao, Z. Yuan, C. Zhang, C. Li, and Z. L. Wang, ACS Nano **12**, 5190 (2018).
[584]Q. Shi, Z. Zhang, T. Chen, and C. Lee, Nano Energy **62**, 355 (2019).
[585]X. Chen, Z. Ren, H. Guo, X. Cheng, and H. Zhang, Appl. Phys. Lett. **116**, 043902 (2020).
[586]H. Chen, Y. Song, H. Guo, L. Miao, X. Chen, Z. Su, and H. Zhang, Nano Energy **51**, 496 (2018).
[587]L. E. Osborn, A. Dragomir, J. L. Betthauser, C. L. Hunt, H. H. Nguyen, R. R. Kaliki, and N. V. Thakor, Sci. Rob. **3**, eaat3818 (2018).
[588]C. Li, C. Guo, V. Fitzpatrick, A. Ibrahim, M. J. Zwierstra, P. Hanna, A. Lechtig, A. Nazarian, S. J. Lin, and D. L. Kaplan, Nat. Rev. Mater. **5**, 61 (2020).

[589]H.-J. Yoon and S.-W. Kim, Joule **4**, 1398 (2020).
[590]H. Basaeri, D. B. Christensen, and S. Roundy, Smart Mater. Struct. **25**, 123001 (2016).
[591]M. A. Parvez Mahmud, N. Huda, S. H. Farjana, M. Asadnia, and C. Lang, Adv. Energy Mater. **8**, 1701210 (2018).
[592]R. Hinchet, H.-J. Yoon, H. Ryu, M.-K. Kim, E.-K. Choi, D.-S. Kim, and S.-W. Kim, Science **365**, 491 (2019).
[593]S. K. Karan, S. Maiti, J. H. Lee, Y. K. Mishra, B. B. Khatua, and J. K. Kim, Adv. Funct. Mater. **30**, 2004446 (2020).
[594]S. Maiti, S. K. Karan, J. K. Kim, and B. B. Khatua, Adv. Energy Mater. **9**, 1803027 (2019).
[595]D. Jiang, B. Shi, H. Ouyang, Y. Fan, Z. L. Wang, and Z. Li, ACS Nano **14**, 6436 (2020).
[596]Q. Zheng, B. Shi, F. Fan, X. Wang, L. Yan, W. Yuan, S. Wang, H. Liu, Z. Li, and Z. L. Wang, Adv. Mater. **26**, 5851 (2014).
[597]W. Tang, J. Tian, Q. Zheng, L. Yan, J. Wang, Z. Li, and Z. L. Wang, ACS Nano **9**, 7867 (2015).
[598]H. Ouyang, J. Tian, G. Sun, Y. Zou, Z. Liu, H. Li, L. Zhao, B. Shi, Y. Fan, Y. Fan, Z. L. Wang, and Z. Li, Adv. Mater. **29**, 1703456 (2017).
[599]Z. Yan, L. Wang, Y. Xia, R. Qiu, W. Liu, M. Wu, Y. Zhu, S. Zhu, C. Jia, M. Zhu, R. Cao, Z. Li, and X. Wang, Adv. Funct. Mater. **31**, 2100709 (2021).
[600]D.-M. Lee, N. Rubab, I. Hyun, W. Kang, Y.-J. Kim, M. Kang, B. O. Choi, and S.-W. Kim, Sci. Adv. **8**, eabl8423 (2022).
[601]W. Deng, A. Libanori, X. Xiao, J. Fang, X. Zhao, Y. Zhou, G. Chen, S. Li, and J. Chen, Nano Energy **91**, 106656 (2022).
[602]Z. Wang, Nanogenerators for Self-Powered Devices and Systems, 2011.
[603]Y. Fang, Y. Zou, J. Xu, G. Chen, Y. Zhou, W. Deng, X. Zhao, M. Roustaei, T. K. Hsiai, and J. Chen, Adv. Mater. **33**, 2104178 (2021).
[604]S. A. Pullano, D. C. Critello, and A. S. Fiorillo, Nano Energy **67**, 104278 (2020).
[605]S. Park, J. Park, Y.-g. Kim, S. Bae, T.-W. Kim, K.-I. Park, B. H. Hong, C. K. Jeong, and S.-K. Lee, Nano Energy **78**, 105266 (2020).
[606]Y. Ma, Q. Zheng, Y. Liu, B. Shi, X. Xue, W. Ji, Z. Liu, Y. Jin, Y. Zou, Z. An, W. Zhang, X. Wang, W. Jiang, Z. Xu, Z. L. Wang, Z. Li, and H. Zhang, Nano Lett. **16**, 6042 (2016).
[607]Z. Lin, J. Yang, X. Li, Y. Wu, W. Wei, J. Liu, J. Chen, and J. Yang, Adv. Funct. Mater. **28**, 1704112 (2018).
[608]Y. Song, J. Min, Y. Yu, H. Wang, Y. Yang, H. Zhang, and W. Gao, Sci. Adv. **6**, eaay9842 (2020).
[609]J.-N. Kim, J. Lee, H. Lee, and I.-K. Oh, Nano Energy **82**, 105705 (2021).
[610]Y. Xi, J. Wang, Y. Zi, X. Li, C. Han, X. Cao, C. Hu, and Z. Wang, Nano Energy **38**, 101 (2017).
[611]Q. Zheng, Y. Zou, Y. Zhang, Z. Liu, B. Shi, X. Wang, Y. Jin, H. Ouyang, Z. Li, and Z. L. Wang, Sci. Adv. **2**, e1501478 (2016).
[612]C. M. Schoellhammer, S. Srinivasan, R. Barman, S. H. Mo, B. E. Polat, R. Langer, and D. Blankschtein, J. Controlled Release **202**, 93 (2015).
[613]L. Jiang, Y. Yang, Y. Chen, and Q. Zhou, Nano Energy **77**, 105131 (2020).
[614]Q. Shi, T. Wang, T. Kobayashi, and C. Lee, Appl. Phys. Lett. **108**, 193902 (2016).
[615]Q. Shi, T. Wang, and C. Lee, Sci. Rep. **6**, 24946 (2016).
[616]H. Feng, C. Zhao, P. Tan, R. Liu, X. Chen, and Z. Li, Adv. Healthcare Mater. **7**, 1701298 (2018).
[617]T. Busolo, P. K. Szewczyk, M. Nair, U. Stachewicz, and S. Kar-Narayan, ACS Appl. Mater. Interfaces **13**, 16876 (2021).
[618]M. Smith and S. Kar-Narayan, Int. Mater. Rev. **67**, 65 (2021).
[619]Q. Jing, Y. S. Choi, M. Smith, N. Ćatić, C. Ou, and S. Kar-Narayan, Adv. Mater. Technol. **4**, 1800328 (2019).

AFFILIATIONS

[1]Univ. Gustave Eiffel, CNRS, ESYCOM, F-77454 Marne-la-Vallée, France
[2]School of Electronics and Computer Science, University of Southampton, Southampton, United Kingdom
[3]Department of Mechanical Engineering, University of Bath, Bath BA2 7AY, United Kingdom
[4]College of Engineering, Mathematics and Physical Sciences, University of Exeter, Exeter, United Kingdom
[5]Wolfson School of Mechanical and Manufacturing Engineering, Loughborough University, Loughborough LE11 3TU, United Kingdom
[6]Department of Electrical and Electronic Engineering, Advanced Technology Institute, University of Surrey, Guildford, Surrey GU2 7XH, United Kingdom
[7]College of Chemistry and Chemical Engineering, Xiamen University, Xiamen 361005, China
[8]Sorbonne Université, LIP6, Paris, France
[9]Department of Applied Physics, Chongqing University, Chongqing 400044, People's Republic of China
[10]Department of Applied Physics, The Hong Kong Polytechnic University, Hong Kong, People's Republic of China
[11]Materials Research Institute, Pennsylvania State University, University Park, Pennsylvania 16802, USA
[12]Department of Materials Science and Metallurgy, University of Cambridge, Cambridge, United Kingdom
[13]State Key Laboratory of Powder Metallurgy, Central South University, Changsha, Hunan 410083, China
[14]James Watt School of Engineering, University of Glasgow, Glasgow, United Kingdom
[15]Department of Materials Science and Engineering, Korea Advanced Institute of Science and Technology (KAIST), 291 Daehak-ro, Yuseong-gu, Daejeon 34141, Republic of Korea
[16]School of Advanced Materials Science and Engineering, Sungkyunkwan University (SKKU), Suwon 16419, Republic of Korea
[17]SKKU Advanced Institute of Nanotechnology (SAINT), Sungkyunkwan University (SKKU), Suwon 16419, Republic of Korea
[18]Key Laboratory of Textile Science and Technology, Ministry of Education, College of Textiles, Donghua University, Shanghai 201620, China
[19]Department of Materials Science and Engineering, University of Wisconsin-Madison, Madison, Wisconsin 53706, USA
[20]School of Materials Science and Engineering, Georgia Institute of Technology, Atlanta, Georgia 30332, USA
[21]School of Industrial Engineering, Purdue University, West Lafayette, Indiana 47907, USA
[22]Flex Laboratory, Purdue University, West Lafayette, Indiana 47907, USA
[23]Birck Nanotechnology Center, Purdue University, West Lafayette, Indiana 47907, USA
[24]ESAT-MNS, University of Leuven, Leuven 3001, Belgium

[a)]**Authors to whom correspondence should be addressed:** qj214@cam.ac.uk and sk568@cam.ac.uk